

Cross-Layer Aided Energy-Efficient Routing Design for Ad Hoc Networks

Jing Zuo, Chen Dong, Soon Xin Ng, Lie-Liang Yang, and Lajos Hanzo

Abstract—In this treatise, we first review some basic routing protocols conceived for *ad hoc* networks, followed by some design examples of cross-layer operation aided routing protocols. Specifically, cross-layer operation across the PHYSICAL layer (PHY), the Data Link layer (DL) and even the NETWORK layer (NET) is exemplified for improving the energy efficiency of the entire system. Moreover, the philosophy of Opportunistic Routing (OR) is reviewed for the sake of further reducing the system's energy dissipation with the aid of optimized Power Allocation (PA). The system's end-to-end throughput is also considered in the context of a design example.

Index Terms—Opportunistic routing, cross-layer, objective function, near-capacity coding, energy consumption, power allocation.

I. INTRODUCTION

SINCE the commencement of the Defense Advanced Research Projects Agency (DARPA) project [1] developed by the American Defense Department in the 1970s, *ad hoc* networks have been widely applied in scenarios, including military applications, crisis response, medical care, conference meetings and space exploration. During the past few decades, *ad hoc* networks attracted substantial research attention as a benefit of their prompt set-up and their ability to self-organize their noncentrally-controlled dynamic topology. Each node of an *ad hoc* network plays the dual role of being both a terminal and a router under the assumption that not all nodes can directly communicate with each other [2]. Fig. 1(a) and (b) show the difference between the classic infrastructure based network and *ad hoc* network. Fig. 1(a) shows that the nodes A, B and C communicate with each other under the control of Base Station (BS) 1 and that A communicates with E via BS 1 and BS 2. However, Fig. 1(b) shows that A can only communicate with E by relying on B, C and D as its Relay Nodes (RNs). Each node has to discover its own neighbor list.

The characteristics of *ad hoc* networks impose a number of open problems, which constitute challenges for the protocol design. For example, the scalability, the energy-efficiency, the

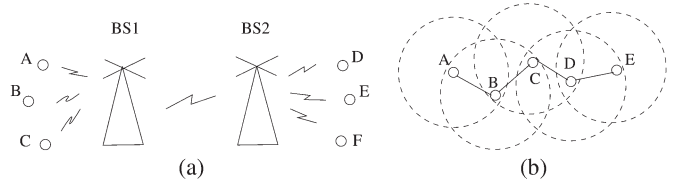


Fig. 1. Categories of wireless networks. (a) The infrastructure network; (b) *Ad hoc* network.

Quality of Service (QoS) and the security are challenging problems to be solved and to be further improved. Hence the emphasis of this treatise is on the design of routing protocols relying on cross-layer interaction for improving the attainable system performance, such as the Normalized Energy Consumption (NEC) and the end-to-end throughput.

A. Cross-Layer Design

The International Standards Organization (ISO) created the SubCommittee 16 (SC16) in 1977 for developing an architecture, which could serve as a framework for the definition of standard protocols. At the end of 1979, the Reference Model of Open System Interconnection (OSI) was adopted by the parent of SC16, namely, Technical Committee (TC97). The OSI Reference Model was also recognized by the International Telegraph and Telephone Consultative Committee (CCITT) Rapporteur's Group on Public Data Network Services. The OSI Reference Model consists of seven layers, which are the PHYSICAL layer (PHY), the Data Link layer (DL), the NETWORK layer (NET), the transport layer, the session layer, the presentation layer and the application layer. The benefit of this layering technique is to group the similar communication functions into these logical layers. A layer has to cooperate with the layer above it and the layer below it. However, when the Transmission Control Protocol (TCP) of the transport layer and the Internet Protocol (IP) of the network layer were defined, the five-layer model (TCP/IP model) became the dominant one. More explicitly, the TCP/IP model consists of the application layer, the transport layer, the NETWORK (NET) layer, the Data Link (DL) layer and the PHYSICAL (PHY) layer [3]–[6]. Fig. 2 illustrates the structure of the TCP/IP model and the main functions of each layer.

The functions of these layers are briefly highlighted below:

- **The physical layer:** The PHY layer concentrates on both the physical devices and on the transmission media. Providing a diversity and/or multiplexing gain with the aid of multiple antennas is capable of improving the integrity and/or throughput of data transmission. Additionally, the

Manuscript received January 9, 2014; revised July 6, 2014 and October 31, 2014; accepted January 17, 2015. The research leading to these results has received funding from the European Union's Seventh Framework Programme (FP7/2012-2014) under grant agreement no 288502. The financial support of the China-UK Scholarship Council, and of the RC-UK under the auspices of the IU-ATC initiative is also gratefully acknowledged.

The authors are with the School of Electronics and Computer Science (ECS), University of Southampton, Southampton SO17 1BJ, U.K. (e-mail: jz08r@ecs.soton.ac.uk; cd2g09@ecs.soton.ac.uk; sxn@ecs.soton.ac.uk; lly@ecs.soton.ac.uk; lh@ecs.soton.ac.uk; http://www-mobile.ecs.soton.ac.uk).

Color versions of one or more of the figures in this paper are available online at <http://ieeexplore.ieee.org>.

Digital Object Identifier 10.1109/COMST.2015.2395378

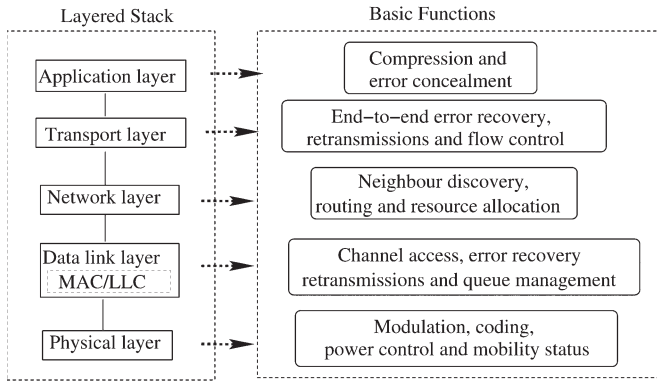


Fig. 2. Layered stack and the main functions in each layer.

77 adjustment of the transmit power, the design of the coding
 78 and modulation schemes as well as the effects of mobil-
 79 ity and/or propagation effects constitute important design
 80 factors of the physical layer.

- 81 • **The data link layer:** The DL layer of Fig. 2 is concerned
 82 with the media access, the error recovery, the retransmission
 83 and the queue management functions. It consists of
 84 two sub-layers, namely the Media Access Control (MAC)
 85 sublayer and the Logical Link Control (LLC) sublayer [7].
- 86 • **The network layer:** The NET layer is responsible for
 87 the neighbor discovery, routing and resource allocation
 88 functions. Routing is the main function of the network
 89 layer, guiding a packet through the network from a source
 90 to the destination [8], [9]. Numerous routing protocols
 91 have been designed based on the IP protocol for satisfy-
 92 ing the requirements of wireless *ad hoc* networks, which
 93 fundamentally predetermines the attainable performance
 94 in terms of the Packet Loss Ratio PLR, the end-to-end
 95 delay and the network's throughput.
- 96 • **The transport layer:** The transport layer is responsible for
 97 flow control, congestion control, error recovery, packet re-
 98 ordering and for the end-to-end connection setup. It assists
 99 the application layer of Fig. 2 in allocating/mapping the
 100 flows to different routes, which are found in the NET layer.
 101 It also assists by monitoring the end-to-end data transmis-
 102 sion and in avoiding network congestion [10], [11].
- 103 • **The application layer:** The application layer constitutes
 104 the interface to the end user in the TCP/IP model of Fig. 2.
 105 By considering the requirements of the end user, it divides
 106 the user services into different categories, such as for
 107 example, real-time and non-real-time services, continuous
 108 and intermittent services, Constant Bit Rate (CBR) and
 109 Variable Bit Rate (VBR) multimedia services, etc. [12].

110 Again, although the layered architecture has its own ad-
 111 vantages and performs well in wired networks in terms of
 112 portability, flexibility and low design complexity, it is not
 113 suitable for wireless networks, especially in wireless *ad hoc*
 114 networks. The reason for its inadequacy in wireless scenarios
 115 is that the services offered by the layers to those above them
 116 in Fig. 2 are realized by specifically tailored protocols for the
 117 different layers and that the architecture forbids direct com-
 118 munication between non-adjacent layers. The communication
 119 between adjacent layers is limited to procedure calls and to their

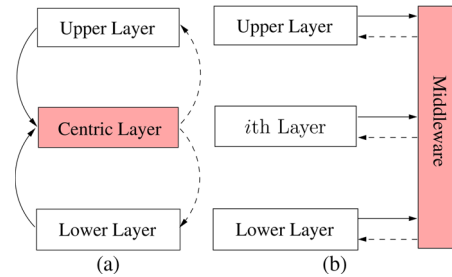


Fig. 3. Conceptual illustration of cross-layer design methods. (a) Layer-centric solution; (b) centralized solution.

120 responses. Moreover, the hostile wireless links impose several
 121 new problems on the associated protocol design that cannot
 122 be readily handled by the layered architecture [13]. More
 123 explicitly, having a strict layered design is not flexible enough to
 124 cope with the dynamics of Mobile *Ad hoc* Network (MANET)
 125 environments and will thus result in a low performance [14].
 126 Thus, the mutual impact of the layers on each other cannot
 127 be ignored [15]. Hence the concept of cross-layer design has
 128 been proposed in an attempt to achieve a performance gain by
 129 exploiting the close interaction amongst the different layers.
 130 Srivastava and Motani [13] defined “Cross-Layer operation”
 131 as: “Protocol design by the violation of a reference layered
 132 communication architecture is cross-layer design with respect
 133 to the particular layered architecture”, while Jurdak [15] define
 134 it as: “Cross-layer design with respect to a reference layered
 135 architecture is the design of algorithms, protocols, or architec-
 136 tures that exploit or provide a set of inter-layer interactions that
 137 is a superset of the standard interfaces provided by the reference
 138 layered architecture”. Therefore, cross-layer operation may be
 139 interpreted as the ‘violation’ of the layered architecture seen
 140 in Fig. 2, which requires more interaction amongst the layers,
 141 beyond the interaction between the adjacent layers. Cross-layer
 142 design clearly requires information exchange between layers, as
 143 well as adaptivity to this information at each layer and a certain
 144 grade of diversity built into each layer for the sake of improving
 145 the achievable robustness [5].

146 There are two basic methods of information sharing in cross-
 147 layer design [16]. One of them makes the variables of a specific
 148 layer visible to the other layers, which is referred to as a layer-
 149 centric solution. The other relies on a shared middleware [15],
 150 [16], which provides the service of storage/retrieval of infor-
 151 mation to all layers, which is termed as a centralized solution.
 152 Fig. 3 illustrates how these two cross-layer solutions operate.

153 The basic principles of the above-mentioned pair of cross-
 154 layer solutions are:

- 155 • **The layer-centric solution:** A certain layer is allowed to
 156 be the central layer, which controls the cross-layer adap-
 157 tation by accessing the internal protocol parameters and
 158 algorithms of the other layers, as shown in Fig. 3(a). Al-
 159 though this approach significantly improves the attainable
 160 system performance, it violates the layered architecture,
 161 since it requires access to the internal variables of other
 162 layers.
- 163 • **The centralized solution:** A middleware or a system-level
 164 monitor (centralized optimizer) is employed for estimating
 165 both the availability of resources and the environmental

TABLE I
MAJOR CONTRIBUTIONS OF CROSS-LAYER DESIGN IN *Ad Hoc* NETWORKS

Year	Authors	Contribution
2005	Setton <i>et al.</i> [18]	Explored the potential synergies of exchanging information between different layers to support real-time video streaming.
2006	Liu <i>et al.</i> [19]	Proposed a scheduling algorithm at the MAC layer for multiple connections under diverse QoS requirements, where each connection employs both adaptive modulation and coding at the PHY layer for transmission over wireless channels.
2007	Huang and Letaief [20]	Proposed a cross-layer optimization framework to jointly design the scheduling, power control and adaptive modulation.
2008	Zhang and Zhang [21]	Reviewed the state-of-the-art on the cross-layer paradigm and discussed the open issues related to cross-layer design for QoS support.
2009	Oh and Chen [22]	Presented a cross-layer design for reliable video transmission based on a multichannel MAC protocol in the context of time division multiple access.
2010	Chu and Wang [23]	Presented cross-layer centralized and distributed scheduling algorithms, which exploited the PHY layer channel information to opportunistically schedule cooperative spatial multiplexed transmissions between MIMO-based nodes.
2011	Ghosh and Hamouda [24]	Proposed a cross-layer antenna selection algorithm for improving the transmission efficiency in cognitive MIMO-aided <i>ad hoc</i> networks.
2012	Mardani <i>et al.</i> [25]	Jointly considered flow control, multipath routing and random access control based on network utility maximization.
2013	Uddin <i>et al.</i> [26]	Studied cross-layer design in random-access-based fixed wireless multihop networks under a physical interference model.
2014	Tang <i>et al.</i> [27]	Proposed a cross-layer distributed approach for maximizing the network throughput by jointly selecting stable routes and assigning channels based on mobility prediction.

166 dynamics, for the sake of coordinating the allocation of
 167 resources across diverse applications as well as nodes, and
 168 for adapting the protocols' parameters within each layer
 169 based on the dynamics experienced, as shown in Fig. 3(b).
 170 This approach requires each layer to forward the complete
 171 information characterizing its protocol parameters and
 172 algorithms to the middleware or system monitor. It also
 173 requires each layer to carry out the actions requested by the
 174 central optimizer. This approach also violates the layered
 175 architecture. The so-called MobileMan [14] and CrossTalk
 176 [17] protocols constitute important centralized cross-layer
 177 solutions.

178 The cross-layer operation aided design of wireless *ad hoc*
 179 networks poses challenges mainly due to the time-variant char-
 180 acteristics of wireless channels. The signal is substantially more
 181 vulnerable to the effects of noise, fading and interference than
 182 in benign fixed networks, leading to potential performance
 183 degradations within the higher layers. For example, a packet has
 184 to be retransmitted in the DL layer or the transmit power has to
 185 be adjusted to guarantee its high-integrity transmission, which
 186 may impose interference on other nodes or promote aggressive
 187 contention for channel access. In the NET layer, the current
 188 route may become invalid and hence route maintenance/repair
 189 has to be activated or even a new route discovery process has to
 190 be initiated. As a result, potentially more energy is consumed
 191 and the end-to-end delay is increased, while the end-to-end
 192 throughput is reduced. Therefore, careful adaptation of the
 193 protocol stack should be used at each layer to compensate for
 194 the variations at that layer, depending on the specific time scale
 195 of these variations [5]. Both the local adaptation of parameters
 196 within each layer and the adaptation based on the other layers
 197 have to be considered. For example, the transmit power, the
 198 signal processing hardware's power dissipation, the information
 199 transmit rate, the coding and modulation schemes, the Frame
 200 Error Ratio (FER) and the mobility in the PHY layer consti-

tute important parameters, which may be beneficially shared 201
 with other layers. The protocol design of the upper layers has 202
 to consider the information gleaned from the PHY layer for 203
 minimizing the energy consumption, the resource allocation, 204
 scheduling and the queueing management, while maintaining 205
 a certain QoS guarantee. Meanwhile, the number of retransmis- 206
 sions, as well as both the routing and network topology related 207
 information received from the upper layers may be beneficially 208
 shared. Additionally, node cooperation also calls for cross-layer 209
 design [13]. Table I is presented for discussing the previous 210
 work on cross-layer design in a compact manner. 211

These cross-layer aided designs may be classified into several 212
 categories according to their different application requirements. 213
 They might be designed for reducing the energy consumption, 214
 the end-to-end delay [21], for improving the network's through- 215
 put [18], [22], [24], [26], [27], for striking a flexible tradeoff 216
 between any two of them [20], [23], and even for multiple- 217
 constraint optimization [19], [21]. 218

As detailed above, cross-layer design has substantial benefits, 219
 but it has its own disadvantages as well. For example, the cross- 220
 layer interactions create dependencies amongst the layers, 221
 which will affect not only the layer concerned, but also the other 222
 layers. Hence, a complete redesign of the operational networks 223
 and protocols will lead to a high implementational cost [16]. 224
 Therefore, cross-layer design should be carefully crafted, be- 225
 cause once the seven-layer OSI structure is violated, the benefits 226
 of independent, layer-specific protocol design will disappear 227
 [13], [28]. The effects of any protocol chosen in every single 228
 layer on the overall system has to be carefully considered. 229

B. Categories of *Ad Hoc* Routing Protocols

230

The NET layer of Fig. 2 plays a key role in *ad hoc* networks, 231
 which substantially influences the performance of the overall 232
 system. The NET layer is responsible both for allocating IP 233

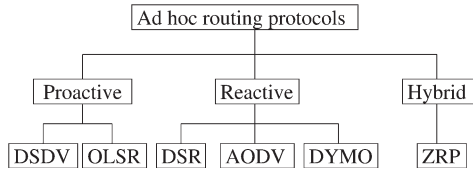


Fig. 4. Categorization of *ad hoc* routing protocols (DSDV: Destination-Sequenced Distance Vector routing; OLSR: Optimized Link State Routing; DSR: Dynamic Source Routing; AODV: Ad-hoc On-demand Distance Vector routing; DYMO: DYnamic Manet On-demand routing; ZRP: Zone Routing Protocol).

addresses and for choosing the right route for communication between the source and destination. The routing protocols of *ad hoc* networks may be classified as proactive routing, reactive routing and hybrid routing [29], as shown in Fig. 4.

The proactive routing periodically transmits “hello” packets for the sake of identifying all possible routes in the network. Hence every node has to maintain a routing table, which stores the route spanning from itself to all other available nodes. The advantage of this kind of routing protocol is that the route discovery time is low. By contrast, its disadvantage is that each node has to maintain a routing table. If the number of nodes in the network becomes high, then the routing table becomes large and hence requires a large memory. On the other hand, periodically sending “hello” packets increases the network control load imposed. The so-called Destination-Sequenced Distance Vector (DSDV) [30] protocol and the Optimized Link State Routing (OLSR) [31] protocol are typical proactive routing protocols, as seen in Fig. 4.

The reactive routing protocols are source-driven, implying that they transmit route discovery packets to find a route to the destination, when there is sufficient data scheduled for transmission in the buffer, instead of periodically broadcasting the “hello” packets. As a benefit, not all nodes have to maintain a route table for storing the routes leading to all other nodes. Instead, they only store routes that were found during the process of route discovery. This technique reduces the network control load compared to the proactive routing protocols of Fig. 4. The disadvantage of this routing protocol family is however that their delay is increased, because a route has to be found to the destination, when no routes leading to the destination exist in the route table. Additionally, the nodes’ movement changes the network’s topology, which hence requires the transmission of more control packets for the sake of maintaining the current communication session. As seen in Fig. 4, the Dynamic Source Routing (DSR) [32], Ad-hoc On-demand Distance Vector (AODV) [33] and DYnamic Manet On-demand (DYMO) [34] routing protocols constitute typical reactive routing protocols.

Based on beneficially combining the advantages, whilst avoiding the disadvantages of the above-mentioned protocol families, hybrid routing protocols may also be conceived. We may divide the entire *ad hoc* network into several small areas and in each area proactive routing may be employed for establishing a link for all nodes. By contrast, between the areas, reactive routing protocols may be adopted for reducing the number of control packets required. Hybrid protocols are widely applied in large *ad hoc* networks. The so-called Zone Routing Protocol (ZRP) [35] is a typical hybrid routing protocol.

C. Review of Cross-Layer Aided Routing Protocols

281

This treatise is mainly dedicated to cross-layer operation aided routing design in *ad hoc* networks, hence we list the major contributions to the literature of cross-layer aided routing protocols conceived for *ad hoc* networks in Table II.

Similarly, these cross-layer aided routing protocols may be classified into several categories according to their different application requirements. They might be designed for reducing the energy consumption [38], [48], [52], the end-to-end delay [47], for improving the network’s throughput [39], [49], [54], for striking a flexible tradeoff between any two of them [26], [42], [45], [46], [50], [51], and even for multiple-constraint optimization [36], [41], [43], [44].

D. Review of Energy-Efficient Routing Protocols

294

As mentioned in Section I-C, cross-layer design may be studied based on diverse application requirements. This paper focuses on cross-layer design techniques conceived for reducing the energy consumption. **since energy saving in wireless *ad hoc* networks is of salient importance in the interest of mitigating the problem of limited battery supply at each node. In *ad hoc* networks the nodes actively and voluntarily participate in constructing a network and act as relays for other nodes. As a result of node-mobility, the Channel State Information (CSI) varies and hence a substantial amount of control messages have to be exchanged across the network to maintain reliable communications between certain pairs of nodes, which potentially imposes a high energy-consumption. Therefore, minimizing the energy consumption becomes extremely important.** Numerous power-aware routing protocols were proposed in [55] for improving the energy efficiency from a multiuser networking perspective. Firstly, a compact-form review of energy-efficient single-layer routing design is provided in Table III.

Moreover, cross-layer optimized power control has been widely exploited [66]–[71] for maintaining the required target-integrity at a low power in realistic propagation environments. A physical-layer-oriented routing protocol supported by sophisticated power control was proposed in [66] for a Line-Of-Sight (LOS) and shadow faded scenario, where the estimated end-to-end BER of a multi-hop path was used as the route selection metric. Furthermore, an adaptive relaying strategy switching between the Amplify-and-Forward (AF) and the Decode-and-Forward (DF) schemes was proposed in [67] for reducing both the energy consumption as well as the delay of the system. As a further design dilemma, the influence of the ‘small number of long hops’ versus the ‘many short hops’ philosophy on the energy consumption was studied in [68]–[70]. It was indicated in [68] that the ‘small number of long hops’ routing scheme was better than the ‘many short hops’ routing scheme provided that near-capacity coding strategies combined with a relatively short block length were employed, because a substantial SNR loss was exhibited by the ‘many short hops’ based routing scheme. Moreover, it was demonstrated in [69] that ‘many short hops’ perform well in energy-limited scenarios relying on spatial reuse, even in the absence of interference cancellation, while using a ‘small number of long hops’ is more suitable for

TABLE II
MAJOR CONTRIBUTIONS OF CROSS-LAYER AIDED ROUTING PROTOCOLS IN *Ad Hoc* NETWORKS

Year	Authors	Contribution
2002	Goldsmith and Wicker [36]	Reviewed each layer's protocol and emphasized the necessity of cross-layer design, particularly in energy-limited scenarios.
2005	Souryal <i>et al.</i> [37]	Proposed efficient channel-quality-aware adaptive routing relying on adaptive modulation.
	Lee <i>et al.</i> [38]	Combined power-aware routing with a MAC layer algorithm for minimizing the total consumed power.
2006	Johansson and Xiao [39]	Jointly optimized the end-to-end communication rates, routing, power allocation and transmission scheduling of a network.
	Mao <i>et al.</i> [40]	proposed a Genetic Algorithm (GA)-based application-centric cross-layer approach for minimizing video distortion.
	Abdrabou and Zhuang [41]	Presented a position-aware QoS routing scheme by considering its interactions with the MAC.
	Zhang <i>et al.</i> [42]	Addressed the topic of energy-efficient routing subject to both packet delay and multi-access interference constraints.
2007	Kompella <i>et al.</i> [43]	Optimized the performance of Multiple Description (MD) video subject to certain routing and link layer constraints.
	Chiang <i>et al.</i> [44]	Surveyed the functional modules, such as congestion control, routing, scheduling, random access, power control and channel coding.
2008	Phan <i>et al.</i> [45]	Presented a cross-layer optimization approach jointly considering the design of the MAC, routing and energy distribution.
	Liu <i>et al.</i> [46]	Jointly optimized the power and bandwidth allocation at each node and designed multihop/multipath routing for a MIMO-based wireless <i>ad hoc</i> network.
2009	Abdrabou and Zhuang [47]	Proposed a routing scheme based on a geographical on-demand routing protocol, which is capable of guaranteeing a certain maximum end-to-end delay.
	Li <i>et al.</i> [48]	Proposed a combined multi-rate power controlled MAC protocol and routing protocol relying on the effective transport capacity as the routing metric.
2010	Ding <i>et al.</i> [49]	Proposed a ROuting and dynamic Spectrum-Allocation (ROSA) algorithm aiming for maximizing the network's throughput by performing joint routing, dynamic spectrum allocation, scheduling and transmit power control.
	Lu <i>et al.</i> [50]	Presented Joint Channel Assignment and Cross-layer Routing (JCACR) by employing two metrics, namely the Channel Utilization Percentage (CUP) and the Channel Selection Metric (CSM).
2011	Ding and Leung [51]	Proposed cross-layer routing applying both cooperative transmission and path selection for striking a tradeoff between the transmit power consumption and the end-to-end reliability.
	Tavli and Heinzelman [52]	Presented real-time multicasting based routing.
2012	Syue <i>et al.</i> [53]	Proposed a relay-aware cooperative routing protocol relying on cross-layer design.
2013	Pan <i>et al.</i> [54]	Investigated the path selection problem based on the cross-layer optimization in on flow routing, multihop Cognitive Radio Networks(CRNs) under constraints link scheduling and CR source's budget.
2014	Uddin <i>et al.</i> [26]	Studied cross-layer design in random-access-based fixed wireless multihop networks under a physical interference model.

TABLE III
MAJOR CONTRIBUTIONS OF SINGLE LAYER ENERGY-EFFICIENT ROUTING PROTOCOLS IN *Ad Hoc* NETWORKS

Year	Authors	Contribution
2005	Muruganathan <i>et al.</i> [56]	Proposed a centralized routing protocol referred to as a base-station controlled dynamic clustering protocol, which distributes the energy dissipation evenly among all sensor nodes for improving the network lifetime and for achieving average energy savings.
2006	Zhu <i>et al.</i> [57]	Proposed a minimum energy dissipation routing protocol based on an accurate model, which took into account the energy consumption of both the data packets, as well as of the control packets and retransmissions.
2007	Baek and Veciana [58]	Investigated the employment of proactive multipath routing to achieve a tradeoff between the energy cost of spreading traffic and the improved spatial balance of energy.
2008	Eidenbenz <i>et al.</i> [59]	Designed an energy-efficient distributed algorithm based on the so-called side payment scheme in conjunction with a game-theoretic technique to achieve truthfulness for the rational selfish nodes.
2009	Liang <i>et al.</i> [60]	Designed energy-efficient routing algorithms, which constructed a shared multicast tree spanning all terminal nodes, while ensuring that the total energy consumption of realizing all-to-all multicasting was minimized.
2010	Li <i>et al.</i> [61]	Proposed a virtual-link-reduction-based broadcasting protocol using directional antennas.
2011	Ma and Yang [62]	Proposed an online computable discrete-time mathematical energy model for characterising the battery discharging behavior and proposed a battery-aware routing scheme that incorporates battery awareness into routing protocols.
2012	Akhtar <i>et al.</i> [63]	Designed a cooperative routing algorithm, which took the electronic power consumption into consideration, when constructing the minimum-power route leading from source to destination.
2013	Lu and Zhu [64]	Proposed an energy-efficient genetic algorithm aided mechanism, which depended on bounded end-to-end delay and minimum energy cost of the multicast tree, to solve QoS based multicast routing problems.
2014	Vazifehdan <i>et al.</i> [65]	Proposed an energy-efficient routing algorithm, which finds routes minimizing the total energy required for end-to-end packet delivery.



Fig. 5. Structure of this treatise.

bandwidth-limited scenarios. Therefore, the routing algorithms should be carefully designed, when jointly considering both the achievable energy-efficiency and the attainable bandwidth-efficiency. The tradeoffs between energy- and bandwidth-efficiency were studied in [70], where it was found that at high end-to-end data rates the routes associated with fewer hops minimize the energy consumption, while at lower end-to-end data rates the routes having more hops mitigate it.

E. Outline

Based on the discussions in the previous sections, the rest of the paper is organized as follows: First, we study the cross-layer aided routing design jointly considering both the PHY layer and the NET layer [72], as shown in Section II; Then in Section III we further investigate the cross-layer aided routing design concept by jointly considering the PHY layer, the DL layer and the NET layer [73], [74]. We commence by considering Traditional Routing (TR) relying on a fixed transmit power in Section III-A, while TR combined with Power Allocation (PA) is discussed in Section III-B and Opportunistic Routing (OR) using PA is studied in Section III-C; Finally, Section IV concludes this treatise and offers some design guidelines. Fig. 5 lists the structure of this paper.

The notations used in this treatise are defined as follows:

- N : the number of nodes in the network;
- H : the number of hops in an established route;
- N_r : the maximum number of MAC retransmissions, including the first transmission attempt;
- P_i : the transmit power of each node;
- P_{i_i} : the transmit power in the i -th node of the established route;
- FER_i : the FER of the i -th link in an established route;
- p_i : the successful reception probability of the i -th link, where $p_i = 1 - FER_i$;
- E_T : the sum of the energy dissipated by all the nodes in the network, including the data packets and the control packets;
- \bar{E}_T : the overall energy dissipation E_T normalized by the number of bits received in the application layer of the destination;
- E_{total} : the sum of the energy dissipated by the data packets during their transmission in the network;
- \bar{E}_{total} : the total energy dissipation E_{total} normalized by the end-to-end successful reception probability, which is the average energy consumption dissipated by the entire system during the successful delivery of a packet from the source to the destination;
- R_{e2e} : the number of information bits successfully delivered to the destination per second.

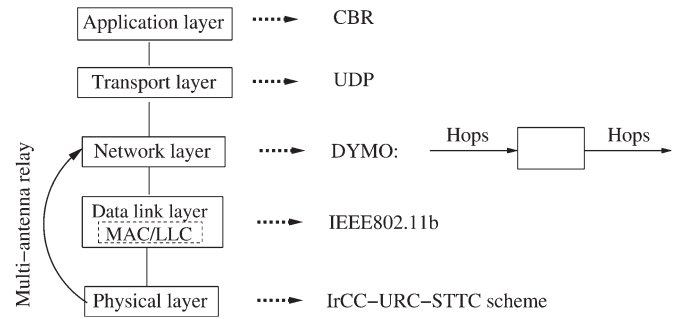


Fig. 6. System model of the energy-efficient routing with PHY & NET cooperation in *ad hoc* networks.

II. ROUTING DESIGN WITH PHY & NET COOPERATION

Energy-efficient wireless network design has recently attracted wide-spread research attention [75]. Diverse resilient Forward Error Correction (FEC) schemes were proposed in [76] for achieving a low Bit Error Ratio (BER) at near-capacity Signal-to-Noise Ratio (SNR) values. Therefore, the effective transmission range can be improved, when the required received signal power is reduced. Again, an Irregular Convolutional Coded, Unity-Rate Coded and Space-Time Trellis Coded (IrCC-URC-STTC) scheme has been proposed for cooperative communications in [77]. Several Single-Antenna RNs (SAs) were activated between the source and the destination. The RNs roaming closest to their optimal locations were activated based on a technique relying on EXtrinsic Information Transfer (EXIT) charts [78] in conjunction with near-capacity code design principles, which were detailed for example in [79].

However, the solution disseminated in [72] aims for minimizing the energy consumption by the joint design of both the PHY and NET layers with the assistance of Multiple-Antenna Aided Relay Nodes (MA-RN), as shown in the system model of Fig. 6. Although the routing metric is still the number of hops, the employment of MA-RNs assists in reducing the potential number of hops from the source to the destination, when dissipating a given transmit power at each node. Therefore MA-RNs are capable of reducing the entire system's energy consumption. The influence of the number of MA-RNs in a system will be studied in Section II-C. Both the perfect capacity-achieving coding abstraction and a realistic near-capacity coding scheme, namely a three-stage-concatenated IrCC-URC-STTC arrangement is employed in the PHY layer. The IEEE802.11b regime [7] is used in the DL layer. In the NET layer, the more efficient DYMO routing protocol [34] is employed, because the DYMO protocol imposes a lower network control load and it is more flexible in a high-mobility environment. However, the scenario considered in [72] is a stationary scenario. The investigation of high-mobility scenarios was set aside for its future study. The User Data Protocol UDP [80] is employed in the transport layer and CBR data streaming is used in the application layer. The channel model employed is an Additive White Gaussian Noise (AWGN) channel subjected to both inverse-second-power free-space path loss and to uncorrelated Rayleigh fading.

A. Near-Capacity Coding Schemes

Each MA-RN is assumed to be equipped with two antennas. If more than one MA-RN exist in the multi-hop *ad hoc*

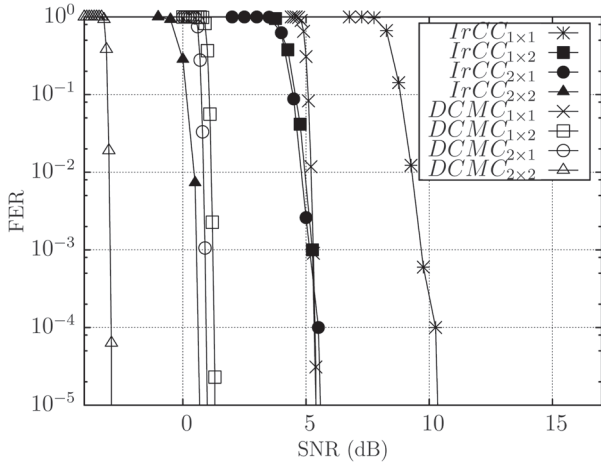


Fig. 7. FER performance of the four types of links, for example at the frame length of 1500 bits, of the uncorrelated Rayleigh fading channel for DCMC-capacity-based scheme and the IrCC-URC-STTC scheme, where $DCMC_{T \times R}$ represents the DCMC-capacity-based scheme, and $IrCC_{T \times R}$ represents the IrCC-URC-STTC scheme. Additionally, the subscript ' $T \times R$ ' represents having T transmit antennas and R receive antennas. Moreover, the overall FEC code rate is $R_c = 0.5$, the effective throughput is 1 bps (bits/symbol), the number of transmitted frames is 10 000 and the IrCC has 17 component codes, associated with the weights [0.049, 0, 0, 0, 0, 0.24, 0.16, 0.12, 0.035, 0.102, 0, 0.071, 0.093, 0, 0.091, 0, 0.039].

network considered, then four different types of links may appear. Specifically, there exists the SA-RN to SA-RN, SA-RN to MA-RN, MA-RN to SA-RN and finally the MA-RN to MA-RN links. All the MA-RNs employ the Quadrature Phase Shift Keying (QPSK)-assisted IrCC-URC-STTC scheme, while all the SA-RNs employ the 8-ary Phase-Shift Keying (8PSK)-assisted IrCC-URC scheme.

For example, the FER performance of all the four links at the frame length of 1500 bits characterized by the Discrete-input Continuous-output Memoryless Channel's (DCMC)-capacity [81] and that of the IrCC-URC-STTC scheme is portrayed in Fig. 7. It can be observed that the IrCC-URC-STTC scheme performs close to the DCMC-capacity based scheme at a given SNR value. Meanwhile, the $IrCC_{2 \times 2}$ scheme has a 5 dB gain compared to $IrCC_{2 \times 1}$ or $IrCC_{1 \times 2}$ arrangements and has a nearly 10 dB gain compared to the $IrCC_{1 \times 1}$ scheme at an FER of 10^{-5} , where $IrCC_{T \times R}$ represents the IrCC-URC-STTC scheme and the subscript ' $T \times R$ ' indicates having T transmit and R receive antennas. Hence, for the sake of guaranteeing the same FER performance, $IrCC_{2 \times 2}$ exhibits a larger transmit range at a given transmit power and may hence potentially reduce the number of hops required for conveying a message from the source to the destination, which can be explained by analyzing the calculation of the transmission range. More explicitly, the average maximum transmission range is defined as the range, over which the receiver node is capable of receiving a transmitted packet with $FER < 10^{-5}$.

The required minimum signal-to-noise ratio SNR_{dB}^* may be calculated from the minimum receive power P_r^* expressed in dBm as follows

$$SNR_{dB}^* = 10 \log_{10} \left(\frac{P_r^*}{N_0} \right), \quad (1)$$

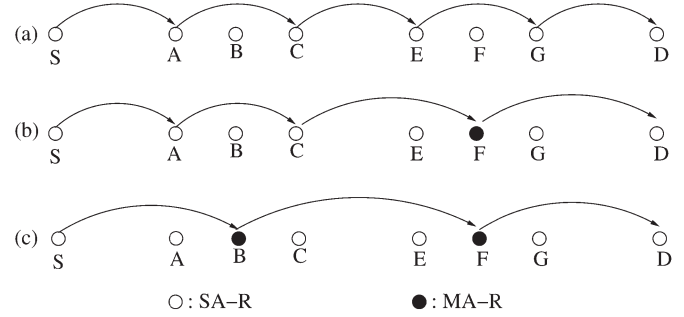


Fig. 8. The influence of MA-RNs on the routing strategy: (a) $H = 5$ hops without MA-RNs; (b) $H = 4$ with 1 MA-RN at point F ; (c) $H = 3$ with 2 MA-RNs at points B and F .

where N_0 is the thermal noise power. Hence, given the transmitted power P_t and SNR_{dB}^* , the average maximum distance d_{max} from the transmitter, where the SNR requirement SNR_{dB}^* may 'just' be satisfied to guarantee $FER < 10^{-5}$, is given by

$$d_{max} = \frac{\sqrt{P_t} \lambda}{4\pi 10^{\left(\frac{SNR_{dB}^* + N_{0dB}}{20}\right)}}, \quad (2)$$

where the carrier's wavelength $\lambda = c/f$ and $N_{0dB} = 10 \log_{10} N_0$. c is the speed of light in vacuum and f is the carrier frequency.

Naturally, if the value of P_t and N_{0dB} are fixed, then it may be readily seen how the adequately 'illuminated' distance, where the required target-FER may be maintained, will vary as a function of the SNR value. As seen from Fig. 7, the maximum adequately covered communication distance from MA-RN to MA-RN is the highest, while that from SA-RN to SA-RN is the lowest. Conversely, if P_t and d_{max} are fixed, then the FER is the lowest for the MA-RN to MA-RN link, while it is the highest for the SA-RN to SA-RN link.

B. Routing Algorithms

It was shown in [77] that the IrCC-URC-STTC scheme is capable of operating near the link's capacity, hence a substantial power saving may be attained. When this scheme is employed by the MA-RNs of the *ad hoc* network considered, the different error correction capability of the four different types of links will influence the routing strategy. Fig. 8 provides an example on how the routing strategy is influenced.

As seen from Fig. 8, the network consists of $N = 8$ nodes, where S is the source and D is the destination. In Fig. 8(a), all nodes are equipped with a single antenna, hence all links are SA-RN to SA-RN links, which yields $H = 5$ hops from S to D . A single MA-RN is employed at point F in Fig. 8(b), where the packets arriving at node C are directly transmitted to node F . Then, node F will forward its received packets further to the destination D . More specifically, the C -to- F link is a SA-RN to MA-RN link, while the F -to- D link is an MA-RN to D link, where the $F - D$ distance is higher than that between the single-antenna nodes of Fig. 8(a). Consequently, the number of hops from S to D is decreased to $H = 4$. In Fig. 8(c), two MA-RNs, namely B and F , are employed. The number of hops is further decreased to $H = 3$ as a benefit of using MA-RNs for nodes B and F .

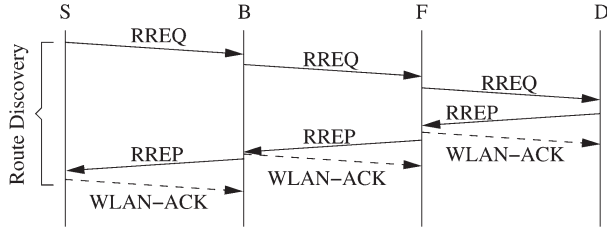


Fig. 9. The process of **route discovery** in the DYMO routing algorithm.

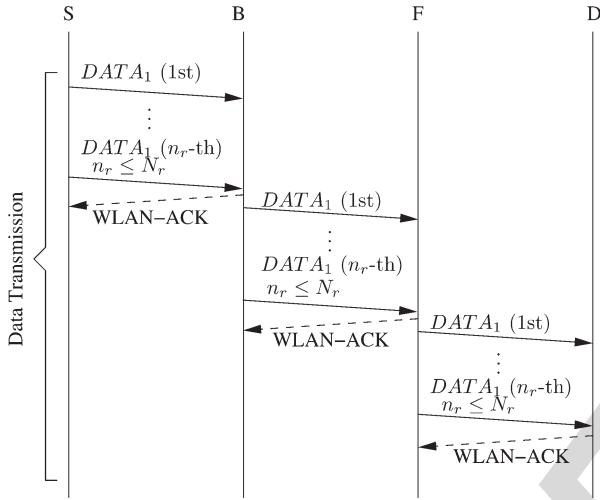


Fig. 10. The process of **data transmission** after a route is found from source A to destination D .

496 The DYMO routing protocol is employed in the NET layer,
 497 which combines most of the benefits of the AODV [33] and
 498 DSR [32] protocols. The DYMO routing protocol always opts
 499 for the specific route having the lowest number of hops to the
 500 destination. When employing the MA-RN aided IrCC-URC-
 501 STTC scheme, it will be demonstrated that the route selected
 502 may be expected to have a further reduced number of hops.
 503 The DYMO routing protocol is constituted by two main stages,
 504 namely the route discovery and route maintenance. During the
 505 route discovery, the Route REQuest (RREQ) and the Route
 506 REPLY (RREP) packets are used for identifying a route from
 507 the source to the destination. By contrast, during the route
 508 maintenance phase, a Route ERRor (RERR) packet is returned
 509 to the source, when a broken link is detected. Figs. 9–11 show
 510 the process of route discovery and data transmission as well
 511 as route maintenance for the DYMO routing protocol, which
 512 assisted us in analyzing the total energy consumption of the
 513 system. The topology considered in Figs. 9–11 has a source S ,
 514 a destination D and the pair of RNs B and F . It is assumed that
 515 each node is only capable of communicating with its neighbour
 516 nodes. For example, node B can only communicate with node
 517 S and node F , while it cannot communicate with node D . The
 518 exchange of the control packets between the neighbour nodes,
 519 such as the exchange of the RREQ packet, RREP packet and
 520 RERR packet, and the associated data transmission process is
 521 detailed as follows:

522 • Route Discovery process of Fig. 9.

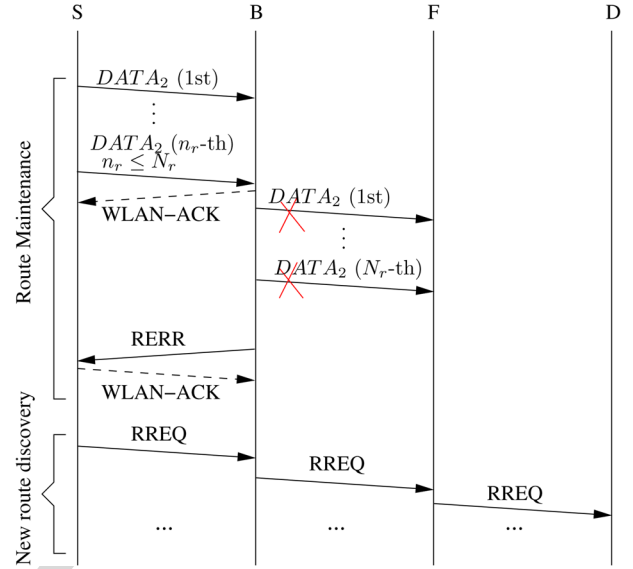


Fig. 11. The process of **route maintenance** in the DYMO routing algorithm.

As seen in Fig. 9, first the source S broadcasts an RREQ 523 packet and when node B receives this RREQ packet, it 524 broadcasts it. Then node F receives the RREQ packet and 525 broadcasts it again. Finally, the destination D receives the 526 RREQ packet, which originated from the source S ; The 527 destination D responds to the RREQ packet with a newly 528 generated RREP packet. The routing table of each node 529 is refreshed, when ever an RREQ/RREP packet arrives 530 at a node. Additionally, a Wireless Local Area Network- 531 Acknowledgement (WLAN-ACK) packet¹ is required for 532 confirming the successful reception of the RREP packet. 533

• Data Transmission process of Fig. 10. 534

When the RREP packet arrives at the source S during 535 the process of route discovery, the source S is informed 536 of a route spanning from the source S to the destination 537 D , with node B being the next hop of this route. Hence, 538 as seen in Fig. 10, the buffered data packet $DATA_1$ is 539 transmitted to node B according to the routing information 540 stored in the routing table of source S . If the packet $DATA_1$ 541 failed to reach node B , then node B has to retransmit 542 the packet $DATA_1$ until the number of retransmission 543 reaches its maximum of N_r . If and only if node B receives 544 the packet $DATA_1$ successfully within n_r retransmissions, 545 where $n_r \leq N_r$, it would respond to source S by sending 546 back a WLAN-ACK packet. The WLAN-ACK is used 547 for confirming the successful transmission of the packet 548 $DATA_1$. Meanwhile, node B forwards the packet $DATA_1$ to 549 node F , since node F is its next hop *en route* to destination 550 D . The routing information stored in node B 's routing table 551 is obtained during the route discovery process as well. In 552 a similar way, if node F successfully receives the packet 553 $DATA_1$, it respond with a WLAN-ACK to node B and 554

¹The Acknowledgement packet is the one, which is returned to the transmitter as the acknowledgement of the correctly received data in the DL layer, hence it is referred to as WLAN-ACK in this treatise, where 'WLAN-ACK' represents the ACK packet employed in the IEEE802.11 standard. It is assumed that no Request-To-Send (RTS)/Clear-To-Send (CTS) mechanism is employed.

555 forwards the packet $DATA_1$ to the destination D according
 556 to its own routing table. Finally, if the destination D suc-
 557 cessfully receives the packet $DATA_1$, it only has to respond
 558 with a WLAN-ACK packet to node F . Destination D
 559 does not forward the packet $DATA_1$, because it is the final
 560 destination of the packet $DATA_1$. Hence the packet from
 561 the source S to the destination D has been completed.

562 • Route Maintenance process of Fig. 11.

563 The process of route maintenance is graphically illus-
 564 trated in Fig. 11, where the transmission of the packet
 565 $DATA_2$ from the source S to the destination D is exem-
 566 plified. First the packet $DATA_2$ is transmitted by the source S
 567 to node B . Node B receives the packet $DATA_2$ successfully
 568 during the n_r -th retransmission, where $1 \leq n_r \leq N_r$ and it
 569 responds with a WLAN-ACK packet to the source S for
 570 confirming the successful reception of the packet $DATA_2$.
 571 Then node B forwards the packet $DATA_2$ to node F .
 572 However, node F fails to receive the packet $DATA_2$ suc-
 573 cessfully after N_r retransmissions by node B . Therefore,
 574 no response is sent from node F to node B . Once the pre-
 575 set timer expires at node B and node B has not received any
 576 WLAN-ACK packet from node F , then node B considers
 577 the link $B - F$ to be broken and actively sends an RERR
 578 packet to its adjacent-node, namely to the source S . Source
 579 S updates its own routing table by deleting all the routes,
 580 which include the link $B - F$. Therefore, the source S does
 581 not have a route to the destination D and a new route
 582 discovery process has to be activated. Hence, an RREQ
 583 packet is broadcast by the source S again, as shown in
 584 Fig. 11.

585 Every node is assumed to has the same transmit power of P_T .
 586 Consequently, the sum of the energy E_T dissipated by all nodes
 587 in the network is given by

$$E_T = \sum E_{Route_Discovery} + \sum E_{Data_Transmission} + \sum E_{Route_Maintenance}, \quad (3)$$

588 where E_T indicates the energy dissipated by a specific network
 589 topology. $\sum E_{Route_Discovery}$ denotes the sum of energy dissi-
 590 pated by the RREQ, the RREP and the WLAN-ACK packets
 591 during the route discovery phase, which is shown in Fig. 9.
 592 Furthermore, $\sum E_{Route_Maintenance}$ includes all the energy during
 593 the route maintenance phase, except for $\sum E_{Data_Transmission}$,
 594 which is the energy dissipated by the data packets and by
 595 the corresponding WLAN-ACK packets, as shown in Figs. 10
 596 and 11.

597 C. System Analysis

598 The overall energy consumption E_T of the entire network is
 599 dependent on numerous parameters, such as the node density
 600 ρ , the number of MA-RNs n_{MA} , the mobile speed, the number
 601 of hops H of the selected route and the amount of bits L_{app}
 602 received in the application layer of the destination. To reduce
 603 the dimensionality of the investigations when characterizing
 604 the benefits of MA-RNs on the node's achievable transmission
 605 range and FER performance, the node density ρ , the mobile
 606 speed and L_{app} are assumed to be constant, then E_T is further
 607 normalized by L_{app} and N of the entire network, where N is re-

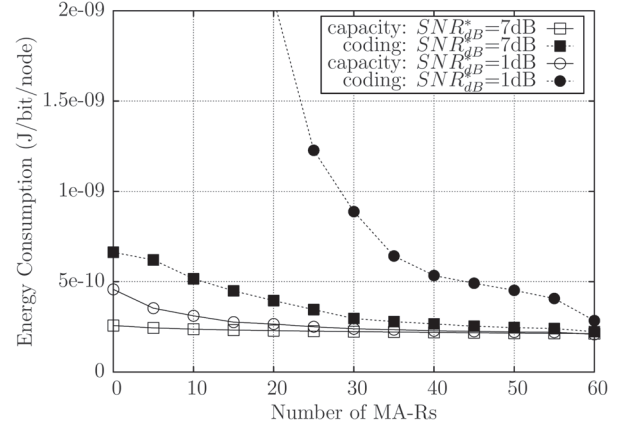


Fig. 12. Energy consumption \bar{E}_T versus the number of MA-RNs n_{MA} aiming for comparing the IrCC-URC-STTC scheme and the DCMC-capacity-based benchmark scheme at SNR_{dB}^* of 7 dB and 1 dB, where ‘coding’ denotes the IrCC-URC-STTC scheme and ‘capacity’ represents the DCMC-capacity-based benchmark scheme.

TABLE IV
SYSTEM PARAMETERS

Path-loss exponent	2
Sensitivity threshold [82], P_r^*	-85 dBm
Mobility	stationary(0 m/s)
Simulation time	30 second
Number of simulation runs	100

608 related to the node density. Finally, the Normalized Energy Con-
 609 sumption (NEC) \bar{E}_T of the entire network can be expressed as: 609

$$\bar{E}_T = \frac{E_T}{NL_{app}} = F(n_{MA}, H). \quad (4)$$

610 Four scenarios are considered to study the relationship be-
 611 tween the number of MA-RNs and the energy consumption, 611
 612 where $N = 60$ stationary nodes are uniformly located in a 612
 613 $500 \text{ m} \times 500 \text{ m}$ field, hence the node density is $\rho = 240$ nodes
 614 per square kilometer. The source S and the destination D are
 615 located in the position (499, 499) and (0, 0), respectively. The
 616 number of MA-RNs² is increased from $n_{MA} = 0$ to $n_{MA} = 60$
 617 in steps of 5. The frame length of the data packets, which are
 618 generated by the application layer, is $L_{app} = 504$ Bytes. The
 619 802.11b standard is employed in the DL layer. The transmit
 620 power is set to $P_T = 1$ mW. The other system parameters
 621 employed for the simulations of Fig. 12 are listed in Table IV,
 622 where the receiver's sensitivity [82] threshold is used to judge
 623 whether the received signal is deemed to be noise, because a
 624 received signal power below the sensitivity level is deemed to
 625 be noise.

626 The energy consumption is quantified for both the IrCC-
 627 URC-STTC scenario³ and the DCMC-capacity-based bench-
 628 mark scenario at SNR_{dB}^* of 7 dB and 1 dB. As seen from
 629 Fig. 12, the energy consumption of the IrCC-URC-STTC
 630 scheme and of the benchmark scheme decrease upon increasing

²The number of MA-RNs also includes the source and the destination. Again, the multi-antenna aided nodes are denoted as MA-RNs and single-antenna nodes are denoted as SA-RNs.

³In the IrCC-URC-STTC scenario the network consists of QPSK-assisted IrCC-URC-STTC aided MA-RNs and 8PSK-assisted IrCC-URC aided SA-RNs.

631 the number of MA-RNs n_{MA} . As mentioned in Section II-A,
 632 a low FER and a relatively high transmission range i.e. cov-
 633 erage area may be ensured by using the IrCC-URC-STTC
 634 scheme advocated. Furthermore, as justified in Section II-B,
 635 the specific routes having the lowest number of hops tend to be
 636 activated in the MA-RNs aided network considered. Therefore,
 637 having a high PHY-layer FER results in an increased number
 638 of retransmissions and hence may trigger route re-discovery,
 639 which results in more control packets being transmitted. Hence,
 640 more energy per payload bit is required for successfully de-
 641 livering the source data to the destination, as demonstrated
 642 in Fig. 12.

643 III. ROUTING DESIGN WITH PHY & 644 DL & NET COOPERATION

645 In recent years, numerous energy-efficient techniques have
 646 been proposed [26], [64], [65], [69], [83]–[106]. However,
 647 simply minimizing the energy consumption results in deficient
 648 designs. It is more beneficial to strike a tradeoff between the
 649 energy consumed and other metrics, such as the attainable
 650 throughput. For example, Multiple-Input and Multiple-Output
 651 (MIMO) schemes and near-capacity Space-Time Codes (STCs)
 652 were employed in [84] for optimizing the RN selection for
 653 the sake of maximizing the end-to-end throughput at a given
 654 total available power. While single-hop transmissions are more
 655 suitable for bandwidth-limited scenarios, multi-hop transmis-
 656 sions combined with spatial frequency-reuse tend to perform
 657 better in power-limited situations [69]. Spatial frequency-reuse
 658 employed in multi-hop scenarios may be beneficially com-
 659 bined with Interference Mitigation (IM) [69], [84] and transmit
 660 beamforming [84] for the sake of finding an attractive balance
 661 between energy minimization and throughput maximization in
 662 both single-hop and multi-hop schemes [69], [85], [86]. As a
 663 further advance, a beneficial tradeoff between the total energy
 664 consumption and throughput was found in [85] by considering
 665 both the transmission strategy of each node as well as the
 666 location of the RNs and the data rate of each node.

667 Moreover, the authors of [26], [57], [86], [89], [92], [95]–
 668 [98], [101]–[104], [107] invoked cross-layer design. For ex-
 669 ample, the impact of the link error rate on the route selection
 670 between a path associated with a large number of short-distance
 671 hops and another with a smaller number of long-distance hops
 672 was studied in [86]. In this paper, the link ‘cost’ was defined as
 673 a function of both the energy required for a single transmission
 674 attempt and the link error rate. This Objective Function (OF)
 675 captures the cumulative energy expended in reliable data trans-
 676 fer for both reliable and unreliable link layers. In [107], several
 677 routing algorithms were proposed, which opted for the route
 678 with minimum energy consumption in a mixed hop-by-hop and
 679 end-to-end retransmission mode. In the end-to-end retransmis-
 680 sion mode, a single unreliable link may require retransmissions
 681 from the source, and hence may require more energy for suc-
 682 cessfully delivering packets. Consequently, routing protocols
 683 play an important role in saving energy. The authors of [57]
 684 took into account both the energy consumed by data packets as
 685 well as by control packets and MAC retransmissions, because
 686 ignoring the energy consumption of exchanging control packets

might underestimate the actual energy consumption and thus 687
 688 may lead to inefficient designs. However, the energy OFs em-
 689 ployed in [57], [86], [107] exploited the assumption of having
 690 access to a potentially infinite number of MAC retransmissions,
 691 which is unrealistic. The employment of the OF proposed in
 692 [57], [86], [107] is feasible only when the affordable number of
 693 MAC retransmissions is infinite, which is formulated as

$$E_{total} = \sum_1^H \frac{E_i}{1 - FER_i}, \quad (5)$$

where $\frac{1}{1 - FER_i}$ is the expected number of transmission at- 694
 695 tempts required for successfully delivering a packet across
 696 link i . As seen from (5), the total energy of all hops is simply
 697 summed, which suggests that the success of the individual links
 698 in a route is deemed to be independent of each other, since the
 699 assumption that an infinite number of MAC retransmissions
 700 is affordable is given. Additionally, although the authors of
 701 [89] considered a limited number of MAC retransmissions, no
 702 specific OF was formulated.

Furthermore, TR relies on a route discovery process invoked 703
 704 for gleaning sufficient routing information for the source to
 705 make meritorious routing decisions, regardless, whether the
 706 routing protocol is proactive or reactive [108]. However, due to
 707 the rapid fluctuation of the channel conditions, the routing in-
 708 formation estimated on the basis of the average Channel Quality
 709 Information (CQI) may become stale, resulting in suboptimum
 710 routing. Therefore, OR [90]–[92], [96], [101], [103], [109]–
 711 [114] has been proposed for avoiding this problem. In OR no
 712 pre-selected route is employed, instead a so-called forwarder
 713 RN set is used for forwarding the packets along a benefi-
 714 cial route. The near-instantaneously varying characteristics of
 715 wireless channels is beneficially exploited considered by OR.
 716 Table V shows that OR is widely used in various networks, such
 717 as *ad hoc* networks [103], [115], wireless sensor networks [91],
 718 cognitive networks [116], vehicular networks [117], [118] and
 719 DTNs [119]–[121].

More specifically, Liu *et al.* [110] illustrated the basic idea 720
 721 behind OR and categorized the potential design criteria, includ-
 722 ing the Estimated Transmission count (ETX), the geographic
 723 distance aided and the energy consumption based philosophies.
 724 Biswas and Morris [101] proposed an Extremely Opportunistic
 725 Routing (ExOR) scheme, which employed the ETX metric at
 726 the destination for deciding the priority order of selecting a
 727 RN from the potential forwarder set. The proposed routing
 728 regime integrated the routing protocol and the MAC protocol
 729 for the sake of increasing the attainable throughput of multi-
 730 hop wireless networks. Their solution [101] also exploited
 731 the less reliable long-distance links, which would have been
 732 ignored by traditional routing protocols. Moreover, Dubois-
 733 Ferrière *et al.* [111] conceived the Least-Cost Anypath Routing
 734 (LCAR) regime, which finds the optimal choice of candidate
 735 RNs relying on the expected ETX cost of forwarding a packet
 736 to the destination. This LCAR algorithm considers the coordi-
 737 nation of the link layer protocols. Laufer *et al.* [114] proposed
 738 a ‘polynomial-time multirate anypath’ routing algorithm and
 739 provided the proof of its optimality. The proposed routing
 740 algorithm employed the Expected Anypath Transmission Time

TABLE V
OPPORTUNISTIC ROUTING PROTOCOLS IN VARIOUS NETWORKS

Year	Authors	Contribution
2006	Pelusi <i>et al.</i> [117]	Surveyed the most promising OR solutions and the taxonomy of the main routing and forwarding approaches in challenging environments.
2008	Conan <i>et al.</i> [121]	Proposed a single copy and multi-hop OR scheme for sparse Delay Tolerant Networks (DTNs).
2009	Khalife <i>et al.</i> [118]	Explored opportunistic forwarding without preestablished routing in multihop cognitive radio networks.
	Spyropoulos <i>et al.</i> [122]	Proposed a class of routing schemes that can identify the nodes of “highest utility” in intermittently connected wireless networks.
2010	Lee <i>et al.</i> [119]	Presented a topology-assisted Geo-OR designed for vehicular networks that combined topology-assisted geographic routing with opportunistic forwarding for mitigating the effects of unreliable wireless channels.
	Li <i>et al.</i> [123]	Investigated energy-efficient opportunistic forwarding and designed different forwarding policies for DTNs.
2011	Mao <i>et al.</i> [91]	Presented an energy-efficient OR strategy conceived for wireless sensor networks, which created a prioritized forwarder list to minimize the total energy consumption of all nodes.
2012	Wang <i>et al.</i> [103]	Proposed a cooperative OR scheme for mobile ad hoc networks for tackling the problem of opportunistic data transfer.
2013	Wu <i>et al.</i> [120]	Proposed a hybrid routing scheme for data dissemination in vehicular ad hoc networks (VANETs), using a carry-and-forward scheme for mitigating the forwarding disconnection problem of sparse VANETs.
2014	Yoon <i>et al.</i> [124]	Investigated the feasibility of OR in power line communications access networks and proposed a customized OR, which used static geographical information.

741 (EATT) as the routing metric, which is a generalization of the
 742 unidirectional ETX metric that takes into account that nodes
 743 transmit at multiple bit rates. The authors of [90], [109], [113]
 744 employed a geographic distance based metric for choosing the
 745 potential forwarder RN set. More specifically, Zorzi and Rao
 746 [109] proposed an OR scheme based on random forwarding,
 747 where the specific node, which is closest to the destination
 748 is chosen as the RN for the next hop. Additionally, they [90]
 749 analyzed the achievable energy as well as latency performance
 750 and provided a detailed description of a MAC scheme based
 751 on both opportunistic concepts and on collision avoidance.
 752 Zeng *et al.* [113] proposed a multirate OR by incorporating
 753 rate adaptation into their candidate-selection algorithm, which
 754 was shown to achieve a higher throughput and lower delay
 755 than the corresponding traditional single-rate routing and its
 756 opportunistic single-rate routing counterpart. The authors of
 757 [91], [92], [96] employed the energy consumption metric for
 758 choosing the potential forwarder RN set. More concretely,
 759 Mao *et al.* [91] presented an energy-efficient OR strategy
 760 relying on sophisticated PA, which prioritizes the forwarder
 761 RNs by directly minimizing the total energy consumption of
 762 all nodes. Dehghan *et al.* [92] developed a minimum-energy
 763 cooperative routing based on many-to-many cooperation and
 764 determines the optimal route with the aid of the Bellman-Ford
 765 algorithm [123]. Wei *et al.* [96] proposed an energy-conserving
 766 Assistant Opportunistic Routing (AsOR) protocol, which clas-
 767 sified a sequence of nodes into three different node sets, namely,
 768 the frame node, the assistant node and the unselected node.
 769 The frame nodes were indispensable for decode-and-forward
 770 operation, while the assistant nodes provided protection against
 771 unsuccessful opportunistic transmissions. Although the authors
 772 of [91], [92], [96] employed the energy consumption as their
 773 routing metric, they have not provided any theoretical bounds
 774 in their performance analysis. Moreover, these authors as-
 775 sumed that the number of affordable MAC retransmissions
 776 was infinite.

777 An appropriate PA scheme combined with an opportunistic
 778 scheme was introduced in [74]. The opportunistic scheme does

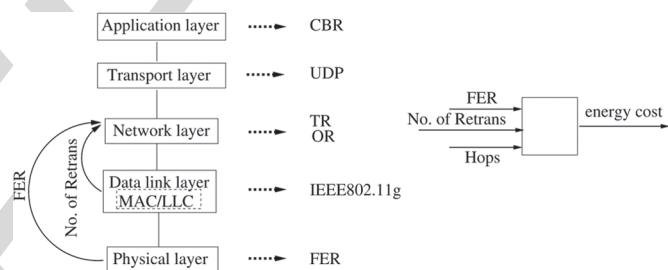


Fig. 13. System model of the energy-efficient routing with PHY & DL & NET cooperation in *ad hoc* networks.

not employ a pre-selected route, while it will fully utilize
 779 the time-variant characteristic of the hostile wireless channel,
 780 where any RN has the chance to forward a packet as long as
 781 the packet arrives at this RN successfully. A pair of energy-
 782 consumption-based OFs are constructed for TR and OR by
 783 exploiting the knowledge of both the corresponding FER within
 784 the PHY layer, as well as that of the number of MAC retrans-
 785 missions and of the number of RNs in the NET layer, as seen
 786 in the system model of Fig. 13. The above-mentioned TR and
 787 OR algorithms employ the corresponding energy-consumption-
 788 based OFs as their routing metrics, respectively. Apart from
 789 the energy consumption, the end-to-end throughput is evaluated
 790 as well. It was demonstrated that the algorithms **proposed in**
 791 [74] are capable of operating close to the theoretical bound
 792 found by the exhaustive search of all routes. In Fig. 13, the
 793 characteristics of the PHY layer are represented with the aid
 794 of the FER, while the DL layer employs the IEEE802.11g
 795 standard. In the NET layer, the above-mentioned TR and
 796 are employed, which make their decisions on the basis of the
 797 above energy-consumption-related OFs. The UDP is employed
 798 in the transport layer and the data streaming relies on a CBR
 799 service in the application layer. As in Section II, the channel
 800 imposes both free-space path-loss and uncorrelated Rayleigh
 801 fading, plus the ubiquitous AWGN.

Based on the system model of Fig. 13, the impact of the
 803 lowest three layers of the OSI model on the total energy 804

805 dissipated of the entire system is considered, which will be
 806 analyzed, whilst relying on an energy-consumption-based OF.
 807 In [73], [74], only the transmit energy consumed by the
 808 data packets during their transmission is considered, which are
 809 generated by the application layer. The energy consumed by
 810 other packets, such as routing and MAC control packets is not
 811 considered. In other words, the idealized simplifying assump-
 812 tion is that the energy consumed during the process of route
 813 discovery is negligible. The elimination of this simplification
 814 was set aside for the future work. **As detailed in** [73], [74],
 815 **the OF is** invoked for making routing-related decisions, which
 816 directly influence the energy consumed by future data packets.
 817 All nodes are assumed to be stationary. Only a single source-
 818 destination pair is supported in the network and only a single
 819 node has the chance of transmitting in a time slot, once the route
 820 was determined. All the data packets are also assumed to have
 821 the same length and all nodes have the same transmission rate.

822 A. Traditional Routing With Fixed Transmit Power

823 Naturally, having an infinite number of MAC retransmis-
 824 sions will impose a potentially infinite end-to-end delay at the
 825 destination, which is not realistic. In realistic environments,
 826 the wireless link may become broken owing to packet errors
 827 if the maximum number of MAC retransmissions has been
 828 exhausted. A broken link may trigger a route-repair or even
 829 route re-discovery for the sake of maintaining the current
 830 source-destination communications session. The route-repair
 831 is often required at the upper-node's broken link, while the
 832 route re-discovery should be initiated by the source. All these
 833 actions may consume more energy and naturally they reduce
 834 the attainable throughput. Additionally, the success of a specific
 835 hop emanating from a node relies on the success of all previous
 836 hops. If any of the previous links is broken, then no packet
 837 will be forwarded towards the destination. Naturally, any link
 838 is more likely to break if the number of MAC retransmissions
 839 is limited to N_r . The energy consumption considered is divided
 840 into two parts: the energy consumed by the data packets which
 841 succeed in reaching the destination and the energy consumed
 842 by the data packets which are dropped before reaching the
 843 destination. The time slot duration of a single transmission
 844 attempt across a given link is defined as T . Given the same data
 845 packet length and the same transmission rate at each node, T is
 846 a constant value. Here, the energy-conscious OF of a two-hop
 847 route is detailed as an example. p_s and p_f are used to denote
 848 the probability of a packet being successfully delivered to the
 849 destination successfully and being dropped before reaching the
 850 destination, respectively. Furthermore, the notation $p_s(\tau)$ repre-
 851 sents the probability that the packet is successfully delivered
 852 all the way from the source to the destination after a time
 853 duration of τ . First, the energy consumption analysis of a 2-hop
 854 route is considered in Fig. 14. The symbol \checkmark indicates that
 855 the link's transmission is successful after $1 \leq \frac{\tau}{T} \leq N_r$ MAC
 856 retransmission attempts. Hence the time duration of the link's
 857 transmission is $T \leq \tau \leq N_r T$. Fig. 14 shows that a packet's
 858 successful transmission over the link $S - R_1$ requires a time
 859 duration of τ_1 , while the successful transmission of a packet
 860 over the link $R_1 - D$ requires a time duration of τ_2 . Hence the

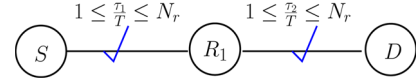


Fig. 14. A packet is successfully delivered from S to D in a 2-hop route.

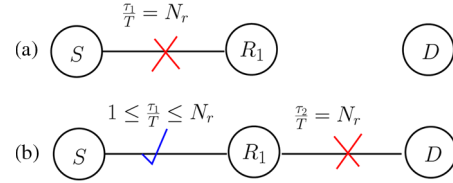


Fig. 15. A packet is dropped before reaching D in a 2-hop route.

total time duration of a packet's passage between S and D is 861
 862 $(\tau_1 + \tau_2)$, where $2T \leq \tau_1 + \tau_2 \leq 2N_r T$.

Therefore, 863

$$p_s(2T) = p_1 p_2, \quad (6)$$

$$p_s(3T) = (1 - p_1) p_1 p_2 + p_1 (1 - p_2) p_2, \quad (7)$$

$$p_s(4T) = (1 - p_1)^2 p_1 p_2 + (1 - p_1) p_1 (1 - p_2) p_2 + p_1 (1 - p_2)^2 p_2, \quad (8)$$

$$\vdots \quad \quad \quad \vdots$$

$$p_s(2N_r T) = (1 - p_1)^{N_r - 1} p_1 (1 - p_2)^{N_r - 1} p_2. \quad (9)$$

While p_s is given by 864

$$p_s = p_s(2T) + p_s(3T) + p_s(4T) + \dots + p_s(2N_r T), \quad (10)$$

$$= \sum_{i=1}^{N_r} \sum_{j=1}^{N_r} (1 - p_1)^{i-1} p_1 (1 - p_2)^{j-1} p_2. \quad (11)$$

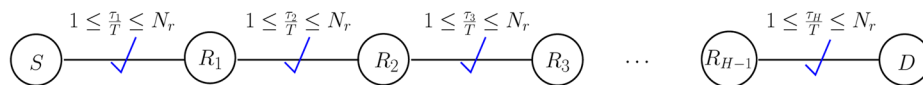
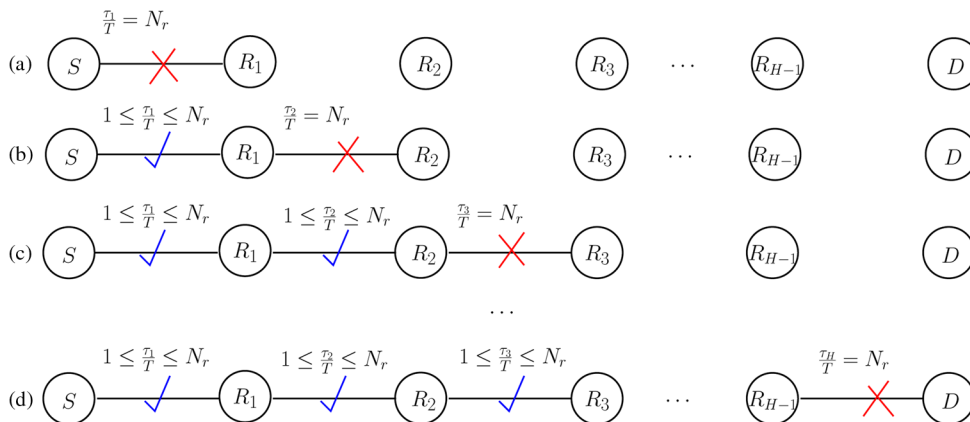
Since during a single time slot T the nodes consume an energy 865
 866 of E , the estimated total energy E_s consumed by a successfully
 867 delivered packet in a two-hop route is

$$E_s = [2p_s(2T) + 3p_s(3T) + 4p_s(4T) + \dots + 2N_r p_s(2N_r T)] E. \quad (12)$$

In a similar way, the time D_s required for a packet, which is 868
 869 successfully delivered from S to D is given by

$$D_s = [2p_s(2T) + 3p_s(3T) + 4p_s(4T) + \dots + 2N_r p_s(2N_r T)] T. \quad (13)$$

Additionally, the packets, which exhausted the maximum 870
 871 number N_r of MAC retransmissions and were finally dropped
 872 before reaching D due to poor channel conditions also consume
 873 energy. This energy should also be taken into account in the
 874 total energy consumption. The energy dissipation analysis of a
 875 packet dropped before reaching the destination in a 2-hop route
 876 is portrayed in Fig. 15. The symbol \times indicates that the link's
 877 transmission fails after $\frac{\tau}{T} = N_r$ MAC retransmission attempts.
 878 As seen in Fig. 15, a transmission failure may occur either in
 879 the $S - R_1$ link or in the $R_1 - D$ link of a 2-hop route. Hence,
 880 even when the data transmission in the $S - R_1$ link is successful
 881 within the time duration of $T \leq \tau_1 \leq N_r T$, the transmission
 882 might fail in the $R_1 - D$ link.


 Fig. 16. A packet is successfully delivered from S to D in a H -hop route.

 Fig. 17. A packet is dropped before reaching D in a H -hop route.

883 The probability of failure p_f of the two-hop route for a single
884 packet is described as follows:

$$p_f(1) = (1 - p_1)^{N_r}, \quad (14)$$

$$p_f(2) = [(1 - p_f(1))] (1 - p_2)^{N_r}, \quad (15)$$

$$p_f = p_f(1) + p_f(2), \quad (16)$$

885 where $p_f(h)$ represents the probability of the packet becoming
886 dropped during the h -th hop. Therefore, the energy E_f con-
887 sumed by a dropped packet is quantified as follows:

$$E_f = \left[N_r p_f(1) + \sum_1^{N_r} (1 - p_1)^{i-1} p_1 (1 - p_2)^{N_r} (i_1 + N_r) \right] E. \quad (17)$$

888 Similarly, the average time D_f required by a packet to propagate
889 from S up to the broken link is formulated as

$$D_f = \left[N_r p_f(1) + \sum_1^{N_r} (1 - p_1)^{i-1} p_1 (1 - p_2)^{N_r} (i_1 + N_r) \right] T. \quad (18)$$

890 The energy dissipation analysis of a packet's successful
891 delivery to the destination and that of a packet dropped before
892 reaching the destination in a H -hop route is characterized in
893 Fig. 16 and Fig. 17, respectively. Fig. 16 portrays the scenario,
894 where each link's transmission is successful after $1 \leq \frac{\tau}{T} \leq N_r$
895 MAC retransmission attempts. By contrast, Fig. 17 shows that
896 a transmission failure could take place within any of the links,
897 where all the previous links' transmissions were successful. The
898 time duration elapsed before reaching the failed link is $\tau = N_r T$,
899 while that elapsing during all the previous link's transmission is
900 $T \leq \tau \leq N_r T$.

901 Therefore, the total normalized transmit energy consumption
902 becomes:

$$\bar{E}_{total} = \frac{E_{total}}{p_s} = \frac{E_s + E_f}{p_s}. \quad (19)$$

Similarly, the end-to-end throughput R_{e2e} is given as

903

$$R_{e2e} = \frac{P_s}{D_s + D_f}. \quad (20)$$

A low-complexity routing algorithm is proposed in [73].
The process of route discovery is shown in Fig. 18, where
 S represents the source, D represents the destination, and the
other nodes are denoted by symbols A, B, C, E, F and G . $E_{S \rightarrow n, t}$
denotes the estimated NEC for the route spanning from S to
node n at time instant t , while $E_{S \rightarrow n}$ is used for storing the
minimum NEC for every node in every time-slot of duration
 T . The routing process may be divided into the following
four steps:

- **Step 1** Node S broadcasts the RREQ packet;
- **Step 2** Every node carries out the operations detailed in Fig. 19 upon receiving the RREQ packet;
- **Step 3** Node S receives the RREP packet and then updates the routing table;
- **Step 4** Then node S sends its data packet along the specific route having the lowest estimated \bar{E}_{total} .

A flow chart is provided in Fig. 19 for specifically highlight-
ing the operations, when each node receives an RREQ packet.
If S receives the RREQ packet, S will simply discard this RREQ
packet. By contrast, if another node n ($n \neq S$) receives the
RREQ packet, it calculates the NEC $E_{S \rightarrow n, t}$ and then compares
 $E_{S \rightarrow n, t}$ to $E_{S \rightarrow n}$. If $E_{S \rightarrow n, t} > E_{S \rightarrow n}$, then node n will discard the
RREQ packet. Otherwise, if node n is D , then D will respond
with a newly created RREP packet. However, if node n is not
 D , node n will broadcast the RREQ packet again.

Now the process of routing discovery is explained in details
for further clarification. During time slot 1, node S broadcasts
the RREQ packet, nodes A, B and C receive the RREQ packet.
According to the actions seen in Fig. 19, nodes A, B and C first
calculate $E_{S \rightarrow A, 1}$, $E_{S \rightarrow B, 1}$ and $E_{S \rightarrow C, 1}$, respectively. Then they
compare these newly calculated values with the aid of $E_{S \rightarrow A}$,

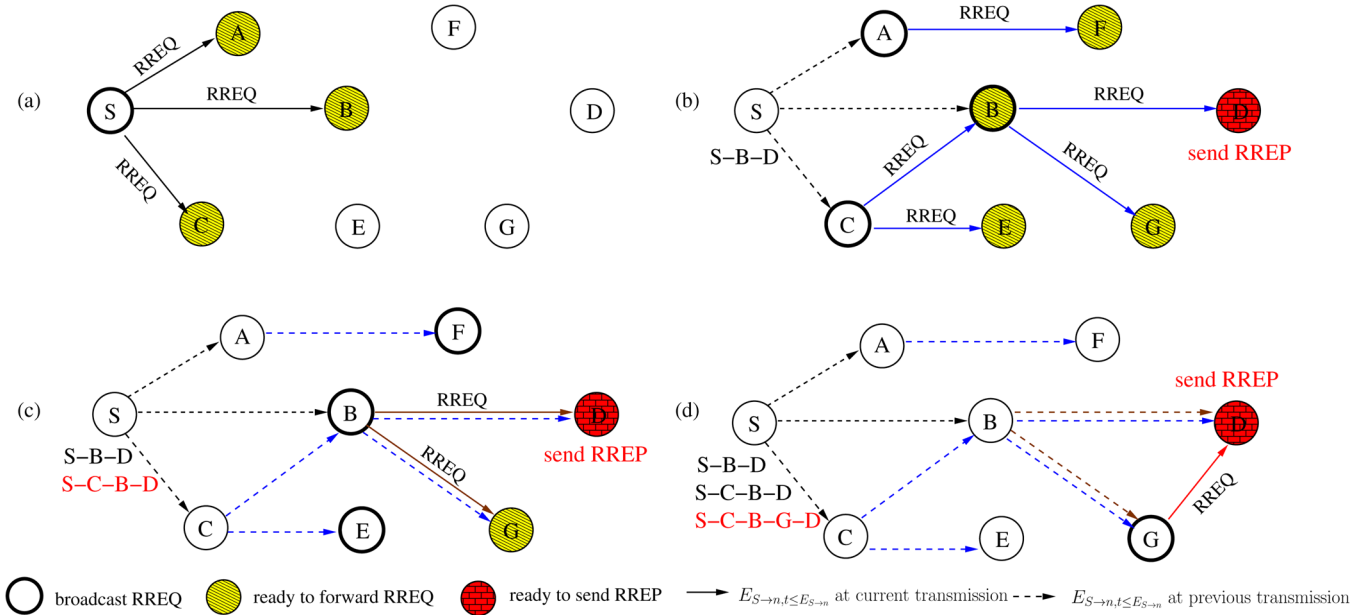


Fig. 18. The process of route discovery in the low-complexity routing algorithm. (a) Actions during time slot 1. (b) Actions during time slot 2 and node S updates its routing table with the route $S-B-D$. (c) Actions during time slot 3 and node S updates its routing table with the route $S-C-B-D$ since the estimated NEC of route $S-C-B-D$ is lower than that of route $S-B-D$. (d) Actions during time slot 4 and node S updates its routing table with the route $S-C-B-G-D$, since the estimated NEC of route $S-C-B-G-D$ is lower than that of route $S-C-B-D$.

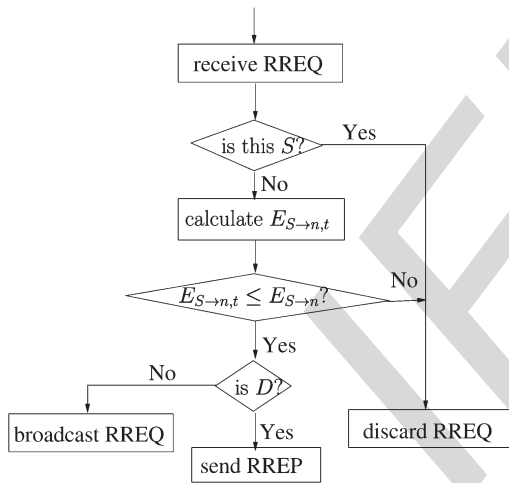


Fig. 19. Operations when each node receives an RREQ packet.

935 $E_{S \rightarrow B}$ and $E_{S \rightarrow A}$, respectively. If $E_{S \rightarrow A, 1} \leq E_{S \rightarrow A}$, then A will
 936 update $E_{S \rightarrow A}$ and will forward the RREQ packet during the
 937 next time slot, otherwise it will discard it. The same actions
 938 are carried out at node B and node C as well.

939 Then during time slot 2, node A , B and C forward the RREQ
 940 packet. According to the actions seen in Fig. 19, nodes B , E , F
 941 and G will forward the RREQ packet in the next time slot, since
 942 $E_{S \rightarrow B, 2} \leq E_{S \rightarrow B}$, $E_{S \rightarrow E, 2} \leq E_{S \rightarrow E}$, $E_{S \rightarrow F, 2} \leq E_{S \rightarrow F}$ and $E_{S \rightarrow G, 2} \leq$
 943 $E_{S \rightarrow G}$. Node D is ready to send back a newly created RREP
 944 packet in the next time slot, since node D is the destination and
 945 $E_{S \rightarrow D, 2} \leq E_{S \rightarrow D}$. Afterwards, S will receive the RREP packet
 946 and updates its routing table with the route $S-B-D$ obtained.
 947 S will send the data packet along the route $S-B-D$.

948 During time slot 3, nodes B , E , F and G forward the RREQ
 949 packet. According to the actions portrayed in Fig. 19, node G
 950 will forward the RREQ packet during the next time slot, since

$E_{S \rightarrow G, 3} \leq E_{S \rightarrow G}$. Node D will then send back a newly created
 951 RREP packet during the next time slot, since node D is the
 952 destination and $E_{S \rightarrow D, 3} \leq E_{S \rightarrow D}$. Afterwards, S will receive the
 953 second RREP packet and updates its routing table again with
 954 the route $S-C-B-D$ obtained, since the estimated NEC of
 955 route $S-C-B-D$ is lower than that of route $S-B-D$. Finally,
 956 node S will send the next data packet along the updated route
 957 $S-C-B-D$. 958

959 During time slot 4, node G forwards the RREQ packet,
 960 then nodes B , E and D receive it. According to the actions
 961 of Fig. 19, then D is ready to send back a newly created
 962 RREP packet during the next time slot, since node D is the
 963 destination and $E_{S \rightarrow D, 4} \leq E_{S \rightarrow D}$. Afterwards, S will receive the
 964 third RREP packet and updates its routing table again with the
 965 route $S-C-B-G-D$ obtained, since the estimated NEC of
 966 route $S-C-B-G-D$ is lower than that of route $S-C-B-D$.
 967 Finally, node S will send the next data packet along the updated
 968 route $S-C-B-G-D$. 968

969 The analytically estimated NEC associated both with an
 970 infinite number as well as a finite number of N_r MAC re-
 971 transmissions was calculated from (5) and (19), respectively.
 972 A simple linear network topology was studied, where all N
 973 nodes are equi-spaced along a line. The frame length of the
 974 data packets, which are generated from the application layer,
 975 is $L_{app} = 1024$ Bytes. The 802.11g standard is employed in the
 976 DL layer. The transmit power is set to $P_{t_i} = 0.016$ mW and the
 977 IrCC-URC-QPSK defined in Section II is employed in the PHY
 978 layer. The channel model is the AWGN channel subjected to
 979 inverse second-power free-space path loss. The other system
 980 parameters employed for the simulations of Figs. 20 and 21 are
 981 listed in Table IV. 981

982 The NEC and the end-to-end throughput evaluated both from
 983 (19) and (20) as well as by simulations are portrayed in Figs. 20
 984 and 21. 984

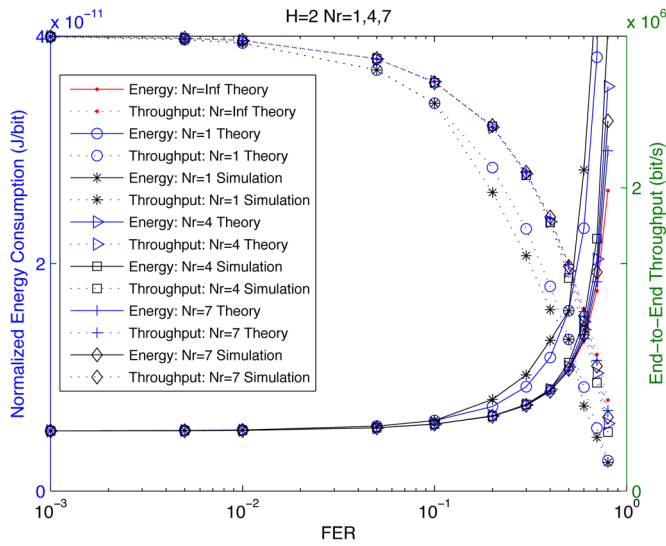


Fig. 20. The NEC and the end-to-end throughput versus FER ($10^{-3} \leq FER \leq 1$) and the maximum number of MAC retransmissions N_r ($N_r = 1, 4, 7$) with the number of hops $H = 2$ for comparing the theoretically analyzed values and simulation based values.

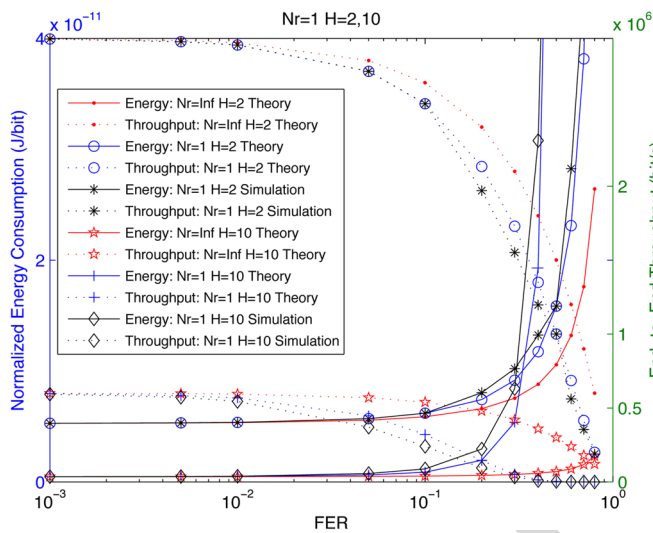


Fig. 21. The NEC and the end-to-end throughput versus FER ($10^{-3} \leq FER \leq 1$) and the number of hops H ($H = 2, 10$) with the maximum number of MAC retransmissions $N_r = 1$ for comparing the theoretically analyzed values and simulation based values.

985 Fig. 20 displays three groups of performance curves recorded
 986 at $N_r = 1, 4$ and 7 , respectively, for both the NEC and for the
 987 end-to-end throughput, where N_r is the maximum number of
 988 MAC retransmissions. The performance figures recorded for
 989 the infinite number of MAC retransmissions scenario, namely
 990 for $N_r = \infty$ are identical for the theory evaluated from (5)
 991 and for the simulations. All the analytical and the simulation
 992 based values recorded for the NEC increase, when the FER
 993 increases. By contrast, the curves representing the end-to-end
 994 throughput decrease, when the FER increases. The reason for
 995 this observation is that a high FER in a link indicates a high
 996 breakage probability not only for the specific link and but
 997 also for the entire route, when retransmissions are required.
 998 However, if N_r is sufficiently high, then the success probability
 999 of a packet across a link or even the entire route becomes higher.

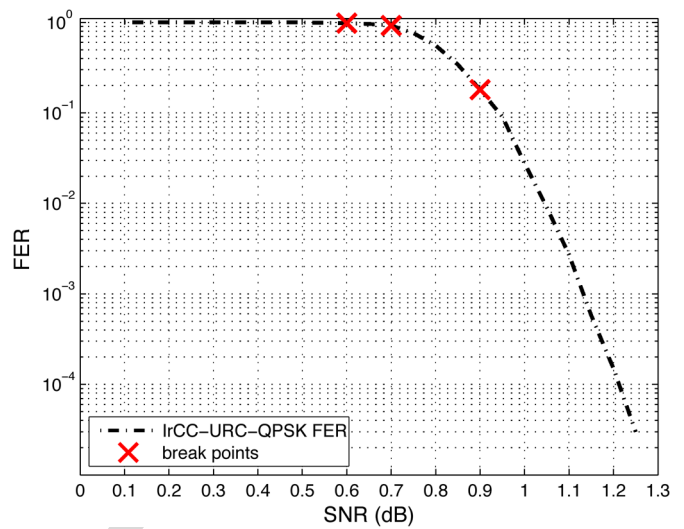


Fig. 22. FER versus SNR for the IrCC-URC-QPSK scheme of Section II-A for the average code rate of $R_c = 0.5$ in an AWGN channel.

This trend is presented in Fig. 20, where the curve recorded for 1000
 $N_r = 7$ is seen to be close to that of $N_r = \infty$. The discrepancy 1001
 between the theoretical value and the simulation-based value 1002
 becomes higher when N_r is reduced and simultaneously the 1003
 FER is increased. Fig. 20 also shows that the theoretical energy 1004
 consumption of (19) based on the energy-conscious OF is closer 1005
 to the simulation based values than those based on the OF rely- 1006
 ing on an infinite number of MAC retransmissions. Naturally, 1007
 the advantage of the OF is more substantial for $N_r = 1$. 1008

Fig. 21 also displays two groups of performance curves, 1009
 one group for the NEC and the other group for the end-to- 1010
 end throughput, which are associated with $H = 2$ and 1011
 respectively. When H is increased, the normalized energy 1012
 consumption is reduced and the end-to-end throughput is de- 1013
 creased, because the distance between a pair of adjacent nodes 1014
 is reduced and therefore the transmit power required at each 1015
 node for successfully delivering a packet is reduced. Similarly, 1016
 as discussed in [73], the theoretical values estimated based 1017
 on the proposed OF are closer to the simulated values than 1018
 to those estimated on the basis of an infinite number of MAC 1019
 retransmissions, especially when both H and the FER are high. 1020

Hence, as elaborated on in [73], the conclusion is reached 1021
from Figs. 20 and 21 that the proposed energy-conscious OF 1022
is more accurate than the one assuming an infinite number of 1023
MAC retransmissions at high FERs, or for a high number of 1024
hops at a low maximum number of MAC retransmissions. 1025

B. Traditional Routing With Adjustable Transmit Power 1026

The FER curve was generated for the AWGN channel model 1027
 with the aid of simulation [74]. According to the approach 1028
 of [102], this will allow us to determine the average FER 1029
 for arbitrary fading channels upon weighting the AWGN-FER 1030
 by the Probability Distribution Function (PDF) of the fading 1031
 channel and averaging it over the legitimate dynamic range. 1032
 More specifically, the channel model considered is the uncor- 1033
 related, non-dispersive Rayleigh fading channel. The average 1034
 FER expression $FER_{Rayleigh}$ is determined for the Rayleigh 1035
 fading channel considered by integrating the specific FER_{AWGN} 1036

1037 value of the AWGN channel experienced at a given SNR after
1038 weighting it by the probability of that specific SNR, which is
1039 given by:

$$FER_{Rayleigh} = \int_0^{\infty} e^{-\gamma} FER_{AWGN}(\gamma) d\gamma, \quad (21)$$

1040 where γ is the channel SNR, $e^{-\gamma}$ represents the Rayleigh
1041 channel while the $FER_{AWGN}(\gamma)$ versus the SNR curve is ap-
1042 proximated by the following four-segment FER vs. SNR model
1043 representing the AWGN channel:

$$FER_{AWGN}(\gamma) \approx \begin{cases} 1, & \text{if } 0 \leq \gamma < \eta_1, \\ 10a_1 \log(\gamma) + a_2, & \text{if } \eta_1 \leq \gamma < \eta_2, \\ 10a_3 \log(\gamma) + a_4, & \text{if } \eta_2 \leq \gamma < \eta_3, \\ a_5 e^{-10a_6 \log(\gamma)}, & \text{if } \gamma \geq \eta_3, \end{cases} \quad (22)$$

1044 with η_1 , η_2 and η_3 being the break-points of the four-segment
1045 FER versus SNR approximation $FER_{AWGN}(\gamma)$. Eqs. (21) and
1046 (22) are suitable for approximating different FER curves by ap-
1047 propriately setting the corresponding parameter values invoked.
1048 Eq. (21) may be readily extended to arbitrary channel models.
1049 Given $FER_{Rayleigh}$, the successful reception probability of a
1050 link can be calculated as $[1 - (FER_{Rayleigh})^{N_r}]$ if the maximum
1051 number of MAC retransmissions (including the first MAC
1052 retransmission attempt) is N_r . Specifically, for the IrCC-URC-
1053 QPSK scheme of Section II-A[72] employed, $a_1 = -0.5889$,
1054 $a_2 = 1.3341$, $a_3 = -3.705$, $a_4 = 3.5169$, $a_5 = 4.4669 \times 10^6$
1055 and $a_6 = 18.9118$. Additionally, the values of the break-points
1056 η_1 , η_2 and η_3 are determined for the SNR points of 0.6 dB,
1057 0.7 dB, and 0.9 dB, which are based on the curves seen
1058 in Fig. 22. Fig. 22 shows the FER performance versus the
1059 SNR, when the IrCC-URC-QPSK scheme of Section II-A is
1060 employed, relying on the average code rate of $R_c = 0.5$ in an
1061 AWGN channel. As seen from Fig. 22, the corresponding hori-
1062 zontal points of the symbol 'x' are 0.6 dB, 0.7 dB and 0.9 dB.
1063 Therefore, by employing a practical coding scheme, such as
1064 the IrCC-URC-QPSK scheme of Section II with the aid of (19),
1065 it arrives at

$$\bar{E}_{total} = \frac{P_{t1}}{p_1} T, \quad (23)$$

1066 which shows that \bar{E}_{total} is independent of the number of retrans-
1067 missions in a single-hop route. In this context, the NEC is the
1068 same as that of a transmitter operating without a transmission
1069 limit, i.e. when $N_r = \text{inf}$. As indicated in [74], optimizing
1070 the transmit power of the source was formulated as a convex
1071 optimization problem.

1072 Once the closed-form expression of (23) for the NEC \bar{E}_{total}
1073 of a single hop, the optimized transmit power P_{t1} may be
1074 calculated by setting the derivative of (23) with respect to P_{t1}
1075 to zero, which yields

$$\frac{1}{p_1} + \frac{P_{t1}}{p_1^2} \frac{d(1-p_1)}{dP_{t1}} = 0$$

$$\frac{p_1}{-P_{t1}} = \frac{d(1-p_1)}{dP_{t1}}, \quad (24)$$

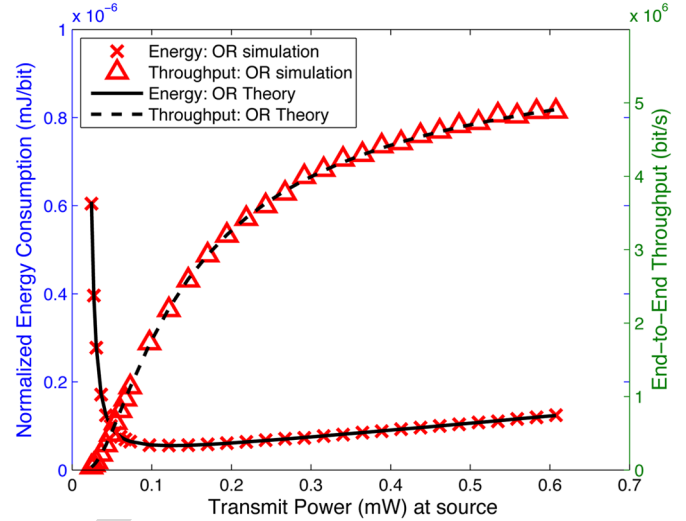


Fig. 23. The NEC \bar{E}_{total} and the end-to-end throughput R_{e2e} versus the transmit power P_{tS} .

1076 where $1 - p_1 = FER_1$. Finally, the analytical expression of the
1077 optimized transmit power P_{t1} can be found. The existence of the
1078 optimized transmit power at the source of a single-hop route
1079 is shown in Fig. 23. Moreover, the end-to-end throughput R_{e2e}
1080 of the TR relying on an adjustable transmit power also obeys
1081 the same expression of (20). Therefore, the NEC \bar{E}_{total} and the
1082 end-to-end throughput R_{e2e} are compared both in terms of sim-
1083 ulation and theoretical results in Fig. 23, where the maximum
1084 number of MAC retransmissions is $N_r = 7$. The frame length
1085 of the data packets, which are generated from the application
1086 layer, is 1024 Bytes. The 802.11g standard is employed in the
1087 DL layer. The distance between S and D is 1000 m. The other
1088 simulation configurations are listed in Table IV.

1089 Fig. 23 shows that the NEC initially decreases and then
1090 increases slowly beyond the transmit power of 0.12 mW, where
1091 0.12 mW is the optimal transmit power obtained by using
1092 (24). The end-to-end throughput increases upon increasing the
1093 transmit power at S . Observe that the simulation results closely
1094 match the theoretical curve.

1095 The idealized multi-hop linear network researched in
1096 Section III-A may be extended to a more realistic random net-
1097 work relying on Dijkstra's routing algorithm [124] and invoking
1098 the NEC \bar{E}_{total} for route selection. **Hence, a heuristic routing**
1099 **algorithm, namely the TR having an adjustable transmit**
1100 **power is invoked in [74] (referred to as Algorithm 1 in [74]),**
1101 **which may be adapted to the random network scenario**
1102 **considered for guaranteeing a high energy efficiency. For**
1103 **ease of interpretation, in this paper, the TR having an**
1104 **adjustable transmit power is exemplified with the aid of**
1105 **its step-by-step execution using the NEC metric \bar{E}_{total} , as**
1106 **shown in Fig. 24. It is assumed that \mathcal{V} is the vertex set, v is**
1107 **a node in the set \mathcal{V} and \bar{E}_{Sv} denotes the NEC. Moreover, \mathcal{S}**
1108 **represents the set of selected nodes, while $P_t^{opt}(u, v)$ denotes**
1109 **the optimal transmit power of node u assigned for transmission**
1110 **to node v .**

1111 As an example, the positions of S , D , R_1 and R_2 are as-
1112 sumed to be (100, 100), (900, 100), (500, 500), and (300,
1113 400), respectively. The IrCC-URC-QPSK is employed in the

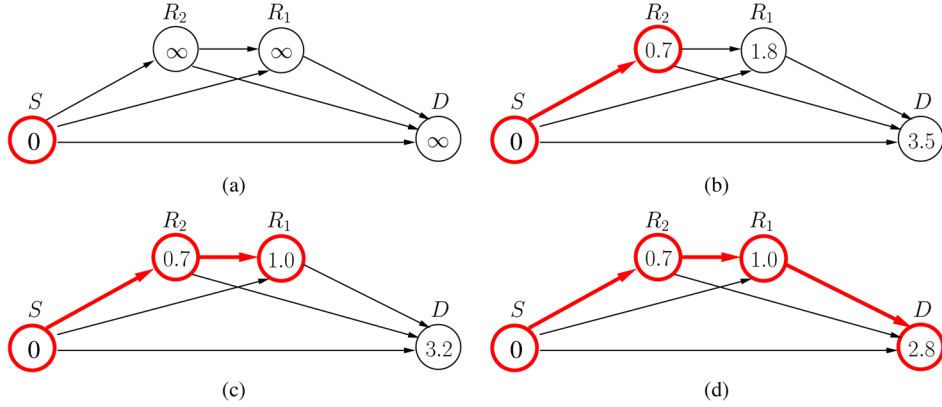


Fig. 24. Execution of the TR associated with an adjustable transmit power in a specific instance, where the positions of S , D , R_1 and R_2 are assumed to be (100, 100), (900, 100), (500, 500), and (300, 400), respectively. The value within a node v is its energy cost $\bar{E}_{total} (\times 10^{-8}$ mJ/bit) for transmission from S to node v . After each iteration one node is incorporated into the set S . The nodes in boldface denote the nodes in S after each iteration and the arrows in boldface represent the shortest route from S to the nodes in boldface after each iteration. Due to the adjustable transmit power of node u , the probability $p_f(u, v)$ of a packet, which is dropped at any link $u - v$ after $N_r = 7$ retransmissions, has nearly the same value of $p_f(u, v) = 0.041$, hence this value next to the arrows is not plotted for simplicity. (a) The situation just after the initialization, where $S = \{S\}$. (b) The first iteration of the algorithm, where $S = \{S\}$ before the iteration, while after the iteration R_2 is incorporated into the set S with the optimum power of $P_t^{opt}(S, R_2) = 0.16$ mW, yielding $S = \{S, R_2\}$. (c) The second iteration of the algorithm, where $S = \{S, R_2\}$ before the iteration, while after the iteration R_1 is incorporated into the set S with the optimum power of $P_t^{opt}(R_2, R_1) = 0.06$ mW, yielding $S = \{S, R_2, R_1\}$. (d) The final iteration of the algorithm, where $S = \{S, R_2, R_1\}$ before the iteration, while after the iteration D is incorporated into the set S with the optimum power of $P_t^{opt}(R_1, D) = 0.39$ mW, yielding $S = \{S, R_2, R_1, D\}$. The algorithm terminates.

1114 PHY layer. The channel imposes both free-space path-loss and
 1115 uncorrelated Rayleigh fading, plus the ubiquitous AWGN. The
 1116 other relevant parameters are listed in Table IV. Each node is
 1117 assumed to be aware of the other nodes' position, hence also
 1118 of their distance. In a compact form, $\mathcal{V} = \{S, R_1, R_2, D\}$ and
 1119 $S = \{S\}$, as shown in Fig. 24(a). In Fig. 24(b), S calculates its
 1120 transmit power optimized for minimizing the NEC from (24),
 1121 which is $\bar{E}_{SR_1} = 1.8 \times 10^{-8}$ mJ/bit, $\bar{E}_{SR_2} = 0.7 \times 10^{-8}$ mJ/bit,
 1122 $\bar{E}_{SD} = 3.5 \times 10^{-8}$ mJ/bit for transmission from S to R_1 , R_2 and
 1123 D , respectively. Since $\bar{E}_{SR_2} = 0.7 \times 10^{-8}$ mJ/bit is the lowest
 1124 in the set of the three energies, S is updated to $\{S, R_2\}$. Then
 1125 in Fig. 24(c), R_2 calculates its transmit power optimized for
 1126 minimizing the NEC from (24) for the transmission, which
 1127 is spanning from S to node R_1 and D via R_2 , respectively.
 1128 Since the updated NEC $\bar{E}_{SR_1} = 1.0 \times 10^{-8}$ mJ/bit is lower than
 1129 $\bar{E}_{SD} = 3.2 \times 10^{-8}$ mJ/bit, S is updated to $\{S, R_2, R_1\}$. Finally, in
 1130 Fig. 24(d), R_1 adjusts its own transmit power to the optimal one,
 1131 which minimizes the NEC $\bar{E}_{SD} = 2.8 \times 10^{-8}$ mJ/bit from S to
 1132 D via R_2 and R_1 . At this stage, D is incorporated into S . Since
 1133 $S = \{S, R_2, R_1, D\}$, the TR with adjustable transmit power may
 1134 be deemed to have converged and the route $S - R_2 - R_1 - D$ is
 1135 deemed to be the optimal route for transmission from S to D .

1136 The computational complexity has three main contributing
 1137 factors: a) the calculation of a single NEC in a specific case;
 1138 b) the number of NEC calculations; c) and finally, finding the
 1139 minimum NEC in each round. They denote the complexity of
 1140 E_s , E_f and p_s , where $p_s = \prod_1^H B(p_i)$, by $C(E_s)$, $C(E_f)$ and
 1141 $C(p_s)$. The complexity of evaluating D_s and D_f is the same
 1142 as that of E_s and E_f , apart from a multiplicative constant.
 1143 The number of NEC calculations is given by the number of
 1144 node pairs, which is $\mathcal{V}(\mathcal{V} - 1)/2$. The minimum NEC can be
 1145 found based on the Fibonacci heap approach of [125], which
 1146 has a complexity on the order of $O(\log \mathcal{V})$. Therefore, the
 1147 complexity imposed by the TR with adjustable transmit power
 1148 is $O[\mathcal{V}^2[C(E_s) + C(E_f) + C(p_s)] + \mathcal{V} \log \mathcal{V}]$.

The performance of TR relying on an adjustable transmit
 power will be characterized in Section III-C in comparison to
 that of the OR of Section III-C.

C. Opportunistic Routing With Adjustable Transmit Power

The TR transmits the packet along the specific pre-selected
 route having the lowest estimated NEC. This pre-selected route
 is determined after the estimation and comparison of the NEC
 of each potential candidate route. The information invoked
 for routing decisions is gleaned during the process of route
 discovery, but this information may become stale owing to
 node-mobility. Instead, OR considers the potential chances of
 success for each candidate RN, bearing in mind their time-
 variant channel conditions. Regardless of which particular RN
 receives the packet from the source successfully, if this RN has
 the highest priority in the forwarder RN list, it will forward the
 packet to the next RN. Naturally, the challenge in the design
 of the OR procedure is the beneficial selection of the forwarder
 RN set, the specific priority order of the potential forwarders
 and the avoidance of duplicate transmissions [110]. All the
 nodes in a node's neighbor list are assumed to belong to this
 node's forwarder R-list. The metric used for determining the
 priority order is the normalized energy required by this par-
 ticular RN for reaching D . Acknowledgement (ACK) packets
 are employed for avoiding the duplicate transmissions. The
 particular RN in the forwarder R-set, which has the highest
 priority owing to requiring the lowest energy will send the ACK
 first. The other RNs, which overhear the ACK will withdraw
 from the competition [126], [127].

A two-hop network is shown in Fig. 25, which has a sin-
 gle source S , a single destination D and M RNs $R_1, R_2, \dots,$
 R_{M-1}, R_M . S and D are capable of communicating with all
 the RNs, as well as with each other. By contrast, the M RNs
 are unable to communicate with each other. The idealized

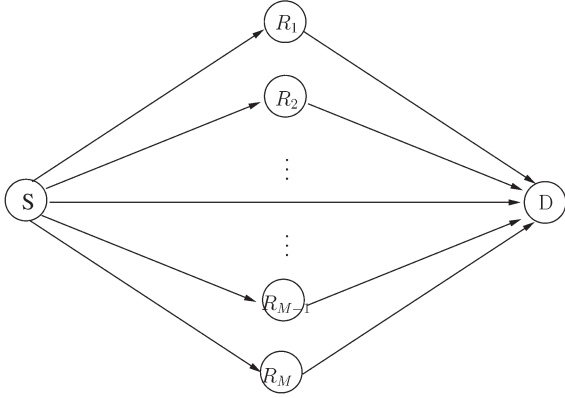


Fig. 25. A two-hop network assisted by a number of RNs.

1182 simplifying assumption is stipulated furthermore that each node
 1183 knows the position of all other nodes. For each RN $R_m, m =$
 1184 $1 \dots M$, the total average energy consumption $E_{R_m D}$ required
 1185 for transmission from R_m to D is given by $E_{R_m D} = E_{R_m D}^s + E_{R_m D}^f$
 1186 where $E_{R_m D}^s$ represents the energy dissipated by a packet, which
 1187 is successfully delivered from R_m to D while $E_{R_m D}^f$ represents
 1188 the energy dissipated by a packet, which is dropped before
 1189 reaching D from R_m after N_r MAC retransmissions. Let E_S
 1190 denote the energy dissipated while sending a packet from
 1191 the source S to any of the RNs R_m , which is $E_S = P_S T$. It
 1192 is assumed that $E_{R_1 D} < E_{R_2 D} < \dots < E_{R_M D}$. Furthermore, for
 1193 convenience, the destination node D is represented as R_0 and
 1194 $\prod_{m=0}^M (1 - p_{SR_m}) = \zeta$, where p_{SR_m} denotes the probability of a
 1195 packet, which is successfully delivered from S to R_m .
 1196 If S successfully sends a packet to the m -th RN, $m =$
 1197 $0, 1, \dots, M$, with the aid of n_r transmissions, the probability of
 1198 this event is

$$p_0(n_r) = \zeta^{n_r-1} p_{SR_0}, \text{ if } m = 0 \quad (25)$$

$$p_m(n_r) = \zeta^{n_r-1} \prod_{i=0}^{m-1} (1 - p_{SR_i}) p_{SR_m}, \text{ if } 1 \leq m \leq M. \quad (26)$$

1199 Correspondingly, the energy dissipated becomes

$$E_0(n_r) = n_r E_S, \text{ if } m = 0 \quad (27)$$

$$E_m(n_r) = n_r E_S + E_{R_m D}, \text{ if } 1 \leq m \leq M. \quad (28)$$

1200 Let $D_{R_m D}$ denote the average delay of a packet travers-
 1201 ing from $R_m, m = 1, \dots, M$, to D , including the delay $D_{R_m D}^s$
 1202 encountered by a packet that is successfully delivered to D
 1203 and the delay $D_{R_m D}^f$ experienced when a packet is dropped
 1204 before reaching D . Then $D_{R_m D} = D_{R_m D}^s + D_{R_m D}^f$, where $D_{R_m D}^s$
 1205 represents D_s and $D_{R_m D}^f$ corresponds to D_f , provided that the
 1206 number of hops is 1. Consequently,

$$D_0(n_r) = n_r D_S, \text{ if } m = 0 \quad (29)$$

$$\begin{aligned} D_m(n_r) &= n_r D_S + D_{R_m D} \\ &= n_r D_S + \left(D_{R_m D}^s + D_{R_m D}^f \right), \text{ if } 1 \leq m \leq M, \end{aligned} \quad (30)$$

1207 where D_S is T , which denotes the duration of a Time Slot (TS).

Consequently, when taking into account all the possible 1208
 events, the total energy consumption is 1209

$$\begin{aligned} E_{total} &= \sum_{n_r=1}^{N_r} p_0(n_r) E_0(n_r) \\ &\quad + \sum_{n_r=1}^{N_r} \sum_{m=1}^M p_m(n_r) E_m(n_r) + \zeta^{N_r} (N_r E_S), \end{aligned} \quad (31)$$

while the total delay becomes: 1210

$$\begin{aligned} D_{total} &= \sum_{n_r=1}^{N_r} p_0(n_r) D_0(n_r) \\ &\quad + \sum_{n_r=1}^{N_r} \sum_{m=1}^M p_m(n_r) D_m(n_r) + \zeta^{N_r} (N_r D_S), \end{aligned} \quad (32)$$

Meanwhile, the packet transmitted from S may be dropped 1211
 in the $S - D$, $S - R_m$ or $R_m - D$ link, where $m = 1, \dots, M$ and 1212
 again, the destination can be replaced by R_0 . Then the end-to- 1213
 end outage probability p_f may be formulated as 1214

$$p_f = p_{f,S-R_0} + p_{f,S-R_m} + p_{f,R_m-D}, \quad m = 1, \dots, M. \quad (33)$$

Furthermore, the NEC \bar{E}_{total} may be formulated as 1215

$$\bar{E}_{total} = \frac{E_{total}}{1 - p_f}, \quad (34)$$

while the end-to-end throughput R_{e2e} is given by 1216

$$R_{e2e} = \frac{1 - p_f}{D_{total}}. \quad (35)$$

Although the network topology in Fig. 25 has only two hops, 1217
 this algorithm may be extended to a large network, where 1218
 the OR principle is employed for each hop. Meanwhile, the 1219
 optimal transmit power of each node is found for the sake 1220
 of minimizing the NEC required for the successful passage 1221
 of a packet from that node to the destination. Therefore, **the** 1222
heuristic routing algorithm, namely the OR associated with 1223
an adjustable transmit power is conceived in [74] (referred 1224
to as Algorithm 2 in [74]), for calculating the minimum NEC 1225
by carrying out optimum distance-dependent power alloca- 1226
tion at each node, hop-by-hop. For ease of interpretation, in 1227
this paper, the OR having an adjustable transmit power is 1228
exemplified with the aid of its step-by-step execution using 1229
the NEC metric \bar{E}_{total} , as shown in Fig. 26. Here, for any 1230
 node v in a given vertex set \mathcal{V} , \bar{E}_{vD} denotes the NEC \bar{E}_{total} 1231
 necessitated for transmission from node v to the destination 1232
 D , where the potential set of receiver nodes is denoted by 1233
 \mathcal{R} . Furthermore, $P_i^{opt}(v)$ is the optimal transmit power, which 1234
 minimizes the NEC required for transmission from node v to 1235
 the destination D . 1236

Again, **as a specific example**, both the topology and the 1237
 relevant parameters **used in** Fig. 26 are similar to those used 1238
in Fig. 24. It was also assumed that each node is aware of 1239
 the other nodes' position, hence also of their distance. In a 1240
 compact form, $\mathcal{V} = \{S, R_1, R_2, D\}$ and $\mathcal{R} = \{D\}$, as shown in 1241

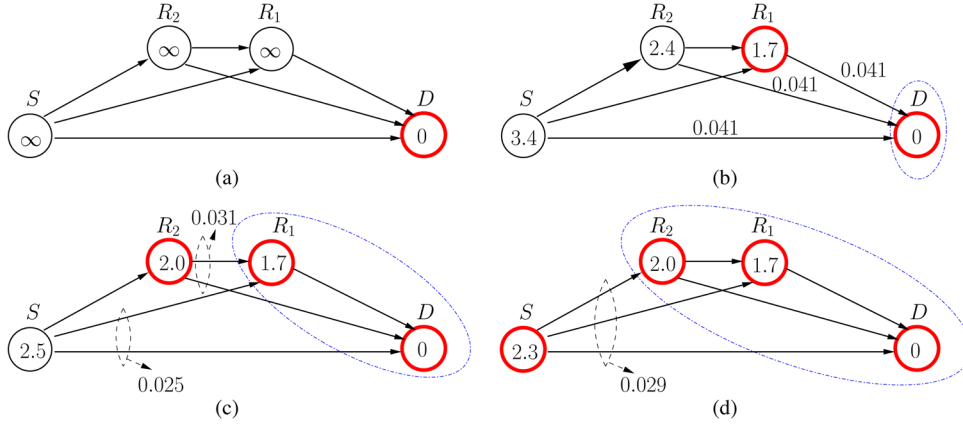


Fig. 26. Execution of the OR associated with an adjustable transmit power in a specific instance, where the positions of S , D , R_1 and R_2 are assumed to be (100, 100), (900, 100), (500, 500) and (300, 400), respectively. The value within a node u is its cost \bar{E}_{total} ($\times 10^{-8}$ mJ/bit) incurred by its transmission from node u to D and the dash-dot ellipse represents the receiver set \mathcal{R} before each iteration. After each iteration one node is incorporated into the set \mathcal{R} . The nodes in boldface denote the nodes in \mathcal{R} after each iteration. The values next to the arrows or the dashed ellipses represent the probability $p_f(u, \mathcal{R})$ of a packet being transmitted from S in conjunction with the event that none of the nodes in the receiver set \mathcal{R} receives it after $N_r = 7$ retransmissions. (a) The situation just after the initialization, where $\mathcal{R} = \{D\}$. (b) The first iteration of the algorithm, where $\mathcal{R} = \{D\}$ before the iteration, while after the iteration R_1 is incorporated into the set \mathcal{R} with the optimum power of $P_t^{opt}(R_1) = 0.39$ mW, yielding $\mathcal{R} = \{R_1, D\}$. (c) The second iteration of the algorithm, where $\mathcal{R} = \{R_1, D\}$ before the iteration while after the iteration R_2 is incorporated into the set \mathcal{R} with the optimum power of $P_t^{opt}(R_2) = 0.36$ mW, yielding $\mathcal{R} = \{R_2, R_1, D\}$. (d) The final iteration of algorithm, where $\mathcal{R} = \{R_2, R_1, D\}$ before the iteration, while after the iteration S is incorporated into the set \mathcal{R} with the optimum power of $P_t^{opt}(S) = 0.41$ mW, yielding $\mathcal{R} = \{S, R_2, R_1, D\}$. The algorithm terminates.

1242 Fig. 26(a). In Fig. 26(b), S , R_1 and R_2 calculate their transmit
 1243 power optimized for minimizing the NEC from (34), yielding
 1244 $\bar{E}_{SD} = 3.4 \times 10^{-8}$ mJ/bit, $\bar{E}_{R_1D} = 1.7 \times 10^{-8}$ mJ/bit, $\bar{E}_{R_2D} =$
 1245 2.4×10^{-8} mJ/bit for transmission to D . Since $\bar{E}_{R_1D} = 1.7 \times$
 1246 10^{-8} mJ/bit is the lowest in the set of the three energies, \mathcal{R} is
 1247 updated to $\{R_1, D\}$. Then in Fig. 26(c), S and R_2 adjust their
 1248 own transmit power and update their NEC for transmission
 1249 to node D by considering $\{R_1, D\}$ as their forwarder relay
 1250 set. Since $\bar{E}_{R_2D} = 2.0 \times 10^{-8}$ mJ/bit is lower than $\bar{E}_{SD} =$
 1251 2.5×10^{-8} mJ/bit, \mathcal{R} is updated to $\{R_2, R_1, D\}$. Finally, in
 1252 Fig. 26(d), S adjusts its own transmit power to the optimal one,
 1253 which minimizes $\bar{E}_{SD} = 2.3 \times 10^{-8}$ mJ/bit, where $\{R_2, R_1, D\}$
 1254 is the resultant forwarder relay set. At this stage, the OR with
 1255 adjustable transmit power may be deemed to have converged,
 1256 since S is incorporated into \mathcal{R} and $\mathcal{R} = \{S, R_2, R_1, D\}$. In this
 1257 algorithm, every node has to find its own forwarder R-set
 1258 by itself upon exploiting the knowledge of the other nodes'
 1259 positions. If more than one node in a node's forwarder R-
 1260 list receives the packet from that node successfully, then that
 1261 particular one, which requires the lowest NEC for transmission
 1262 to the destination has the highest priority for forwarding this
 1263 packet. The nodes of the forwarder R-set communicate with
 1264 each other similarly to the technique of [126] and again, the
 1265 NEC required for successful transmission to D is invoked for
 1266 deciding the priority order of the forwarders.

1267 The complexity of finding the transmit power and the for-
 1268 warder set also depends on three contributing factors, just like
 1269 for the TR scenario. They denote the complexity of E_{total} in
 1270 (34) and of p_f in (33) by $C(E_{total})$ and $C(p_f)$, respectively.
 1271 The OR with adjustable transmit power has to invoke \mathcal{V} times
 1272 for the sake of adding a further node into \mathcal{R} in each round. The
 1273 optimal transmit power of any node in $(\mathcal{V} - \mathcal{R})$ is calculated
 1274 in a specific round and the complexity of this calculation is
 1275 given by $C(E_{total}) + C(p_f)$. Again, the complexity of finding
 1276 the optimal transmit power can be calculated by Fibonacci

heap [125] which has a complexity on the order of $O(\log \mathcal{V})$.
 Therefore, the complexity of the OR with adjustable transmit
 power is $O[\mathcal{V}^2[C(E_{total}) + C(p_f)] + \mathcal{V} \log \mathcal{V}]$.

Now the performance of the networks associated with a total
 of $N = 4$ and 15 nodes are analyzed. The positions of S and
 D are (100, 100) and (900, 100), respectively, while the other
 nodes are uniformly located within a circle centered at (400,
 100) with a radius of 400 m. The NEC \bar{E}_{total} and the end-
 to-end throughput R_{e2e} are shown in Fig. 27 and Fig. 28 as
 a function of the maximum number of MAC retransmissions
 N_r . The theoretical NEC bound of both TR and OR was also
 investigated when $N = 4$, which was found by the exhaustive
 search of all the routes spanning from S to D , while for $N = 15$
 no theoretical bounds were given, since the exhaustive search
 has an excessive computation complexity.

Fig. 27 shows that the performance of the energy-
 consumption OF based algorithm is close to the theoretical
 bound when $N = 4$, especially in the case of a high N_r . Both
 Figs. 27 and 28 show that the energy-efficient OR outperforms
 both the Adjustable Energy-Efficient Opportunistic Routing
 (A-EEOR) algorithm defined in [91] and the energy-efficient
 TR. Here, the A-EEOR algorithm selects and prioritizes the
 forwarding set during the initialization stage according to the
 total energy cost of forwarding a packet to the destination node,
 which is estimated under the assumption of allowing a poten-
 tially infinite number of MAC retransmissions N_r . However,
 N_r is finite in practical scenarios. Hence, more specifically,
 compared to the A-EEOR algorithm the OR algorithm has
 a lower normalized energy consumption for $N_r < 4$, as seen
 in Fig. 27, while exhibiting a higher end-to-end throughput
 for $N_r < 6$, as shown in Fig. 28. Moreover, both the OR and
 TR simulation results closely match the theoretical curves.
 When $N_r = 1$ or 2 for the network topology of $N = 4$, both
 the exhaustive search, labelled by "TR bound" and the TR
 algorithm proposed in [74], labelled by "TR theory", selected

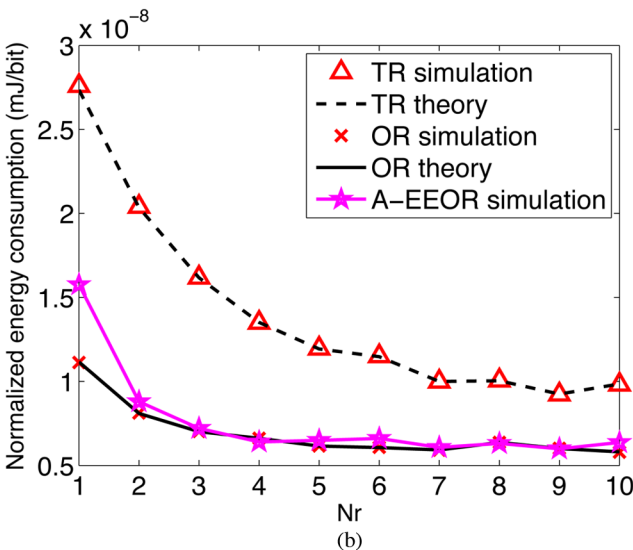
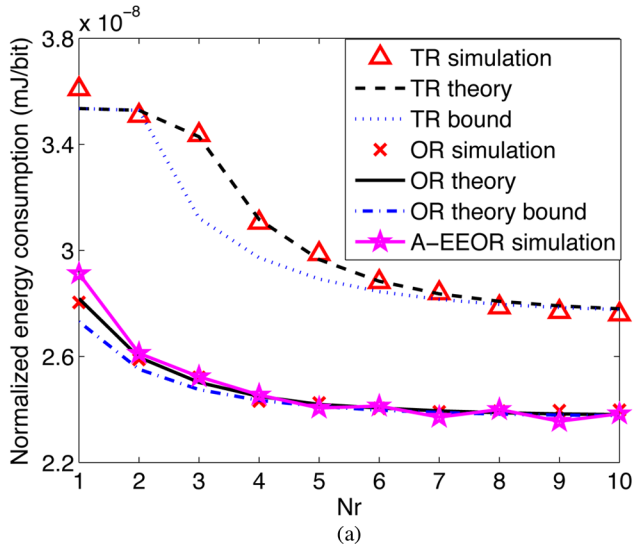


Fig. 27. The NEC \bar{E}_{total} versus the maximum number of MAC retransmissions N_r , when $N = 4$ and 15. (a) Network topology $N = 4$. (b) Network topology $N = 15$.

1312 the route ‘S-D’. Hence the NEC is the same for both. When
 1313 $2 < N_r < 8$, the exhaustive search and **the TR algorithm**
 1314 **proposed in [74]** choose different routes, since the exhaustive
 1315 search represents the globally optimal algorithm, while the TR
 1316 algorithm is a locally optimal algorithm. More specifically, the
 1317 TR algorithm is optimal for every single hop. Moreover, the
 1318 simulation results corresponding to the ‘TR simulation’ label
 1319 closely match the theoretical value represented by the label
 1320 ‘TR theory’. Therefore, the ‘TR simulation/theory’ and the ‘TR
 1321 bound’ scenarios exhibit a performance discrepancy, when $2 <$
 1322 $N_r < 8$, as seen in Fig. 27. Note that the NEC \bar{E}_{total} decreases
 1323 upon increasing N_r . However, the end-to-end throughput R_{e2e} of
 1324 the A-EEOR and OR regimes first increases and then saturates.
 1325 Additionally, the end-to-end throughput of TR is in fact higher
 1326 than that of OR for $N_r = 1$ and 2 when $N = 4$, but it is lower
 1327 for $N_r \geq 3$, as seen in Fig. 28. This is because in case of a low
 1328 number of MAC retransmissions, the direct near-line-of-sight
 1329 route spanning from S to D in the TR has a more dominant
 1330 priority than the other routes.

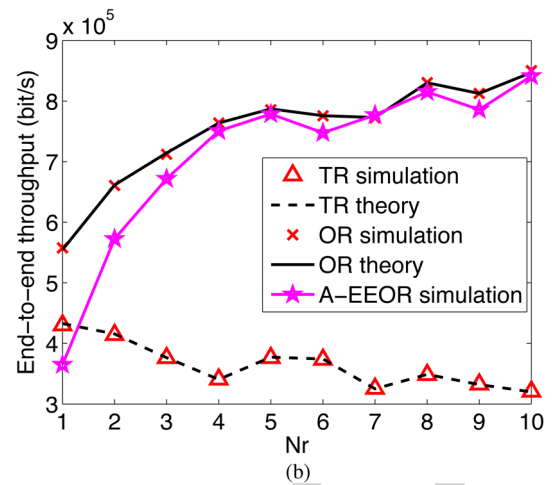
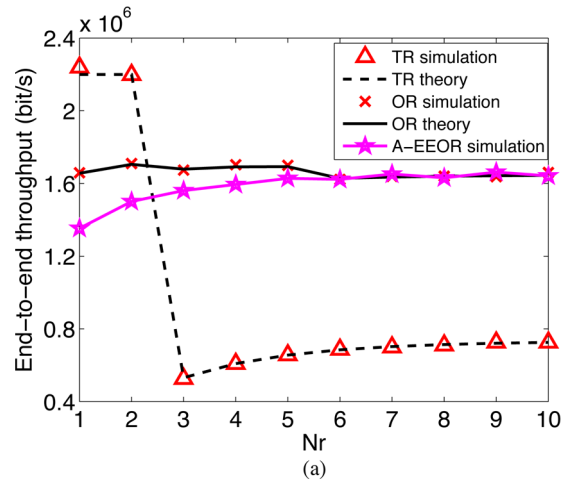


Fig. 28. The end-to-end throughput R_{e2e} versus the maximum number of MAC retransmissions N_r when $N = 4$ and 15. (a) Network topology $N = 4$. (b) Network topology $N = 15$.

IV. CONCLUSIONS AND DESIGN GUIDELINES

1331

A. Conclusions

1332

In this paper diverse routing schemes were studied, investi- 1333
 gating the benefits of multi-antenna aided RNs, the FER, the 1334
 number of MAC retransmissions and the number of hops on 1335
 the performance energy consumption. 1336

- In Section I, we described the main functions of the OSI 1337
 model layer by layer, then we highlighted the common 1338
 methods of cross-layer design. The historical develop- 1339
 ment of cross-layer aided routing protocol designs was 1340
 portrayed in Table II. Then, we categorized the family 1341
 of *ad hoc* routing protocols, which were improved in the 1342
 following chapters. 1343
- In Section II, we focused our attention on the reduction 1344
 of the energy consumption by exploiting the benefits of 1345
 the coordination between the PHY layer and the NET 1346
 layer. Specifically, the advantages of near-capacity coding 1347
 schemes were quantified in terms of their energy saving. A 1348
 near-capacity three-stage concatenated IrCC-URC-STTC 1349
 relay-transceiver equipped with two transmit antennas was 1350
 proposed in [72] for the *ad hoc* network considered, 1351
 since it achieved a low FER at a low transmit power. 1352

1353 The high effective transmission range of the IrCC-URC-
 1354 STTC aided MA-RNs facilitated cross-layer design for
 1355 activating beneficial routes having the lowest number of
 1356 longer hops.

- 1357 • Section III was specifically dedicated to minimizing the
 1358 energy consumed by the data packets during the process
 1359 of data transmission, where the NEC was quantified by
 1360 considering both the PHY layer as well as the DL layer
 1361 and the NET layer. Additionally, a cross-layer operation
 1362 aided energy-efficient OR algorithm for *ad hoc* networks
 1363 and an energy-consumption-based OF combined with PA
 1364 was analyzed, which was proposed in [74] both for finding
 1365 a theoretical bound and for conveying the packets through
 1366 the network.

1367 B. Design Guidelines

1368 In general, three basic steps may be identified, when design-
 1369 ing routing algorithms in *ad hoc* networks, which are:

- 1370 1) Determining the design targets, such as the network's
 1371 throughput and/or energy consumption;
- 1372 2) Determining the key factors, which influence the design
 1373 targets most crucially. These key factors may be related
 1374 to different layers, including the channel categories, the
 1375 protocol parameters and so on;
- 1376 3) Determining the routing metrics used for making routing
 1377 decisions, such as the number of hops and/or the normal-
 1378 ized end-to-end energy consumption.

1379 Let us now detail these three design steps as follows:

- 1380 • Throughput and energy consumption constitute a pair of
 1381 important specifications in analyzing a network's perfor-
 1382 mance, which critically depend on the parameters of the
 1383 different OSI layers. Hence, combining the functions of
 1384 multiple layers with the aid of cross-layer operation is ben-
 1385 efiticial in terms of improving the attainable performance, as
 1386 demonstrated in this tutorial with the assistance of several
 1387 cross-layer aided routing algorithms designed for *ad hoc*
 1388 networks.
- 1389 • The number of hops is one of the most popular routing
 1390 metrics in routing design, as we demonstrated in the con-
 1391 text of the classic routing algorithm, namely the DYMO
 1392 protocol.
- 1393 • One of the most important factors we have to consider
 1394 in the PHY layer is constituted by the specific charac-
 1395 teristics of the time-variant wireless channel, which in-
 1396 flict bit/symbol errors and even packet loss events at the
 1397 receiver node. Hence, strong and robust channel coding
 1398 schemes have to be employed for mitigating the channel-
 1399 induced degradations. The BER and FER are the two rep-
 1400 resentative parameters, which are capable of characteriz-
 1401 ing the influence of both the time-variant wireless channel
 1402 and of the FEC coding schemes, hence representing the
 1403 overall performance of the PHY layer.
- 1404 • For the sake of reducing the system's total transmit energy
 1405 consumption, a near-capacity coding scheme, such as the
 1406 IrCC-URC-STTC scheme of Section II-A is the most
 1407 appropriate choice, since it requires a reduced transmit

- power at a given BER/FER value, which may also be
 viewed as reducing the BER/FER at a given transmit
 power. This is the reason, why the IrCC-URC-STTC aided
 MA transceivers operate close to the achievable capacity
 and this is, why they are capable of reducing the num-
 ber of hops spanning from the source to the destination.
 Requiring less hops implies that less nodes are involved,
 hence reducing the energy dissipation. An energy-efficient
 routing algorithm relying on the employment of IrCC-
 URC-STTC aided MA transceivers [72] was analyzed in
 Section II-B and Section II-C, showing that the system's
 total transmit energy consumption was reduced.
- Furthermore, having considered the factors influencing the
 design of both the PHY layer and of the NET layer, we
 have to proceed by characterizing the influence of the DL
 layer in the cross-layer aided routing design. Our goal
 is that of achieving a throughput improvement and for
 energy reduction. One of the representative factors in the
 DL layer is constituted by the number of maximum MAC
 retransmissions. The larger the number of maximum MAC
 retransmissions, the more energy will be consumed and
 the higher the delay becomes. As a benefit, the success-
 ful packet reception probability is improved. Hence, we
 have to find the most appropriate number of maximum
 MAC retransmissions for the sake of striking an attractive
 compromise.
- Additionally, we emphasize that the energy assigned to
 the data packets plays a dominant role in determining the
 system's total energy dissipation, which hence has to be
 optimized. For the sake of achieving an improved network
 throughput and a reduced energy consumption, the joint
 influence of the FER in the PHY layer, of the maximum
 number of retransmissions in the DL layer and of the
 number of hops in the NET layer has to be carefully con-
 sidered. Additionally, opting for the NEC as the routing
 metric instead of the number of hops is more beneficial in
 terms of reducing energy consumption. Hence, an accurate
 energy-consumption-based OF is required for combining
 all the three factors corresponding to the lower three
 layers of the seven-layer OSI architecture, as indicated
 in Section III-A of the tutorial. The routing algorithm
 proposed strikes an attractive tradeoff between the normal-
 ized energy consumption and the end-to-end throughput
 in the context of real-world scenarios, as exemplified in
 Section III-A.
- A hop-length-dependent PA is beneficial in terms of re-
 ducing the energy consumption. If the transmit power of
 each node is assumed to be the same, a certain amount of
 extra energy will be dissipated, since the distance between
 each pair of nodes is different, which would necessitate a
 different amount of transmit energy. An energy-efficient
 TR algorithm was designed with the aid of the hop-length-
 dependent power allocation of Section III-B, which also
 jointly considered the FER in the PHY layer, the maximum
 number of retransmissions in the DL layer and the number
 of hops in the NET layer. A reliable routing metric is
 constituted by the NEC quantified in terms of the energy-
 based OF exemplified in Section III-B.

1466 • Additionally, the violently time-varying fading channel
 1467 will impose extra energy dissipation as well, because it
 1468 may render a pre-selected route inadequate for reliable
 1469 data transmission. This led to the concept of OR, which
 1470 is capable of reducing the energy consumption. Hence an
 1471 energy-efficient OR regime was designed with the aid of
 1472 hop-length-dependent PA in Section III-C, which also re-
 1473 lied on cross-layer operation across the lower three layers
 1474 of the TCP/IP model. Again, a reliable routing metric is
 1475 constituted by the NEC quantified in terms of the energy-
 1476 based OF exemplified in Section III-C.

1477 **All operational systems rely on a vital form of cross-**
 1478 **layer operation, which makes wireless systems different**
 1479 **from wireline based systems. Explicitly, both handovers and**
 1480 **power-control rely on cross-layer cooperation in all wireless**
 1481 **systems. This is why they are usually shown diagrammati-**
 1482 **cally as a block bridging the lowest three layers. Going back**
 1483 **as far as the old second-generation GSM system, the total**
 1484 **control-channel bitrate was as low as 961 bits/sec, which**
 1485 **limited the efficiency of the power-control and handover**
 1486 **operations, especially at high velocity and for small traffic**
 1487 **cells, when handovers are frequent. For the 3G systems the**
 1488 **control-channel rates were increased by an order of mag-**
 1489 **nitude to about 10 kbits/s, which facilitated more prompt**
 1490 **handovers and power-control actions, when for example**
 1491 **the mobile turned at a street-corner. The 4G LTE system**
 1492 **also followed this trend, since an increased control-channel**
 1493 **rate supports more sophisticated cross-layer cooperation.**
 1494 Although the main focus of this tutorial is on the energy dis-
 1495 sipated by data packets during the process of data transmission,
 1496 we note that cross-layer cooperation imposes an extra network
 1497 overhead, since the control **information also plays** an impor-
 1498 tant role in determining the system's total energy consumption,
 1499 especially in mobile scenarios where the control **information**
 1500 **assists** in maintaining seamless communications [128]. **The**
 1501 **extra control information is generated, when the informa-**
 1502 **tion exchange takes place amongst layers or different nodes,**
 1503 **including the control bits and the extra control packets.**
 1504 Additionally, a plethora of control packets are required for both
 1505 route discovery and for route maintenance. For example, node-
 1506 mobility might cause the following problems:

- 1507 • In TR, both the pre-selected route and the pre-stored
 1508 backup routes become invalid, which will activate route
 1509 re-discovery and hence may deplete the residual energy of
 1510 each node;
- 1511 • In OR, both the pre-computed optimal transmit power and
 1512 the forwarder set might become invalid, which requires the
 1513 re-computation of these two parameters. Hence, the effects
 1514 of the route life-time have to be considered for estimating
 1515 the energy consumption in a mobile scenario [128]–[131].

1516 Hence, the energy-consumption-based OFs formulated in the
 1517 stationary scenario may require further adjustments, if the en-
 1518 ergy dissipated by the control packets is also considered. It may
 1519 be promising to employ bio-inspired algorithms, such as the
 1520 ant colony algorithm [132], for accommodating a dynamically
 1521 changing topology, which requires future research.

REFERENCES

- 1522
- [1] H. Labiod, Ed., *Wireless Ad Hoc and Sensor Networks*. Hoboken, NJ, USA: Wiley, 2008. 1523
 - [2] R. Ramanathan and J. Redi, "A brief overview of Ad Hoc networks: Challenges and directions," *IEEE Commun. Mag.*, vol. 40, no. 5, pp. 20–22, May 2002. 1524
 - [3] H. Zimmermann, "OSI reference model—the ISO model of architecture for open systems interconnection," *IEEE Trans. Commun.*, vol. 28, no. 4, pp. 425–432, Apr. 1980. 1525
 - [4] *Reference Model of Open Systems Interconnection*, ISO/TC97/SC16 Std. Doc. N227, 1979. 1526
 - [5] A. Goldsmith, *Wireless Communications*. New York, NY, USA: Cambridge Univ. Press, 2005. 1527
 - [6] W. Stallings, *Wireless Communications & Networks*, 2nd ed. Englewood Cliffs, NJ, USA: Prentice-Hall, 2005. 1528
 - [7] *Information Technology-Telecommunications and Information Exchange Between Systems-Local and Metropolitan Area Networks-Specific Requirements*, IEEE Std. 802.11, 2007. 1529
 - [8] "Internet protocol," IETF Draft, 1981. 1530
 - [9] S. Deering and R. Hinden, "Internet protocol, version 6 (IPv6) specification," IETF Draft, 1998. 1531
 - [10] "Transmission control protocol," IETF Draft, 1981. 1532
 - [11] "User datagram protocol," IETF Draft, 1980. 1533
 - [12] *Definitions of Terms Related to Quality of Service*, ITU-T E.800, 2008. 1534
 - [13] V. Srivastava and M. Motani, "Cross-layer design: A survey and the road ahead," *IEEE Commun. Mag.*, vol. 43, no. 12, pp. 112–119, Dec. 2005. 1535
 - [14] M. Conti, G. Maselli, G. Turi, and S. Giordano, "Cross-layering in mobile Ad Hoc network design," *Computer*, vol. 37, no. 2, pp. 48–51, Feb. 2004. 1536
 - [15] R. Jurdak, *Wireless Ad Hoc and Sensor Networks: A Cross-layer Design Perspective*. New York, NY, USA: Springer-Verlag, 2010. 1537
 - [16] F. Fu and M. V. D. Schaar, "A new systematic framework for autonomous cross-layer optimization," *IEEE Trans. Veh. Technol.*, vol. 58, no. 4, pp. 1887–1903, May 2009. 1538
 - [17] R. Winter, J. H. Schiller, N. Nikaein, and C. Bonnet, "Crosstalk: Cross-layer decision support based on global knowledge," *IEEE Commun. Mag.*, vol. 44, no. 1, pp. 93–99, Jan. 2006. 1539
 - [18] E. Setton, T. Yoo, X. Zhu, A. Goldsmith, and B. Girod, "Crosslayer design of Ad Hoc networks for real-time video streaming," *IEEE Wireless Commun.*, vol. 12, no. 4, pp. 59–65, Aug. 2005. 1540
 - [19] Q. Liu, X. Wang, and G. B. Giannakis, "A cross-layer scheduling algorithm with QoS support in wireless networks," *IEEE Trans. Veh. Technol.*, vol. 55, no. 3, pp. 839–847, May 2006. 1541
 - [20] W. L. Huang and K. B. Letaief, "Cross-layer scheduling and power control combined with adaptive modulation for wireless Ad Hoc networks," *IEEE Trans. Commun.*, vol. 55, no. 4, pp. 728–739, Apr. 2007. 1542
 - [21] Q. Zhang and Y.-Q. Zhang, "Cross-layer design for QoS support in multihop wireless networks," *Proc. IEEE*, vol. 96, no. 1, pp. 64–76, Jan. 2008. 1543
 - [22] B. J. Oh and C. W. Chen, "A cross-layer approach to multichannel MAC protocol design for video streaming over wireless Ad Hoc networks," *IEEE Trans. Multimedia*, vol. 11, no. 6, pp. 1052–1061, Oct. 2009. 1544
 - [23] S. Chu and X. Wang, "Opportunistic and cooperative spatial multiplexing in MIMO Ad Hoc networks," *IEEE/ACM Trans. Netw.*, vol. 18, no. 5, pp. 1610–1623, Oct. 2010. 1545
 - [24] A. Ghosh and W. Hamouda, "Cross-layer antenna selection and channel allocation for MIMO cognitive radios," *IEEE Trans. Wireless Commun.*, vol. 10, no. 11, pp. 3666–3674, Nov. 2011. 1546
 - [25] M. Mardani, S.-J. Kim, and G. B. Giannakis, "Cross-layer design of wireless multihop random access networks," *IEEE Trans. Signal Process.*, vol. 60, no. 5, pp. 2562–2574, May 2012. 1547
 - [26] M. Uddin, C. Rosenberg, W. Zhuang, P. Mitran, and A. Girard, "Joint routing and medium access control in fixed random access wireless multihop networks," *IEEE/ACM Trans. Netw.*, vol. 22, no. 1, pp. 80–93, Feb. 2014. 1548
 - [27] F. Tang, L. Barolli, and J. Li, "A joint design for distributed stable routing and channel assignment over multihop and multiframe mobile Ad Hoc cognitive networks," *IEEE Trans. Ind. Informat.*, vol. 10, no. 2, pp. 1606–1615, May 2014. 1549
 - [28] V. Kawadia and P. R. Kumar, "A cautionary perspective on cross-layer design," *IEEE Wireless Commun.*, vol. 12, no. 1, pp. 3–11, Feb. 2005. 1550
 - [29] E. M. Royer and C.-K. Toh, "A review of current routing protocols for Ad Hoc mobile wireless networks," *IEEE Pers. Commun.*, vol. 6, no. 2, pp. 46–55, Apr. 1999. 1551
 - [30] C. E. Perkins and P. Bhagwat, "Highly dynamic destination-sequenced distance vector (DSDV) for mobile computers," in *Proc. ACM SIGCOMM*, Aug. 31–Sep. 2, 1994, pp. 234–244. 1552

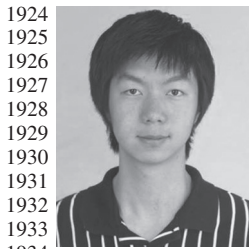
- 1599 [31] T. Clausen and P. Jacquet, Optimized Link State Routing Protocol
1600 (OLSR) (RFC 3626) 2003, IETF Draft.
- 1601 [32] *The Dynamic Source Routing Protocol (DSR) for Mobile Ad Hoc Net-*
1602 *works for IPv4*. [Online]. Available: <http://tools.ietf.org/html/rfc4728>
- 1603 [33] *Ad hoc On-Demand Distance Vector (AODV) Routing*. [Online]. Avail-
1604 able: <http://tools.ietf.org/html/rfc3561>
- 1605 [34] *Dynamic MANET On-Demand (DYMO) Routing Routing*. [Online].
1606 Available: <http://tools.ietf.org/html/draft-ietf-manet-dymo-19>
- 1607 [35] *The Zone Routing Protocol (ZRP) for Ad Hoc Networks*. [Online]. Avail-
1608 able: <http://tools.ietf.org/html/draft-ietf-manet-zone-zrp-04>
- 1609 [36] A. Goldsmith and S. B. Wicker, "Design challenges for energycon-
1610 strained Ad Hoc wireless networks," *IEEE Wireless Commun.*, vol. 9,
1611 no. 4, pp. 8–27, Aug. 2002.
- 1612 [37] M. R. Souryal, B. R. Vojcic, and R. L. Pickholtz, "Information efficiency
1613 of multihop packet radio networks with channel-adaptive routing," *IEEE*
1614 *J. Sel. Areas Commun.*, vol. 23, no. 1, pp. 40–50, Jan. 2005.
- 1615 [38] S.-H. Lee, E. Choi, and D.-H. Cho, "Timer-based broadcasting for
1616 power-aware routing in power-controlled wireless Ad Hoc networks,"
1617 *IEEE Commun. Lett.*, vol. 9, no. 3, pp. 222–224, Mar. 2005.
- 1618 [39] M. Johansson and L. Xiao, "Cross-layer optimization of wireless
1619 networks using nonlinear column generation," *IEEE Trans. Wireless*
1620 *Commun.*, vol. 5, no. 2, pp. 435–445, Feb. 2006.
- 1621 [40] S. Mao *et al.*, "On routing for multiple description video over wireless
1622 Ad Hoc networks," *IEEE Trans. Multimedia*, vol. 8, no. 5, pp. 1063–
1623 1074, Oct. 2006.
- 1624 [41] A. Abdrabou and W. H. Zhuang, "A position-based QoS routing scheme
1625 for UWB mobile Ad Hoc networks," *IEEE J. Sel. Areas Commun.*,
1626 vol. 24, no. 4, pp. 850–856, Apr. 2006.
- 1627 [42] J. Zhang, Q. Zhang, B. Li, X. Luo, and W. Zhu, "Energy-efficient routing
1628 in mobile Ad Hoc networks: Mobility-assisted case," *IEEE Trans. Veh.*
1629 *Technol.*, vol. 55, no. 1, pp. 369–379, Jan. 2006.
- 1630 [43] S. Kompella, S. Mao, Y. T. Hou, and H. D. Sherali, "Cross-layer opti-
1631 mized multipath routing for video communications in wireless net-
1632 works," *IEEE J. Sel. Areas Commun.*, vol. 25, no. 4, pp. 831–840,
1633 May 2007.
- 1634 [44] M. Chiang, S. H. Low, A. R. Calderbank, and J. C. Doyle, "Layering as
1635 optimization decomposition: A mathematical theory of network archi-
1636 tectures," *Proc. IEEE*, vol. 95, no. 1, pp. 255–312, Jan. 2007.
- 1637 [45] K. T. Phan, H. Jiang, C. Tellambura, S. A. Vorobyov, and R. Fan,
1638 "Joint medium access control, routing and energy distribution in multi-
1639 hop wireless networks," *IEEE Trans. Wireless Commun.*, vol. 7, no. 12,
1640 pp. 5244–5249, Dec. 2008.
- 1641 [46] J. Liu, Y. T. Hou, Y. Shi, and H. D. Sherali, "Cross-layer optimization
1642 for MIMO-based wireless Ad Hoc networks: Routing, power allocation,
1643 bandwidth allocation," *IEEE J. Sel. Areas Commun.*, vol. 26, no. 6,
1644 pp. 913–926, Aug. 2008.
- 1645 [47] A. Abdrabou and W. H. Zhuang, "Statistical QoS routing for IEEE
1646 802.11 multihop Ad Hoc networks," *IEEE Trans. Wireless Commun.*,
1647 vol. 8, no. 3, pp. 1542–1552, Mar. 2009.
- 1648 [48] P. Li, Q. Shen, Y. Fang, and H. Zhang, "Power controlled network proto-
1649 cols for multi-rate Ad Hoc networks," *IEEE Trans. Wireless Commun.*,
1650 vol. 8, no. 4, pp. 2142–2149, Apr. 2009.
- 1651 [49] L. Ding, T. Melodia, S. N. Batalama, J. D. Matyjas, and M. J. Medley,
1652 "Cross-layer routing and dynamic spectrum allocation in cognitive radio
1653 Ad Hoc networks," *IEEE Trans. Veh. Technol.*, vol. 59, no. 4, pp. 1969–
1654 1979, May 2010.
- 1655 [50] Y. Lu, J. Guan, Z. Wei, and Q. Wu, "Joint channel assignment and cross-
1656 layer routing protocol for multi-radio multi-channel Ad Hoc networks,"
1657 *J. Syst. Eng. Electron.*, vol. 21, no. 6, pp. 1095–1102, Dec. 2010.
- 1658 [51] Z. Ding and K. K. Leung, "Cross-layer routing using cooperative trans-
1659 mission in vehicular Ad-Hoc networks," *IEEE Journal on Selected Areas*
1660 *in Communications*, vol. 29, no. 3, pp. 571–581, Mar. 2011.
- 1661 [52] B. Tavli and W. B. Heinzelman, "Energy-efficient real-time multicast
1662 routing in mobile Ad Hoc networks," *IEEE Trans. Comput.*, vol. 60,
1663 no. 5, pp. 707–722, May 2011.
- 1664 [53] S.-J. Syue, C.-L. Wang, T. Aguilar, V. Gauthier, and H. Afifi, "Coop-
1665 erative geographic routing with radio coverage extension for SER con-
1666 strained wireless relay networks," *IEEE J. Sel. Areas Commun.*, vol. 30,
1667 no. 2, pp. 271–279, Feb. 2012.
- 1668 [54] M. Pan, H. Yue, C. Zhang, and Y. Fang, "Path selection under budget
1669 constraints in multihop cognitive radio networks," *IEEE Trans. Mobile*
1670 *Comput.*, vol. 12, no. 6, pp. 1133–1145, Jun. 2013.
- 1671 [55] J. G. Li, D. Cordes, and J. Y. Zhang, "Power-aware routing protocols
1672 in Ad Hoc wireless networks," *IEEE Wireless Commun.*, vol. 12, no. 6,
1673 pp. 69–81, Dec. 2005.
- 1674 [56] S. D. Muruganathan, D. C. F. Ma, R. I. Bhasin, and A. Fapojuwo, "A cen-
1675 tralized energy-efficient routing protocol for wireless sensor networks,"
1676 *IEEE Commun. Mag.*, vol. 43, no. 3, pp. S8–S13, Mar. 2005.
- [57] J. Zhu, C. Qiao, and X. Wang, "On accurate energy consumption models
for wireless Ad Hoc networks," *IEEE Trans. Wireless Commun.*, vol. 5,
no. 11, pp. 3077–3086, Nov. 2006. 1677 1678 1679 AQ2
- [58] S. J. Baek and G. Veciana, "Spatial energy balancing through proactive
multipath routing in wireless multihop networks," *IEEE/ACM Trans.*
Netw., vol. 15, no. 1, pp. 93–104, Feb. 2007. 1680 1681 1682
- [59] S. Eidenbenz, G. Resta, and P. Santi, "The COMMIT protocol for
truthful and cost-efficient routing in Ad Hoc networks with self-
ish nodes," *IEEE Trans. Mobile Comput.*, vol. 7, no. 1, pp. 19–33,
Jan. 2008. 1683 1684 1685 1686
- [60] W. Liang, R. Brent, Y. Xu, and Q. Wang, "Minimum-energy all-
toall multicasting in wireless Ad Hoc networks," *IEEE Trans. Wireless*
Commun., vol. 8, no. 11, pp. 5490–5499, Nov. 2009. 1687 1688 1689
- [61] M. Li, L. Ding, Y. Shao, Z. Zhang, and B. Li, "On reducing broadcast
transmission cost and redundancy in Ad Hoc wireless networks using di-
rectional antennas," *IEEE Trans. Veh. Technol.*, vol. 59, no. 3, pp. 1433–
1442, Mar. 2010. 1690 1691 1692
- [62] C. Ma and Y. Yang, "A battery-aware scheme for routing in wireless
Ad Hoc networks," *IEEE Trans. Veh. Technol.*, vol. 60, no. 8, pp. 3919–
3932, Oct. 2011. 1693 1694 1695 1696
- [63] A. M. Akhtar, M. R. Nakhai, and A. H. Aghvami, "Power aware cooper-
ative routing in wireless mesh networks," *IEEE Commun. Lett.*, vol. 16,
no. 5, pp. 670–673, May 2012. 1697 1698 1699
- [64] T. Lu and J. Zhu, "Genetic algorithm for energy-efficient QoS multicast
routing," *IEEE Commun. Lett.*, vol. 17, no. 1, pp. 31–34, Jan. 2013. 1700 1701
- [65] J. Vazifehdan, R. Prasad, and I. Niemegeers, "Energy-efficient reliable
routing considering residual energy in wireless Ad Hoc networks," *IEEE*
Trans. Mobile Comput., vol. 13, no. 2, pp. 434–447, Feb. 2014. 1702 1703 1704
- [66] G. Ferrari, S. A. Malvassori, and O. K. Tonguz, "On physical layeror-
iented routing with power control in Ad Hoc wireless networks," *IET*
Commun., vol. 2, no. 2, pp. 306–319, Feb. 2008. 1705 1706 1707
- [67] J. C. Fricke, M. M. Butt, and P. A. Hoehner, "Quality-oriented adaptive
forwarding for wireless relaying," *IEEE Commun. Lett.*, vol. 12, no. 3,
pp. 200–202, Mar. 2008. 1708 1709 1710
- [68] M. Haenggi and D. Puccinelli, "Routing in Ad Hoc networks: A case
for long hops," *IEEE Commun. Mag.*, vol. 43, no. 10, pp. 93–101,
Oct. 2005. 1711 1712 1713
- [69] M. Sikora, J. N. Laneman, M. Haenggi, D. J. Costello, and T. E. Fuja,
"Bandwidth-and power-efficient routing in linear wireless networks,"
IEEE Trans. Inf. Theory, vol. 52, no. 6, pp. 2624–2633, Jun. 2006. 1714 1715 1716
- [70] C. Bae and W. E. Stark, "End-to-end energy and bandwidth tradeoff in
multihop wireless networks," *IEEE Trans. Inf. Theory*, vol. 55, no. 9,
pp. 4051–4066, Sep. 2009. 1717 1718 1719
- [71] J. Niu, L. Cheng, Y. Gu, L. Shu, and S. K. Das, "R3E: Reliable reactive
routing enhancement for wireless sensor networks," *IEEE Trans. Inf.*
Informat., vol. 10, no. 1, pp. 784–794, Feb. 2014. 1720 1721 1722
- [72] J. Zuo, H. V. Nguyen, S. X. Ng, and L. Hanzo, "Energy-efficient relay
aided Ad Hoc networks using iteratively detected irregular convolu-
tional coded, unity-rate coded and space-time trellis coded transceivers,"
in *Proc. IEEE WCNC*, Quintana-Roo, Mexico, Mar. 28–31, 2011,
pp. 1179–1184. 1723 1724 1725 1726 1727
- [73] J. Zuo, C. Dong, S. X. Ng, L.-L. Yang, and L. Hanzo, "Energy-efficient
routing in Ad Hoc networks relying on channel state information and
limited mac retransmissions," in *Proc. IEEE VTC-Fall*, San Francisco,
CA, USA, Sep. 5–8, 2011, pp. 1–5. 1728 1729 1730 1731
- [74] J. Zuo *et al.*, "Cross-layer aided energy-efficient opportunistic routing in
Ad Hoc networks," *IEEE Trans. Commun.*, vol. 62, no. 2, pp. 522–535,
Feb. 2014. 1732 1733 1734
- [75] D. Feng *et al.*, "A survey of energy-efficient wireless communications,"
IEEE Commun. Surveys Tuts., vol. 15, no. 1, pp. 167–178, 2013. 1735 1736
- [76] M. C. Vuran and I. F. Akyildiz, "Error control in wireless sensor net-
works: A cross layer analysis," *IEEE/ACM Trans. Netw.*, vol. 17, no. 4,
pp. 1186–1199, Aug. 2009. 1737 1738 1739
- [77] H. V. Nguyen, S. X. Ng, and L. Hanzo, "Distributed three-stage concate-
nated irregular convolutional, unity-rate and space-time trellis coding for
single-antenna aided cooperative communications," in *Proc. IEEE 72nd*
VTC-Fall, Ottawa, ON, Canada, Sep. 6–9, 2010, pp. 1–5. 1740 1741 1742 1743
- [78] S. T. Brink, "Convergence behavior of iteratively decoded parallel con-
catenated codes," *IEEE Trans. Commun.*, vol. 49, no. 10, pp. 1727–1737,
Oct. 2001. 1744 1745 1746
- [79] L. Hanzo, O. Alamri, M. El-Hajjar, and N. Wu, *Near-Capacity Multi-*
Functional MIMO Systems. New York, NY, USA: Wiley, 2009. 1747 1748
- [80] *User Datagram Protocol*. [Online]. Available: [http://tools.ietf.org/html/](http://tools.ietf.org/html/rfc768)
[rfc768](http://tools.ietf.org/html/rfc768) 1749 1750
- [81] L. Hanzo, S.-X. Ng, T. Keller, and W. Webb, *Quadrature Amplitude*
Modulation: From Basics to Adaptive Trellis-Coded, Turbo-Equalised
and Space-Time Coded OFDM, CDMA, and MC-CDMA Systems,
2nd ed. Hoboken, NJ, USA: Wiley-IEEE Press, 2004. 1751 1752 1753 1754

- [82] J. Zuo, S. X. Ng, and L. Hanzo, "Fuzzy logic aided dynamic source routing in cross-layer operation assisted Ad Hoc networks," in *Proc. IEEE 72nd VTC-Fall*, Ottawa, ON, Canada, Sep. 6–9, 2010, pp. 1–5.
- [83] A. Ibrahim, H. Zhu, and K. J. R. Liu, "Distributed energy-efficient cooperative routing in wireless networks," *IEEE Trans. Wireless Commun.*, vol. 7, no. 10, pp. 3930–3941, Oct. 2008.
- [84] E. Baccarelli, M. Biagi, C. Pelizzoni, and N. Cordeschi, "Maximum-rate node selection for power-limited multi-antenna relay backbones," *IEEE Trans. Mobile Comput.*, vol. 8, no. 6, pp. 807–820, Jun. 2009.
- [85] C. Bae and W. E. Stark, "End-to-end energy-bandwidth tradeoff in multihop wireless networks," *IEEE Trans. Inf. Theory*, vol. 55, no. 9, pp. 4051–4066, Sep. 2009.
- [86] S. Banerjee and A. Misra, "Minimum energy paths for reliable communication in multi-hop wireless networks," in *Proc. 3rd ACM Int. Symp. MobiHoc*, Lausanne, Switzerland, Jun. 9–11, 2002, pp. 146–156.
- [87] S. Cui, R. Madan, A. Goldsmith, and S. Lall, "Cross-layer energy and delay optimization in small-scale sensor networks," *IEEE Trans. Wireless Commun.*, vol. 6, no. 10, pp. 3688–3699, Oct. 2007.
- [88] H. Alwan and A. Agarwal, "Multi-objective QoS routing for wireless sensor networks," in *Proc. ICNC*, Jan. 28–31, 2013, pp. 1074–1079.
- [89] X.-Y. Li *et al.*, "Reliable and energy-efficient routing for static wireless Ad Hoc networks with unreliable links," *IEEE Trans. Parallel Distrib. Syst.*, vol. 20, no. 10, pp. 1408–1421, Oct. 2009.
- [90] M. Zorzi and R. R. Rao, "Geographic random forwarding (GeRaF) for Ad Hoc and sensor networks: Energy and latency performance," *IEEE Trans. Mobile Comput.*, vol. 2, no. 4, pp. 349–365, Oct.–Dec. 2003.
- [91] X. Mao, S. Tang, X. Xu, X.-Y. Li, and H. Ma, "Energy-efficient opportunistic routing in wireless sensor networks," *IEEE Trans. Parallel Distrib. Syst.*, vol. 22, no. 11, pp. 1934–1942, Nov. 2011.
- [92] M. Dehghan, M. Ghaderi, and D. Goeckel, "Minimum-energy cooperative routing in wireless networks with channel variations," *IEEE Trans. Wireless Commun.*, vol. 10, no. 11, pp. 3813–3823, Nov. 2011.
- [93] J. Zhu and X. Wang, "Model and protocol for energy-efficient routing over mobile Ad Hoc networks," *IEEE Trans. Mobile Comput.*, vol. 10, no. 11, pp. 1546–1557, Nov. 2011.
- [94] T. Luo, M. Motani, and V. Srinivasan, "Energy-efficient strategies for cooperative multichannel MAC protocols," *IEEE Trans. Mobile Comput.*, vol. 11, no. 4, pp. 553–566, Apr. 2012.
- [95] S. Kwon and N. B. Shroff, "Energy-efficient SINR-based routing for multihop wireless networks," *IEEE Trans. Mobile Comput.*, vol. 8, no. 5, pp. 668–681, May 2009.
- [96] C. Wei, C. Zhi, P. Fan, and K. B. Letaief, "AsOR: An energy efficient multi-hop opportunistic routing protocol for wireless sensor networks over Rayleigh fading channels," *IEEE Trans. Wireless Commun.*, vol. 8, no. 5, pp. 2452–2463, May 2009.
- [97] M. C. Vuran and I. F. Akyildiz, "XLP: A cross-layer protocol for efficient communication in wireless sensor networks," *IEEE Trans. Mobile Comput.*, vol. 9, no. 11, pp. 1578–1591, Nov. 2010.
- [98] H. Kwon, T. H. Kim, S. Choi, and B. G. Lee, "A cross-layer strategy for energy-efficient reliable delivery in wireless sensor networks," *IEEE Trans. Wireless Commun.*, vol. 5, no. 12, pp. 3689–3699, Dec. 2006.
- [99] A. N. Pantazis, S. A. Nikolidakis, and D. D. Vergados, "Energy efficient routing protocols in wireless sensor networks: A survey," *IEEE Commun. Surveys Tuts.*, vol. 15, no. 2, pp. 551–591, 2013.
- [100] M. A. Rahman, S. Anwar, M. I. Pramanik, and M. F. Rahman, "A survey on energy efficient routing techniques in wireless sensor network," in *Proc. 15th ICACT*, Jan. 27–30, 2013, pp. 200–205.
- [101] S. Biswas and R. Morris, "Opportunistic routing in multi-hop wireless networks," *ACM SIGCOMM Comput. Commun. Rev.*, vol. 34, no. 1, pp. 69–74, Jan. 2004.
- [102] Q. W. Liu, S. L. Zhou, and G. B. Giannakis, "Cross-layer combining of adaptive modulation and coding with truncated ARQ over wireless links," *IEEE Trans. Wireless Commun.*, vol. 3, no. 5, pp. 1746–1755, Sep. 2004.
- [103] Z. Wang, Y. Chen, and C. Li, "CORMAN: A novel cooperative opportunistic routing scheme in mobile Ad Hoc networks," *IEEE J. Sel. Areas Commun.*, vol. 30, no. 2, pp. 289–296, Feb. 2012.
- [104] A. M. Akhtar, M. R. Nakhai, and A. H. Aghvami, "On the use of cooperative physical layer network coding for energy efficient routing," *IEEE Trans. Commun.*, vol. 61, no. 4, pp. 1498–1509, Apr. 2013.
- [105] R. C. Shah and J. M. Rabaey, "Energy aware routing for low energy Ad Hoc sensor networks," in *Proc. IEEE Wireless Commun. Netw. Conf.*, Mar. 2002, vol. 1, pp. 350–355.
- [106] Y. Xu, J. Heidemann, and D. Estrin, "Geography-informed energy conservation for Ad Hoc routing," in *Proc. 7th Annu. Int. Conf. MobiCom*, Rome, Italy, Jul. 2001, pp. 70–84.
- [107] Q. F. Dong and S. Banerjee, "Minimum energy reliable paths using unreliable wireless links," in *Proc. 6th ACM Int. Symp. MobiHoc*, Urbana-Champaign, IL, USA, May 25–28, 2005, pp. 449–459.
- [108] C.-E. Perkins, E.-M. Royer, S.-R. Das, and M.-K. Marina, "Performance comparison of two on-demand routing protocols for Ad Hoc networks," *IEEE Pers. Commun.*, vol. 8, no. 1, pp. 16–28, Feb. 2001.
- [109] M. Zorzi and R. R. Rao, "Geographic random forwarding (GeRaF) for Ad Hoc and sensor networks: Multihop performance," *IEEE Trans. Mobile Comput.*, vol. 2, no. 4, pp. 337–348, Oct.–Dec. 2003.
- [110] H. Liu, B. Zhang, H. Mouttah, X. Shen, and J. Ma, "Opportunistic routing for wireless Ad Hoc and sensor networks: Present and future 24 directions," *IEEE Commun. Mag.*, vol. 47, no. 12, pp. 103–109, Dec. 2009.
- [111] H. Dubois-Ferrière, M. Grossglauser, and M. Vetterli, "Valuable detours: Least-cost anypath routing," *IEEE/ACM Trans. Netw.*, vol. 19, no. 2, pp. 333–346, Apr. 2011.
- [112] A. A. Bhorkar, M. Naghshvar, T. Javidi, and B. D. Rao, "Adaptive opportunistic routing for wireless Ad Hoc networks," *IEEE/ACM Trans. Netw.*, vol. 20, no. 1, pp. 243–256, Feb. 2012.
- [113] K. Zeng, Z. Yang, and W. Lou, "Location-aided opportunistic forwarding in multirate and multihop wireless networks," *IEEE Trans. Veh. Technol.*, vol. 58, no. 6, pp. 3032–3040, Jul. 2009.
- [114] R. Laufer, H. Dubois-Ferrière, and L. Kleinrock, "Polynomial-time algorithms for multirate anypath routing in wireless multihop networks," *IEEE/ACM Trans. Netw.*, vol. 20, no. 3, pp. 742–755, Jun. 2012.
- [115] L. Pelusi, A. Passarella, and M. Conti, "Opportunistic networking: Data forwarding in disconnected mobile Ad Hoc networks," *IEEE Commun. Mag.*, vol. 44, no. 11, pp. 134–141, Nov. 2006.
- [116] H. Khalife, N. Malouch, and S. Fdida, "Multihop cognitive radio networks: To route or not to route," *IEEE Netw.*, vol. 23, no. 4, pp. 20–25, Jul. 2009.
- [117] K. C. Lee, U. Lee, and M. Gerla, "Geo-opportunistic routing for vehicular networks [topics in automotive networking]," *IEEE Commun. Mag.*, vol. 48, no. 5, pp. 164–170, May 2010.
- [118] D. Wu, Y. Zhang, L. Bao, and A. C. Regan, "Location-based crowdsourcing for vehicular communication in hybrid networks," *IEEE Trans. Intell. Transp. Syst.*, vol. 14, no. 2, pp. 837–846, Jun. 2013.
- [119] V. Conan, J. Leguay, and T. Friedman, "Fixed point opportunistic routing in delay tolerant networks," *IEEE J. Sel. Areas Commun.*, vol. 26, no. 5, pp. 773–782, Jun. 2008.
- [120] T. Spyropoulos, T. Turtletti, and K. Obraczka, "Routing in delay-tolerant networks comprising heterogeneous node populations," *IEEE Trans. Mobile Comput.*, vol. 8, no. 8, pp. 1132–1147, Aug. 2009.
- [121] Y. Li *et al.*, "Energy-efficient optimal opportunistic forwarding for delay-tolerant networks," *IEEE Trans. Veh. Technol.*, vol. 59, no. 9, pp. 4500–4512, Nov. 2010.
- [122] S.-G. Yoon, S. Jang, Y.-H. Kim, and S. Bahk, "Opportunistic routing for smart grid with power line communication access networks," *IEEE Trans. Smart Grid*, vol. 5, no. 1, pp. 303–311, Jan. 2014.
- [123] T. H. Cormen, C. E. Leiserson, R. L. Rivest, and C. Stein, *Introduction to Algorithms*, 3rd ed. Upper Saddle River, NJ, USA: MIT Press, 2009.
- [124] E. W. Dijkstra, "A note on two problems in connexion with graphs," *Numerische Mathematik*, vol. 1, no. 1, pp. 269–271, 1959.
- [125] M. L. Fredman and R. E. Tarjan, "Fibonacci heaps and their uses in improved network optimization algorithms," *J. Assoc. Comput. Mach.*, vol. 34, no. 3, pp. 596–615, Jul. 1987.
- [126] C. Dong, L.-L. Yang, and L. Hanzo, "Multi-hop diversity aided multihop communications: A cumulative distribution function aware approach," *IEEE Trans. Commun.*, vol. 61, no. 11, pp. 4486–4499, Nov. 2013.
- [127] C. Dong, L.-L. Yang, and L. Hanzo, "Performance analysis of multihop-diversity-aided multihop links," *IEEE Trans. Veh. Technol.*, vol. 61, no. 6, pp. 2504–2516, Jul. 2012.
- [128] W. C. Tan, S. K. Bose, and T.-H. Cheng, "Power and mobility aware routing in wireless Ad Hoc networks," *IET Commun.*, vol. 6, no. 11, pp. 1425–1437, Jul. 2012.
- [129] F. D. Rango, F. Guerriero, and P. Fazio, "Link-stability and energy aware routing protocol in distributed wireless networks," *IEEE Trans. Parallel Distrib. Syst.*, vol. 23, no. 4, pp. 713–726, Apr. 2012.
- [130] A. A. Jeng and R.-H. Jan, "Adaptive topology control for mobile Ad Hoc networks," *IEEE Trans. Parallel Distrib. Syst.*, vol. 22, no. 12, pp. 1953–1960, Dec. 2011.
- [131] G. Ferrari and O. K. Tonguz, "Impact of mobility on the BER performance of Ad Hoc wireless networks," *IEEE Trans. Veh. Technol.*, vol. 56, no. 1, pp. 271–286, Jan. 2007.
- [132] S. L. Correia, J. Celestino, and O. Cherkaoui, "Mobility-aware ant colony optimization routing for vehicular Ad Hoc networks," in *Proc. IEEE WCNC*, Quintana-Roo, Mexico, Mar. 28–31, 2011, pp. 1125–1130.



1911
1912
1913
1914
1915
1916
1917
1918
1919
1920
1921
1922
1923

Jing Zuo received the B.Eng. degree in communications engineering and the M.Sc. degree in communications and information system from Jilin University, Changchun, China, in 2006 and 2008, respectively, and the Ph.D. degree in wireless communications from University of Southampton, U.K., in 2013. She is the recipient of scholarship under the UK-China Scholarships for Excellence programme from 2008 to 2011. From 2009 to 2013, she was involved in the OPTIMIX and CONCERTO European projects. She is currently with Huawei, Shenzhen, China and her current research interests include protocols and algorithms design, cross-layer optimization and opportunistic communications.



1924
1925
1926
1927
1928
1929
1930
1931
1932
1933
1934
1935
1936

Chen Dong received the B.S. degree in electronic information sciences and technology from University of Science and Technology of China (USTC), Hefei, China, in 2004, and the M.Eng. degree in pattern recognition and automatic equipment from the University of Chinese Academy of Sciences, Beijing, China in 2007. He received the Ph.D. degree from the University of Southampton, UK. In 2014. Now he is a post-doc in the same University. He was the recipient of scholarship under the UK-China Scholarships for Excellence programme and he has been awarded Best Paper Award at IEEE VTC 2014-Fall. His research interests include applied math, relay system, channel modelling and cross-layer optimization.



1937
1938
1939
1940
1941
1942
1943
1944
1945
1946
1947
1948
1949
1950
1951
1952
1953
1954
1955
1956
1957

Soon Xin Ng (S'99–M'03–SM'08) received the B.Eng. degree (first class) in electronic engineering and the Ph.D. degree in telecommunications from the University of Southampton, Southampton, U.K., in 1999 and 2002, respectively. From 2003 to 2006, he was a postdoctoral research fellow working on collaborative European research projects known as SCOUT, NEWCOM and PHOENIX. Since August 2006, he has been a member of academic staff in the School of Electronics and Computer Science, University of Southampton. He is involved in the OPTIMIX and CONCERTO European projects as well as the IU-ATC and UC4G projects. He is currently an associate professor in telecommunications at the University of Southampton. His research interests include adaptive coded modulation, coded modulation, channel coding, space-time coding, joint source and channel coding, iterative detection, OFDM, MIMO, cooperative communications, distributed coding, quantum error correction codes and joint wireless-and-optical-fiber communications. He has published over 180 papers and co-authored two John Wiley/IEEE Press books in this field. He is a Chartered Engineer and a Fellow of the Higher Education Academy in the U.K.



Lie-Liang Yang (M'98–SM'02) received the 1958 B.Eng. degree in communications engineering from 1959 Shanghai TieDao University, Shanghai, China, 1960 in 1988, and the M.Eng. and Ph.D. degrees in 1961 communications and electronics from Northern 1962 (Beijing) Jiaotong University, Beijing, China in 1963 1991 and 1997, respectively. From June 1997 to 1964 December 1997 he was a visiting scientist of the 1965 Institute of Radio Engineering and Electronics, 1966 Academy of Sciences of the Czech Republic. Since 1967 December 1997, he has been with the University 1968 of Southampton, United Kingdom, where he is the professor of wireless 1969 communications in the School of Electronics and Computer Science. His 1970 research has covered a wide range of topics in wireless communications, 1971 networking and signal processing. He has published over 300 research papers, 1972 in journals and conference proceedings, authored/co-authored three books 1973 and also published several book chapters. The details about his publications 1974 can be found at <http://www-mobile.ecs.soton.ac.uk/lly/>. He is a Fellow of 1975 the IET, served as an associate editor to the IEEE TRANS. ON VEHICULAR 1976 TECHNOLOGY and JOURNAL OF COMMUNICATIONS AND NETWORKS 1977 (JCN), and is currently an associate editor to the *IEEE Access* and the *Security 1978 and Communication Networks (SCN) Journal*. 1979



Lajos Hanzo received the degree in electronics in 1980 1976 and the doctorate degree in 1983. In 2009 he 1981 was awarded the honorary doctorate "Doctor Hon- 1982 oris Causa" by the Technical University of Budapest. 1983 During his 37-year career in telecommunications he 1984 has held various research and academic posts in 1985 Hungary, Germany and the UK. Since 1986 he has 1986 been with the School of Electronics and Computer 1987 Science, University of Southampton, UK, where he 1988 holds the chair in telecommunications. He has suc- 1989 cessfully supervised more than 80 Ph.D. students, 1990 co-authored 20 John Wiley/IEEE Press books on mobile radio communications 1991 totalling in excess of 10 000 pages, published 1460 research entries at IEEE 1992 Xplore, acted both as TPC and General Chair of IEEE conferences, presented 1993 keynote lectures and has been awarded a number of distinctions. Currently 1994 he is directing a 60-strong academic research team, working on a range of 1995 research projects in the field of wireless multimedia communications sponsored 1996 by industry, the Engineering and Physical Sciences Research Council (EPSRC) 1997 UK, the European Research Council's Advanced Fellow Grant and the Royal 1998 Society's Wolfson Research Merit Award. He is an enthusiastic supporter of 1999 industrial and academic liaison and he offers a range of industrial courses. He 2000 is also a Governor of the IEEE VTS. During 2008–2012 he was the Editor-in- 2001 Chief of the IEEE Press and a Chaired Professor also at Tsinghua University, 2002 Beijing. His research is funded by the European Research Council's Senior 2003 Research Fellow Grant. For further information on research in progress and 2004 associated publications please refer to <http://www-mobile.ecs.soton.ac.uk>. 2005

AUTHOR QUERIES

AUTHOR PLEASE ANSWER ALL QUERIES

AQ1 = Note that reference [26] and [105] are the same. Therefore, reference [105] was deleted from the list.
Citations were renumbered accordingly. Please check.

AQ2 = Note that reference [57] and [109] are the same. Therefore, reference [109] was deleted from the list.
Citations were renumbered accordingly. Please check.

END OF ALL QUERIES

IEEE
Proof

Cross-Layer Aided Energy-Efficient Routing Design for Ad Hoc Networks

Jing Zuo, Chen Dong, Soon Xin Ng, Lie-Liang Yang, and Lajos Hanzo

Abstract—In this treatise, we first review some basic routing protocols conceived for *ad hoc* networks, followed by some design examples of cross-layer operation aided routing protocols. Specifically, cross-layer operation across the PHYSICAL layer (PHY), the Data Link layer (DL) and even the NETWORK layer (NET) is exemplified for improving the energy efficiency of the entire system. Moreover, the philosophy of Opportunistic Routing (OR) is reviewed for the sake of further reducing the system's energy dissipation with the aid of optimized Power Allocation (PA). The system's end-to-end throughput is also considered in the context of a design example.

Index Terms—Opportunistic routing, cross-layer, objective function, near-capacity coding, energy consumption, power allocation.

I. INTRODUCTION

SINCE the commencement of the Defense Advanced Research Projects Agency (DARPA) project [1] developed by the American Defense Department in the 1970s, *ad hoc* networks have been widely applied in scenarios, including military applications, crisis response, medical care, conference meetings and space exploration. During the past few decades, *ad hoc* networks attracted substantial research attention as a benefit of their prompt set-up and their ability to self-organize their noncentrally-controlled dynamic topology. Each node of an *ad hoc* network plays the dual role of being both a terminal and a router under the assumption that not all nodes can directly communicate with each other [2]. Fig. 1(a) and (b) show the difference between the classic infrastructure based network and *ad hoc* network. Fig. 1(a) shows that the nodes A, B and C communicate with each other under the control of Base Station (BS) 1 and that A communicates with E via BS 1 and BS 2. However, Fig. 1(b) shows that A can only communicate with E by relying on B, C and D as its Relay Nodes (RNs). Each node has to discover its own neighbor list.

The characteristics of *ad hoc* networks impose a number of open problems, which constitute challenges for the protocol design. For example, the scalability, the energy-efficiency, the

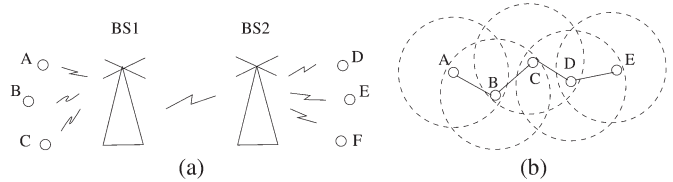


Fig. 1. Categories of wireless networks. (a) The infrastructure network; (b) *Ad hoc* network.

Quality of Service (QoS) and the security are challenging problems to be solved and to be further improved. Hence the emphasis of this treatise is on the design of routing protocols relying on cross-layer interaction for improving the attainable system performance, such as the Normalized Energy Consumption (NEC) and the end-to-end throughput.

A. Cross-Layer Design

The International Standards Organization (ISO) created the SubCommittee 16 (SC16) in 1977 for developing an architecture, which could serve as a framework for the definition of standard protocols. At the end of 1979, the Reference Model of Open System Interconnection (OSI) was adopted by the parent of SC16, namely, Technical Committee (TC97). The OSI Reference Model was also recognized by the International Telegraph and Telephone Consultative Committee (CCITT) Rapporteur's Group on Public Data Network Services. The OSI Reference Model consists of seven layers, which are the PHYSICAL layer (PHY), the Data Link layer (DL), the NETWORK layer (NET), the transport layer, the session layer, the presentation layer and the application layer. The benefit of this layering technique is to group the similar communication functions into these logical layers. A layer has to cooperate with the layer above it and the layer below it. However, when the Transmission Control Protocol (TCP) of the transport layer and the Internet Protocol (IP) of the network layer were defined, the five-layer model (TCP/IP model) became the dominant one. More explicitly, the TCP/IP model consists of the application layer, the transport layer, the NETWORK (NET) layer, the Data Link (DL) layer and the PHYSICAL (PHY) layer [3]–[6]. Fig. 2 illustrates the structure of the TCP/IP model and the main functions of each layer.

The functions of these layers are briefly highlighted below:

- **The physical layer:** The PHY layer concentrates on both the physical devices and on the transmission media. Providing a diversity and/or multiplexing gain with the aid of multiple antennas is capable of improving the integrity and/or throughput of data transmission. Additionally, the

Manuscript received January 9, 2014; revised July 6, 2014 and October 31, 2014; accepted January 17, 2015. The research leading to these results has received funding from the European Union's Seventh Framework Programme (FP7/2012-2014) under grant agreement no 288502. The financial support of the China-UK Scholarship Council, and of the RC-UK under the auspices of the IU-ATC initiative is also gratefully acknowledged.

The authors are with the School of Electronics and Computer Science (ECS), University of Southampton, Southampton SO17 1BJ, U.K. (e-mail: jz08r@ecs.soton.ac.uk; cd2g09@ecs.soton.ac.uk; sxn@ecs.soton.ac.uk; lly@ecs.soton.ac.uk; lh@ecs.soton.ac.uk; http://www-mobile.ecs.soton.ac.uk).

Color versions of one or more of the figures in this paper are available online at <http://ieeexplore.ieee.org>.

Digital Object Identifier 10.1109/COMST.2015.2395378

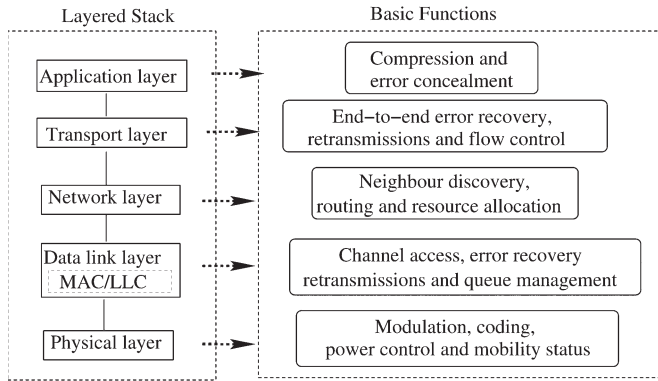


Fig. 2. Layered stack and the main functions in each layer.

77 adjustment of the transmit power, the design of the coding
 78 and modulation schemes as well as the effects of mobil-
 79 ity and/or propagation effects constitute important design
 80 factors of the physical layer.

- 81 • **The data link layer:** The DL layer of Fig. 2 is concerned
 82 with the media access, the error recovery, the retransmission
 83 and the queue management functions. It consists of
 84 two sub-layers, namely the Media Access Control (MAC)
 85 sublayer and the Logical Link Control (LLC) sublayer [7].
- 86 • **The network layer:** The NET layer is responsible for
 87 the neighbor discovery, routing and resource allocation
 88 functions. Routing is the main function of the network
 89 layer, guiding a packet through the network from a source
 90 to the destination [8], [9]. Numerous routing protocols
 91 have been designed based on the IP protocol for satisfy-
 92 ing the requirements of wireless *ad hoc* networks, which
 93 fundamentally predetermines the attainable performance
 94 in terms of the Packet Loss Ratio PLR, the end-to-end
 95 delay and the network's throughput.
- 96 • **The transport layer:** The transport layer is responsible for
 97 flow control, congestion control, error recovery, packet re-
 98 ordering and for the end-to-end connection setup. It assists
 99 the application layer of Fig. 2 in allocating/mapping the
 100 flows to different routes, which are found in the NET layer.
 101 It also assists by monitoring the end-to-end data transmis-
 102 sion and in avoiding network congestion [10], [11].
- 103 • **The application layer:** The application layer constitutes
 104 the interface to the end user in the TCP/IP model of Fig. 2.
 105 By considering the requirements of the end user, it divides
 106 the user services into different categories, such as for
 107 example, real-time and non-real-time services, continuous
 108 and intermittent services, Constant Bit Rate (CBR) and
 109 Variable Bit Rate (VBR) multimedia services, etc. [12].

110 Again, although the layered architecture has its own ad-
 111 vantages and performs well in wired networks in terms of
 112 portability, flexibility and low design complexity, it is not
 113 suitable for wireless networks, especially in wireless *ad hoc*
 114 networks. The reason for its inadequacy in wireless scenarios
 115 is that the services offered by the layers to those above them
 116 in Fig. 2 are realized by specifically tailored protocols for the
 117 different layers and that the architecture forbids direct com-
 118 munication between non-adjacent layers. The communication
 119 between adjacent layers is limited to procedure calls and to their

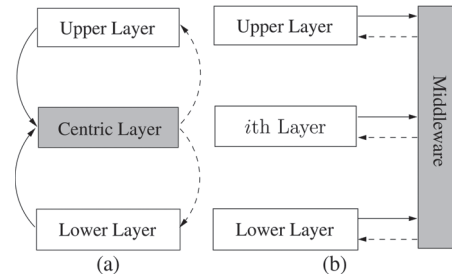


Fig. 3. Conceptual illustration of cross-layer design methods. (a) Layer-centric solution; (b) centralized solution.

120 responses. Moreover, the hostile wireless links impose several
 121 new problems on the associated protocol design that cannot
 122 be readily handled by the layered architecture [13]. More
 123 explicitly, having a strict layered design is not flexible enough to
 124 cope with the dynamics of Mobile *Ad hoc* Network (MANET)
 125 environments and will thus result in a low performance [14].
 126 Thus, the mutual impact of the layers on each other cannot
 127 be ignored [15]. Hence the concept of cross-layer design has
 128 been proposed in an attempt to achieve a performance gain by
 129 exploiting the close interaction amongst the different layers.
 130 Srivastava and Motani [13] defined “Cross-Layer operation”
 131 as: “Protocol design by the violation of a reference layered
 132 communication architecture is cross-layer design with respect
 133 to the particular layered architecture”, while Jurdak [15] define
 134 it as: “Cross-layer design with respect to a reference layered
 135 architecture is the design of algorithms, protocols, or architec-
 136 tures that exploit or provide a set of inter-layer interactions that
 137 is a superset of the standard interfaces provided by the reference
 138 layered architecture”. Therefore, cross-layer operation may be
 139 interpreted as the ‘violation’ of the layered architecture seen
 140 in Fig. 2, which requires more interaction amongst the layers,
 141 beyond the interaction between the adjacent layers. Cross-layer
 142 design clearly requires information exchange between layers, as
 143 well as adaptivity to this information at each layer and a certain
 144 grade of diversity built into each layer for the sake of improving
 145 the achievable robustness [5].

146 There are two basic methods of information sharing in cross-
 147 layer design [16]. One of them makes the variables of a specific
 148 layer visible to the other layers, which is referred to as a layer-
 149 centric solution. The other relies on a shared middleware [15],
 150 [16], which provides the service of storage/retrieval of infor-
 151 mation to all layers, which is termed as a centralized solution.
 152 Fig. 3 illustrates how these two cross-layer solutions operate.

153 The basic principles of the above-mentioned pair of cross-
 154 layer solutions are:

- 155 • **The layer-centric solution:** A certain layer is allowed to
 156 be the central layer, which controls the cross-layer adap-
 157 tation by accessing the internal protocol parameters and
 158 algorithms of the other layers, as shown in Fig. 3(a). Al-
 159 though this approach significantly improves the attainable
 160 system performance, it violates the layered architecture,
 161 since it requires access to the internal variables of other
 162 layers.
- 163 • **The centralized solution:** A middleware or a system-level
 164 monitor (centralized optimizer) is employed for estimating
 165 both the availability of resources and the environmental

TABLE I
MAJOR CONTRIBUTIONS OF CROSS-LAYER DESIGN IN *Ad Hoc* NETWORKS

Year	Authors	Contribution
2005	Setton <i>et al.</i> [18]	Explored the potential synergies of exchanging information between different layers to support real-time video streaming.
2006	Liu <i>et al.</i> [19]	Proposed a scheduling algorithm at the MAC layer for multiple connections under diverse QoS requirements, where each connection employs both adaptive modulation and coding at the PHY layer for transmission over wireless channels.
2007	Huang and Letaief [20]	Proposed a cross-layer optimization framework to jointly design the scheduling, power control and adaptive modulation.
2008	Zhang and Zhang [21]	Reviewed the state-of-the-art on the cross-layer paradigm and discussed the open issues related to cross-layer design for QoS support.
2009	Oh and Chen [22]	Presented a cross-layer design for reliable video transmission based on a multichannel MAC protocol in the context of time division multiple access.
2010	Chu and Wang [23]	Presented cross-layer centralized and distributed scheduling algorithms, which exploited the PHY layer channel information to opportunistically schedule cooperative spatial multiplexed transmissions between MIMO-based nodes.
2011	Ghosh and Hamouda [24]	Proposed a cross-layer antenna selection algorithm for improving the transmission efficiency in cognitive MIMO-aided <i>ad hoc</i> networks.
2012	Mardani <i>et al.</i> [25]	Jointly considered flow control, multipath routing and random access control based on network utility maximization.
2013	Uddin <i>et al.</i> [26]	Studied cross-layer design in random-access-based fixed wireless multihop networks under a physical interference model.
2014	Tang <i>et al.</i> [27]	Proposed a cross-layer distributed approach for maximizing the network throughput by jointly selecting stable routes and assigning channels based on mobility prediction.

166 dynamics, for the sake of coordinating the allocation of
 167 resources across diverse applications as well as nodes, and
 168 for adapting the protocols' parameters within each layer
 169 based on the dynamics experienced, as shown in Fig. 3(b).
 170 This approach requires each layer to forward the complete
 171 information characterizing its protocol parameters and
 172 algorithms to the middleware or system monitor. It also
 173 requires each layer to carry out the actions requested by the
 174 central optimizer. This approach also violates the layered
 175 architecture. The so-called MobileMan [14] and CrossTalk
 176 [17] protocols constitute important centralized cross-layer
 177 solutions.

178 The cross-layer operation aided design of wireless *ad hoc*
 179 networks poses challenges mainly due to the time-variant char-
 180 acteristics of wireless channels. The signal is substantially more
 181 vulnerable to the effects of noise, fading and interference than
 182 in benign fixed networks, leading to potential performance
 183 degradations within the higher layers. For example, a packet has
 184 to be retransmitted in the DL layer or the transmit power has to
 185 be adjusted to guarantee its high-integrity transmission, which
 186 may impose interference on other nodes or promote aggressive
 187 contention for channel access. In the NET layer, the current
 188 route may become invalid and hence route maintenance/repair
 189 has to be activated or even a new route discovery process has to
 190 be initiated. As a result, potentially more energy is consumed
 191 and the end-to-end delay is increased, while the end-to-end
 192 throughput is reduced. Therefore, careful adaptation of the
 193 protocol stack should be used at each layer to compensate for
 194 the variations at that layer, depending on the specific time scale
 195 of these variations [5]. Both the local adaptation of parameters
 196 within each layer and the adaptation based on the other layers
 197 have to be considered. For example, the transmit power, the
 198 signal processing hardware's power dissipation, the information
 199 transmit rate, the coding and modulation schemes, the Frame
 200 Error Ratio (FER) and the mobility in the PHY layer consti-

tute important parameters, which may be beneficially shared 201
 with other layers. The protocol design of the upper layers has 202
 to consider the information gleaned from the PHY layer for 203
 minimizing the energy consumption, the resource allocation, 204
 scheduling and the queueing management, while maintaining 205
 a certain QoS guarantee. Meanwhile, the number of retransmis- 206
 sions, as well as both the routing and network topology related 207
 information received from the upper layers may be beneficially 208
 shared. Additionally, node cooperation also calls for cross-layer 209
 design [13]. Table I is presented for discussing the previous 210
 work on cross-layer design in a compact manner. 211

These cross-layer aided designs may be classified into several 212
 categories according to their different application requirements. 213
 They might be designed for reducing the energy consumption, 214
 the end-to-end delay [21], for improving the network's through- 215
 put [18], [22], [24], [26], [27], for striking a flexible tradeoff 216
 between any two of them [20], [23], and even for multiple- 217
 constraint optimization [19], [21]. 218

As detailed above, cross-layer design has substantial benefits, 219
 but it has its own disadvantages as well. For example, the cross- 220
 layer interactions create dependencies amongst the layers, 221
 which will affect not only the layer concerned, but also the other 222
 layers. Hence, a complete redesign of the operational networks 223
 and protocols will lead to a high implementational cost [16]. 224
 Therefore, cross-layer design should be carefully crafted, be- 225
 cause once the seven-layer OSI structure is violated, the benefits 226
 of independent, layer-specific protocol design will disappear 227
 [13], [28]. The effects of any protocol chosen in every single 228
 layer on the overall system has to be carefully considered. 229

B. Categories of *Ad Hoc* Routing Protocols

230

The NET layer of Fig. 2 plays a key role in *ad hoc* networks, 231
 which substantially influences the performance of the overall 232
 system. The NET layer is responsible both for allocating IP 233

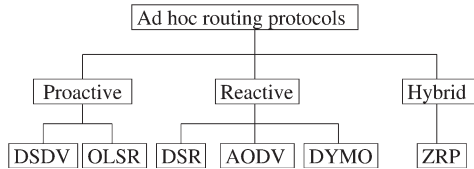


Fig. 4. Categorization of *ad hoc* routing protocols (DSDV: Destination-Sequenced Distance Vector routing; OLSR: Optimized Link State Routing; DSR: Dynamic Source Routing; AODV: Ad-hoc On-demand Distance Vector routing; DYMO: DYnamic Manet On-demand routing; ZRP: Zone Routing Protocol).

addresses and for choosing the right route for communication between the source and destination. The routing protocols of *ad hoc* networks may be classified as proactive routing, reactive routing and hybrid routing [29], as shown in Fig. 4.

The proactive routing periodically transmits “hello” packets for the sake of identifying all possible routes in the network. Hence every node has to maintain a routing table, which stores the route spanning from itself to all other available nodes. The advantage of this kind of routing protocol is that the route discovery time is low. By contrast, its disadvantage is that each node has to maintain a routing table. If the number of nodes in the network becomes high, then the routing table becomes large and hence requires a large memory. On the other hand, periodically sending “hello” packets increases the network control load imposed. The so-called Destination-Sequenced Distance Vector (DSDV) [30] protocol and the Optimized Link State Routing (OLSR) [31] protocol are typical proactive routing protocols, as seen in Fig. 4.

The reactive routing protocols are source-driven, implying that they transmit route discovery packets to find a route to the destination, when there is sufficient data scheduled for transmission in the buffer, instead of periodically broadcasting the “hello” packets. As a benefit, not all nodes have to maintain a route table for storing the routes leading to all other nodes. Instead, they only store routes that were found during the process of route discovery. This technique reduces the network control load compared to the proactive routing protocols of Fig. 4. The disadvantage of this routing protocol family is however that their delay is increased, because a route has to be found to the destination, when no routes leading to the destination exist in the route table. Additionally, the nodes’ movement changes the network’s topology, which hence requires the transmission of more control packets for the sake of maintaining the current communication session. As seen in Fig. 4, the Dynamic Source Routing (DSR) [32], Ad-hoc On-demand Distance Vector (AODV) [33] and DYnamic Manet On-demand (DYMO) [34] routing protocols constitute typical reactive routing protocols.

Based on beneficially combining the advantages, whilst avoiding the disadvantages of the above-mentioned protocol families, hybrid routing protocols may also be conceived. We may divide the entire *ad hoc* network into several small areas and in each area proactive routing may be employed for establishing a link for all nodes. By contrast, between the areas, reactive routing protocols may be adopted for reducing the number of control packets required. Hybrid protocols are widely applied in large *ad hoc* networks. The so-called Zone Routing Protocol (ZRP) [35] is a typical hybrid routing protocol.

C. Review of Cross-Layer Aided Routing Protocols

281

This treatise is mainly dedicated to cross-layer operation aided routing design in *ad hoc* networks, hence we list the major contributions to the literature of cross-layer aided routing protocols conceived for *ad hoc* networks in Table II.

Similarly, these cross-layer aided routing protocols may be classified into several categories according to their different application requirements. They might be designed for reducing the energy consumption [38], [48], [52], the end-to-end delay [47], for improving the network’s throughput [39], [49], [54], for striking a flexible tradeoff between any two of them [26], [42], [45], [46], [50], [51], and even for multiple-constraint optimization [36], [41], [43], [44].

D. Review of Energy-Efficient Routing Protocols

294

As mentioned in Section I-C, cross-layer design may be studied based on diverse application requirements. This paper focuses on cross-layer design techniques conceived for reducing the energy consumption. **since energy saving in wireless *ad hoc* networks is of salient importance in the interest of mitigating the problem of limited battery supply at each node. In *ad hoc* networks the nodes actively and voluntarily participate in constructing a network and act as relays for other nodes. As a result of node-mobility, the Channel State Information (CSI) varies and hence a substantial amount of control messages have to be exchanged across the network to maintain reliable communications between certain pairs of nodes, which potentially imposes a high energy-consumption. Therefore, minimizing the energy consumption becomes extremely important.** Numerous power-aware routing protocols were proposed in [55] for improving the energy efficiency from a multiuser networking perspective. Firstly, a compact-form review of energy-efficient single-layer routing design is provided in Table III.

Moreover, cross-layer optimized power control has been widely exploited [66]–[71] for maintaining the required target-integrity at a low power in realistic propagation environments. A physical-layer-oriented routing protocol supported by sophisticated power control was proposed in [66] for a Line-Of-Sight (LOS) and shadow faded scenario, where the estimated end-to-end BER of a multi-hop path was used as the route selection metric. Furthermore, an adaptive relaying strategy switching between the Amplify-and-Forward (AF) and the Decode-and-Forward (DF) schemes was proposed in [67] for reducing both the energy consumption as well as the delay of the system. As a further design dilemma, the influence of the ‘small number of long hops’ versus the ‘many short hops’ philosophy on the energy consumption was studied in [68]–[70]. It was indicated in [68] that the ‘small number of long hops’ routing scheme was better than the ‘many short hops’ routing scheme provided that near-capacity coding strategies combined with a relatively short block length were employed, because a substantial SNR loss was exhibited by the ‘many short hops’ based routing scheme. Moreover, it was demonstrated in [69] that ‘many short hops’ perform well in energy-limited scenarios relying on spatial reuse, even in the absence of interference cancellation, while using a ‘small number of long hops’ is more suitable for

TABLE II
MAJOR CONTRIBUTIONS OF CROSS-LAYER AIDED ROUTING PROTOCOLS IN *Ad Hoc* NETWORKS

Year	Authors	Contribution
2002	Goldsmith and Wicker [36]	Reviewed each layer's protocol and emphasized the necessity of cross-layer design, particularly in energy-limited scenarios.
2005	Souryal <i>et al.</i> [37]	Proposed efficient channel-quality-aware adaptive routing relying on adaptive modulation.
	Lee <i>et al.</i> [38]	Combined power-aware routing with a MAC layer algorithm for minimizing the total consumed power.
2006	Johansson and Xiao [39]	Jointly optimized the end-to-end communication rates, routing, power allocation and transmission scheduling of a network.
	Mao <i>et al.</i> [40]	proposed a Genetic Algorithm (GA)-based application-centric cross-layer approach for minimizing video distortion.
	Abdrabou and Zhuang [41]	Presented a position-aware QoS routing scheme by considering its interactions with the MAC.
	Zhang <i>et al.</i> [42]	Addressed the topic of energy-efficient routing subject to both packet delay and multi-access interference constraints.
2007	Kompella <i>et al.</i> [43]	Optimized the performance of Multiple Description (MD) video subject to certain routing and link layer constraints.
	Chiang <i>et al.</i> [44]	Surveyed the functional modules, such as congestion control, routing, scheduling, random access, power control and channel coding.
2008	Phan <i>et al.</i> [45]	Presented a cross-layer optimization approach jointly considering the design of the MAC, routing and energy distribution.
	Liu <i>et al.</i> [46]	Jointly optimized the power and bandwidth allocation at each node and designed multihop/multipath routing for a MIMO-based wireless <i>ad hoc</i> network.
2009	Abdrabou and Zhuang [47]	Proposed a routing scheme based on a geographical on-demand routing protocol, which is capable of guaranteeing a certain maximum end-to-end delay.
	Li <i>et al.</i> [48]	Proposed a combined multi-rate power controlled MAC protocol and routing protocol relying on the effective transport capacity as the routing metric.
2010	Ding <i>et al.</i> [49]	Proposed a ROuting and dynamic Spectrum-Allocation (ROSA) algorithm aiming for maximizing the network's throughput by performing joint routing, dynamic spectrum allocation, scheduling and transmit power control.
	Lu <i>et al.</i> [50]	Presented Joint Channel Assignment and Cross-layer Routing (JCACR) by employing two metrics, namely the Channel Utilization Percentage (CUP) and the Channel Selection Metric (CSM).
2011	Ding and Leung [51]	Proposed cross-layer routing applying both cooperative transmission and path selection for striking a tradeoff between the transmit power consumption and the end-to-end reliability.
	Tavli and Heinzelman [52]	Presented real-time multicasting based routing.
2012	Syue <i>et al.</i> [53]	Proposed a relay-aware cooperative routing protocol relying on cross-layer design.
2013	Pan <i>et al.</i> [54]	Investigated the path selection problem based on the cross-layer optimization in on flow routing, multihop Cognitive Radio Networks(CRNs) under constraints link scheduling and CR source's budget.
2014	Uddin <i>et al.</i> [26]	Studied cross-layer design in random-access-based fixed wireless multihop networks under a physical interference model.

TABLE III
MAJOR CONTRIBUTIONS OF SINGLE LAYER ENERGY-EFFICIENT ROUTING PROTOCOLS IN *Ad Hoc* NETWORKS

Year	Authors	Contribution
2005	Muruganathan <i>et al.</i> [56]	Proposed a centralized routing protocol referred to as a base-station controlled dynamic clustering protocol, which distributes the energy dissipation evenly among all sensor nodes for improving the network lifetime and for achieving average energy savings.
2006	Zhu <i>et al.</i> [57]	Proposed a minimum energy dissipation routing protocol based on an accurate model, which took into account the energy consumption of both the data packets, as well as of the control packets and retransmissions.
2007	Baek and Veciana [58]	Investigated the employment of proactive multipath routing to achieve a tradeoff between the energy cost of spreading traffic and the improved spatial balance of energy.
2008	Eidenbenz <i>et al.</i> [59]	Designed an energy-efficient distributed algorithm based on the so-called side payment scheme in conjunction with a game-theoretic technique to achieve truthfulness for the rational selfish nodes.
2009	Liang <i>et al.</i> [60]	Designed energy-efficient routing algorithms, which constructed a shared multicast tree spanning all terminal nodes, while ensuring that the total energy consumption of realizing all-to-all multicasting was minimized.
2010	Li <i>et al.</i> [61]	Proposed a virtual-link-reduction-based broadcasting protocol using directional antennas.
2011	Ma and Yang [62]	Proposed an online computable discrete-time mathematical energy model for characterising the battery discharging behavior and proposed a battery-aware routing scheme that incorporates battery awareness into routing protocols.
2012	Akhtar <i>et al.</i> [63]	Designed a cooperative routing algorithm, which took the electronic power consumption into consideration, when constructing the minimum-power route leading from source to destination.
2013	Lu and Zhu [64]	Proposed an energy-efficient genetic algorithm aided mechanism, which depended on bounded end-to-end delay and minimum energy cost of the multicast tree, to solve QoS based multicast routing problems.
2014	Vazifehdan <i>et al.</i> [65]	Proposed an energy-efficient routing algorithm, which finds routes minimizing the total energy required for end-to-end packet delivery.



Fig. 5. Structure of this treatise.

bandwidth-limited scenarios. Therefore, the routing algorithms should be carefully designed, when jointly considering both the achievable energy-efficiency and the attainable bandwidth-efficiency. The tradeoffs between energy- and bandwidth-efficiency were studied in [70], where it was found that at high end-to-end data rates the routes associated with fewer hops minimize the energy consumption, while at lower end-to-end data rates the routes having more hops mitigate it.

E. Outline

Based on the discussions in the previous sections, the rest of the paper is organized as follows: First, we study the cross-layer aided routing design jointly considering both the PHY layer and the NET layer [72], as shown in Section II; Then in Section III we further investigate the cross-layer aided routing design concept by jointly considering the PHY layer, the DL layer and the NET layer [73], [74]. We commence by considering Traditional Routing (TR) relying on a fixed transmit power in Section III-A, while TR combined with Power Allocation (PA) is discussed in Section III-B and Opportunistic Routing (OR) using PA is studied in Section III-C; Finally, Section IV concludes this treatise and offers some design guidelines. Fig. 5 lists the structure of this paper.

The notations used in this treatise are defined as follows:

- N : the number of nodes in the network;
- H : the number of hops in an established route;
- N_r : the maximum number of MAC retransmissions, including the first transmission attempt;
- P_i : the transmit power of each node;
- P_{i_i} : the transmit power in the i -th node of the established route;
- FER_i : the FER of the i -th link in an established route;
- p_i : the successful reception probability of the i -th link, where $p_i = 1 - FER_i$;
- E_T : the sum of the energy dissipated by all the nodes in the network, including the data packets and the control packets;
- \bar{E}_T : the overall energy dissipation E_T normalized by the number of bits received in the application layer of the destination;
- E_{total} : the sum of the energy dissipated by the data packets during their transmission in the network;
- \bar{E}_{total} : the total energy dissipation E_{total} normalized by the end-to-end successful reception probability, which is the average energy consumption dissipated by the entire system during the successful delivery of a packet from the source to the destination;
- R_{e2e} : the number of information bits successfully delivered to the destination per second.

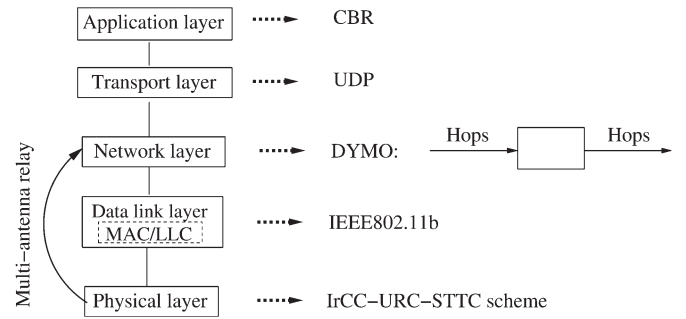


Fig. 6. System model of the energy-efficient routing with PHY & NET cooperation in *ad hoc* networks.

II. ROUTING DESIGN WITH PHY & NET COOPERATION

Energy-efficient wireless network design has recently attracted wide-spread research attention [75]. Diverse resilient Forward Error Correction (FEC) schemes were proposed in [76] for achieving a low Bit Error Ratio (BER) at near-capacity Signal-to-Noise Ratio (SNR) values. Therefore, the effective transmission range can be improved, when the required received signal power is reduced. Again, an Irregular Convolutional Coded, Unity-Rate Coded and Space-Time Trellis Coded (IrCC-URC-STTC) scheme has been proposed for cooperative communications in [77]. Several Single-Antenna RNs (SAs) were activated between the source and the destination. The RNs roaming closest to their optimal locations were activated based on a technique relying on EXtrinsic Information Transfer (EXIT) charts [78] in conjunction with near-capacity code design principles, which were detailed for example in [79].

However, the solution disseminated in [72] aims for minimizing the energy consumption by the joint design of both the PHY and NET layers with the assistance of Multiple-Antenna Aided Relay Nodes (MA-RN), as shown in the system model of Fig. 6. Although the routing metric is still the number of hops, the employment of MA-RNs assists in reducing the potential number of hops from the source to the destination, when dissipating a given transmit power at each node. Therefore MA-RNs are capable of reducing the entire system's energy consumption. The influence of the number of MA-RNs in a system will be studied in Section II-C. Both the perfect capacity-achieving coding abstraction and a realistic near-capacity coding scheme, namely a three-stage-concatenated IrCC-URC-STTC arrangement is employed in the PHY layer. The IEEE802.11b regime [7] is used in the DL layer. In the NET layer, the more efficient DYMO routing protocol [34] is employed, because the DYMO protocol imposes a lower network control load and it is more flexible in a high-mobility environment. However, the scenario considered in [72] is a stationary scenario. The investigation of high-mobility scenarios was set aside for its future study. The User Data Protocol UDP [80] is employed in the transport layer and CBR data streaming is used in the application layer. The channel model employed is an Additive White Gaussian Noise (AWGN) channel subjected to both inverse-second-power free-space path loss and to uncorrelated Rayleigh fading.

A. Near-Capacity Coding Schemes

Each MA-RN is assumed to be equipped with two antennas. If more than one MA-RN exist in the multi-hop *ad hoc*

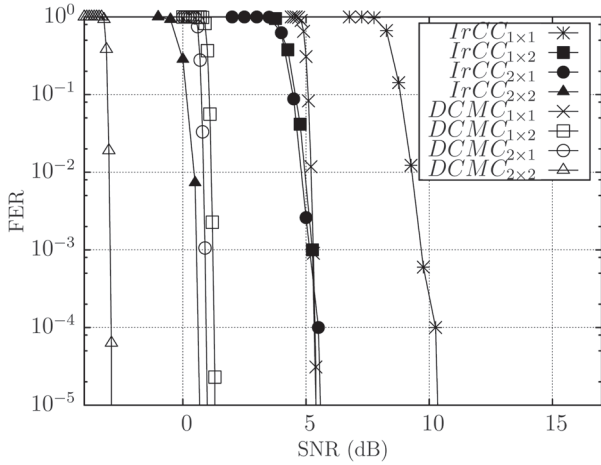


Fig. 7. FER performance of the four types of links, for example at the frame length of 1500 bits, of the uncorrelated Rayleigh fading channel for DCMC-capacity-based scheme and the IrCC-URC-STTC scheme, where $DCMC_{T \times R}$ represents the DCMC-capacity-based scheme, and $IrCC_{T \times R}$ represents the IrCC-URC-STTC scheme. Additionally, the subscript ' $T \times R$ ' represents having T transmit antennas and R receive antennas. Moreover, the overall FEC code rate is $R_c = 0.5$, the effective throughput is 1 bps (bits/symbol), the number of transmitted frames is 10 000 and the IrCC has 17 component codes, associated with the weights [0.049, 0, 0, 0, 0, 0.24, 0.16, 0.12, 0.035, 0.102, 0, 0.071, 0.093, 0, 0.091, 0, 0.039].

network considered, then four different types of links may appear. Specifically, there exists the SA-RN to SA-RN, SA-RN to MA-RN, MA-RN to SA-RN and finally the MA-RN to MA-RN links. All the MA-RNs employ the Quadrature Phase-Shift Keying (QPSK)-assisted IrCC-URC-STTC scheme, while all the SA-RNs employ the 8-ary Phase-Shift Keying (8PSK)-assisted IrCC-URC scheme.

For example, the FER performance of all the four links at the frame length of 1500 bits characterized by the Discrete-input Continuous-output Memoryless Channel's (DCMC)-capacity [81] and that of the IrCC-URC-STTC scheme is portrayed in Fig. 7. It can be observed that the IrCC-URC-STTC scheme performs close to the DCMC-capacity based scheme at a given SNR value. Meanwhile, the $IrCC_{2 \times 2}$ scheme has a 5 dB gain compared to $IrCC_{2 \times 1}$ or $IrCC_{1 \times 2}$ arrangements and has a nearly 10 dB gain compared to the $IrCC_{1 \times 1}$ scheme at an FER of 10^{-5} , where $IrCC_{T \times R}$ represents the IrCC-URC-STTC scheme and the subscript ' $T \times R$ ' indicates having T transmit and R receive antennas. Hence, for the sake of guaranteeing the same FER performance, $IrCC_{2 \times 2}$ exhibits a larger transmit range at a given transmit power and may hence potentially reduce the number of hops required for conveying a message from the source to the destination, which can be explained by analyzing the calculation of the transmission range. More explicitly, the average maximum transmission range is defined as the range, over which the receiver node is capable of receiving a transmitted packet with $FER < 10^{-5}$.

The required minimum signal-to-noise ratio SNR_{dB}^* may be calculated from the minimum receive power P_r^* expressed in dBm as follows

$$SNR_{dB}^* = 10 \log_{10} \left(\frac{P_r^*}{N_0} \right), \quad (1)$$

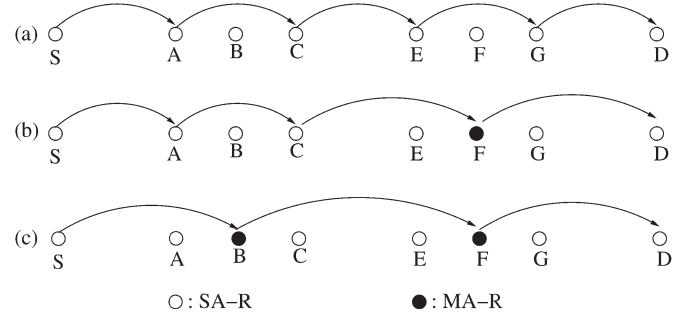


Fig. 8. The influence of MA-RNs on the routing strategy: (a) $H = 5$ hops without MA-RNs; (b) $H = 4$ with 1 MA-RN at point F ; (c) $H = 3$ with 2 MA-RNs at points B and F .

where N_0 is the thermal noise power. Hence, given the transmitted power P_t and SNR_{dB}^* , the average maximum distance d_{max} from the transmitter, where the SNR requirement SNR_{dB}^* may 'just' be satisfied to guarantee $FER < 10^{-5}$, is given by

$$d_{max} = \frac{\sqrt{P_t} \lambda}{4\pi 10^{\left(\frac{SNR_{dB}^* + N_{0dB}}{20}\right)}}, \quad (2)$$

where the carrier's wavelength $\lambda = c/f$ and $N_{0dB} = 10 \log_{10} N_0$. c is the speed of light in vacuum and f is the carrier frequency.

Naturally, if the value of P_t and N_{0dB} are fixed, then it may be readily seen how the adequately 'illuminated' distance, where the required target-FER may be maintained, will vary as a function of the SNR value. As seen from Fig. 7, the maximum adequately covered communication distance from MA-RN to MA-RN is the highest, while that from SA-RN to SA-RN is the lowest. Conversely, if P_t and d_{max} are fixed, then the FER is the lowest for the MA-RN to MA-RN link, while it is the highest for the SA-RN to SA-RN link.

B. Routing Algorithms

It was shown in [77] that the IrCC-URC-STTC scheme is capable of operating near the link's capacity, hence a substantial power saving may be attained. When this scheme is employed by the MA-RNs of the *ad hoc* network considered, the different error correction capability of the four different types of links will influence the routing strategy. Fig. 8 provides an example on how the routing strategy is influenced.

As seen from Fig. 8, the network consists of $N = 8$ nodes, where S is the source and D is the destination. In Fig. 8(a), all nodes are equipped with a single antenna, hence all links are SA-RN to SA-RN links, which yields $H = 5$ hops from S to D . A single MA-RN is employed at point F in Fig. 8(b), where the packets arriving at node C are directly transmitted to node F . Then, node F will forward its received packets further to the destination D . More specifically, the C -to- F link is a SA-RN to MA-RN link, while the F -to- D link is an MA-RN to D link, where the $F - D$ distance is higher than that between the single-antenna nodes of Fig. 8(a). Consequently, the number of hops from S to D is decreased to $H = 4$. In Fig. 8(c), two MA-RNs, namely B and F , are employed. The number of hops is further decreased to $H = 3$ as a benefit of using MA-RNs for nodes B and F .

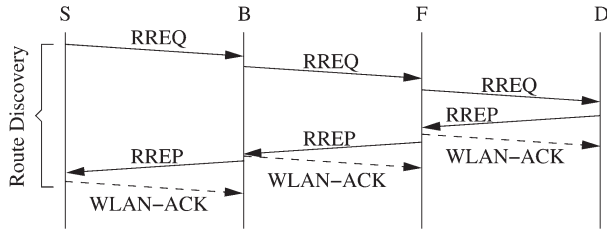


Fig. 9. The process of **route discovery** in the DYMO routing algorithm.

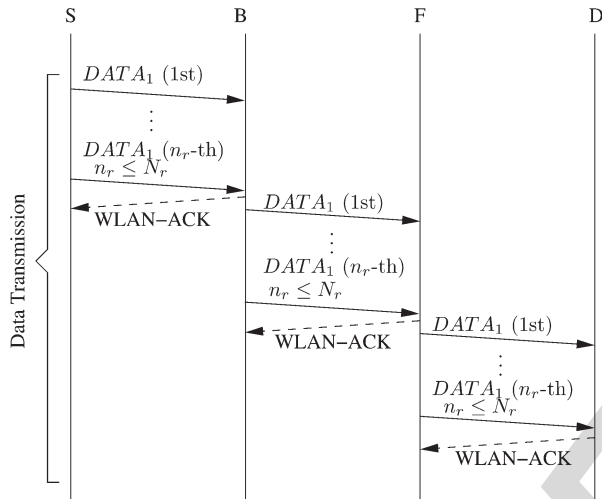


Fig. 10. The process of **data transmission** after a route is found from source A to destination D.

496 The DYMO routing protocol is employed in the NET layer,
 497 which combines most of the benefits of the AODV [33] and
 498 DSR [32] protocols. The DYMO routing protocol always opts
 499 for the specific route having the lowest number of hops to the
 500 destination. When employing the MA-RN aided IrCC-URC-
 501 STTC scheme, it will be demonstrated that the route selected
 502 may be expected to have a further reduced number of hops.
 503 The DYMO routing protocol is constituted by two main stages,
 504 namely the route discovery and route maintenance. During the
 505 route discovery, the Route REQuest (RREQ) and the Route
 506 REPLY (RREP) packets are used for identifying a route from
 507 the source to the destination. By contrast, during the route
 508 maintenance phase, a Route ERRor (RERR) packet is returned
 509 to the source, when a broken link is detected. Figs. 9–11 show
 510 the process of route discovery and data transmission as well
 511 as route maintenance for the DYMO routing protocol, which
 512 assisted us in analyzing the total energy consumption of the
 513 system. The topology considered in Figs. 9–11 has a source S,
 514 a destination D and the pair of RNs B and F. It is assumed that
 515 each node is only capable of communicating with its neighbour
 516 nodes. For example, node B can only communicate with node
 517 S and node F, while it cannot communicate with node D. The
 518 exchange of the control packets between the neighbour nodes,
 519 such as the exchange of the RREQ packet, RREP packet and
 520 RERR packet, and the associated data transmission process is
 521 detailed as follows:

522 • Route Discovery process of Fig. 9.

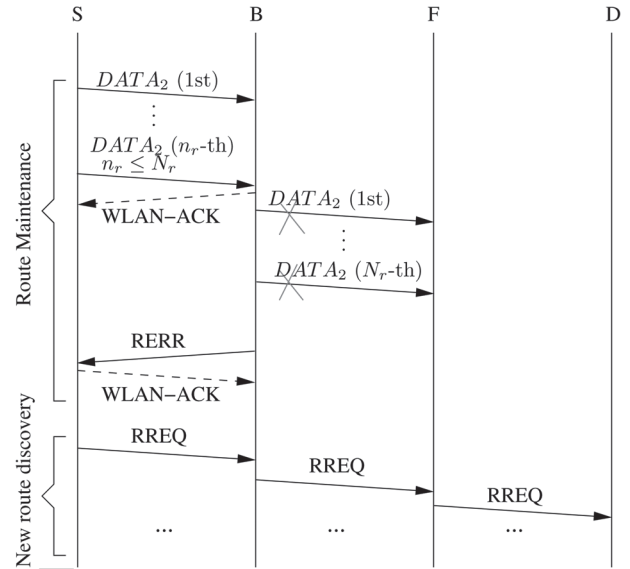


Fig. 11. The process of **route maintenance** in the DYMO routing algorithm.

As seen in Fig. 9, first the source S broadcasts an RREQ 523 packet and when node B receives this RREQ packet, it 524 broadcasts it. Then node F receives the RREQ packet and 525 broadcasts it again. Finally, the destination D receives the 526 RREQ packet, which originated from the source S; The 527 destination D responds to the RREQ packet with a newly 528 generated RREP packet. The routing table of each node 529 is refreshed, when ever an RREQ/RREP packet arrives 530 at a node. Additionally, a Wireless Local Area Network- 531 Acknowledgement (WLAN-ACK) packet¹ is required for 532 confirming the successful reception of the RREP packet. 533

- Data Transmission process of Fig. 10. 534

When the RREP packet arrives at the source S during 535 the process of route discovery, the source S is informed 536 of a route spanning from the source S to the destination 537 D, with node B being the next hop of this route. Hence, 538 as seen in Fig. 10, the buffered data packet $DATA_1$ is 539 transmitted to node B according to the routing information 540 stored in the routing table of source S. If the packet $DATA_1$ 541 failed to reach node B, then node B has to retransmit 542 the packet $DATA_1$ until the number of retransmission 543 reaches its maximum of N_r . If and only if node B receives 544 the packet $DATA_1$ successfully within n_r retransmissions, 545 where $n_r \leq N_r$, it would respond to source S by sending 546 back a WLAN-ACK packet. The WLAN-ACK is used 547 for confirming the successful transmission of the packet 548 $DATA_1$. Meanwhile, node B forwards the packet $DATA_1$ to 549 node F, since node F is its next hop *en route* to destination 550 D. The routing information stored in node B's routing table 551 is obtained during the route discovery process as well. In 552 a similar way, if node F successfully receives the packet 553 $DATA_1$, it respond with a WLAN-ACK to node B and 554

¹The Acknowledgement packet is the one, which is returned to the transmitter as the acknowledgement of the correctly received data in the DL layer, hence it is referred to as WLAN-ACK in this treatise, where 'WLAN-ACK' represents the ACK packet employed in the IEEE802.11 standard. It is assumed that no Request-To-Send (RTS)/Clear-To-Send (CTS) mechanism is employed.

555 forwards the packet $DATA_1$ to the destination D according
 556 to its own routing table. Finally, if the destination D suc-
 557 cessfully receives the packet $DATA_1$, it only has to respond
 558 with a WLAN-ACK packet to node F . Destination D
 559 does not forward the packet $DATA_1$, because it is the final
 560 destination of the packet $DATA_1$. Hence the packet from
 561 the source S to the destination D has been completed.

562 • Route Maintenance process of Fig. 11.

563 The process of route maintenance is graphically illus-
 564 trated in Fig. 11, where the transmission of the packet
 565 $DATA_2$ from the source S to the destination D is exem-
 566 plified. First the packet $DATA_2$ is transmitted by the source S
 567 to node B . Node B receives the packet $DATA_2$ successfully
 568 during the n_r -th retransmission, where $1 \leq n_r \leq N_r$ and it
 569 responds with a WLAN-ACK packet to the source S for
 570 confirming the successful reception of the packet $DATA_2$.
 571 Then node B forwards the packet $DATA_2$ to node F .
 572 However, node F fails to receive the packet $DATA_2$ suc-
 573 cessfully after N_r retransmissions by node B . Therefore,
 574 no response is sent from node F to node B . Once the pre-
 575 set timer expires at node B and node B has not received any
 576 WLAN-ACK packet from node F , then node B considers
 577 the link $B - F$ to be broken and actively sends an RERR
 578 packet to its adjacent-node, namely to the source S . Source
 579 S updates its own routing table by deleting all the routes,
 580 which include the link $B - F$. Therefore, the source S does
 581 not have a route to the destination D and a new route
 582 discovery process has to be activated. Hence, an RREQ
 583 packet is broadcast by the source S again, as shown in
 584 Fig. 11.

585 Every node is assumed to has the same transmit power of P_T .
 586 Consequently, the sum of the energy E_T dissipated by all nodes
 587 in the network is given by

$$E_T = \sum E_{Route_Discovery} + \sum E_{Data_Transmission} + \sum E_{Route_Maintenance}, \quad (3)$$

588 where E_T indicates the energy dissipated by a specific network
 589 topology. $\sum E_{Route_Discovery}$ denotes the sum of energy dissi-
 590 pated by the RREQ, the RREP and the WLAN-ACK packets
 591 during the route discovery phase, which is shown in Fig. 9.
 592 Furthermore, $\sum E_{Route_Maintenance}$ includes all the energy during
 593 the route maintenance phase, except for $\sum E_{Data_Transmission}$,
 594 which is the energy dissipated by the data packets and by
 595 the corresponding WLAN-ACK packets, as shown in Figs. 10
 596 and 11.

597 C. System Analysis

598 The overall energy consumption E_T of the entire network is
 599 dependent on numerous parameters, such as the node density
 600 ρ , the number of MA-RNs n_{MA} , the mobile speed, the number
 601 of hops H of the selected route and the amount of bits L_{app}
 602 received in the application layer of the destination. To reduce
 603 the dimensionality of the investigations when characterizing
 604 the benefits of MA-RNs on the node's achievable transmission
 605 range and FER performance, the node density ρ , the mobile
 606 speed and L_{app} are assumed to be constant, then E_T is further
 607 normalized by L_{app} and N of the entire network, where N is re-

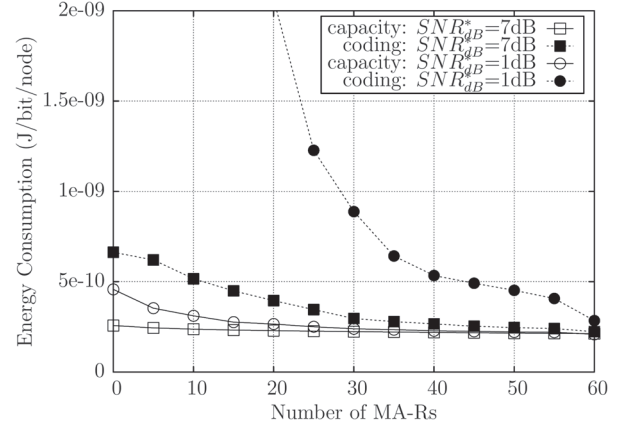


Fig. 12. Energy consumption \bar{E}_T versus the number of MA-RNs n_{MA} aiming for comparing the IrCC-URC-STTC scheme and the DCMC-capacity-based benchmark scheme at SNR_{dB}^* of 7 dB and 1 dB, where ‘coding’ denotes the IrCC-URC-STTC scheme and ‘capacity’ represents the DCMC-capacity-based benchmark scheme.

TABLE IV
SYSTEM PARAMETERS

Path-loss exponent	2
Sensitivity threshold [82], P_r^*	-85 dBm
Mobility	stationary(0 m/s)
Simulation time	30 second
Number of simulation runs	100

608 related to the node density. Finally, the Normalized Energy Con-
 609 sumption (NEC) \bar{E}_T of the entire network can be expressed as: 609

$$\bar{E}_T = \frac{E_T}{NL_{app}} = F(n_{MA}, H). \quad (4)$$

610 Four scenarios are considered to study the relationship be-
 611 tween the number of MA-RNs and the energy consumption, 611
 612 where $N = 60$ stationary nodes are uniformly located in a 612
 613 $500 \text{ m} \times 500 \text{ m}$ field, hence the node density is $\rho = 240$ nodes
 614 per square kilometer. The source S and the destination D are
 615 located in the position (499, 499) and (0, 0), respectively. The
 616 number of MA-RNs² is increased from $n_{MA} = 0$ to $n_{MA} = 60$
 617 in steps of 5. The frame length of the data packets, which are
 618 generated by the application layer, is $L_{app} = 504$ Bytes. The
 619 802.11b standard is employed in the DL layer. The transmit
 620 power is set to $P_T = 1$ mW. The other system parameters
 621 employed for the simulations of Fig. 12 are listed in Table IV,
 622 where the receiver's sensitivity [82] threshold is used to judge
 623 whether the received signal is deemed to be noise, because a
 624 received signal power below the sensitivity level is deemed to
 625 be noise.

626 The energy consumption is quantified for both the IrCC-
 627 URC-STTC scenario³ and the DCMC-capacity-based bench-
 628 mark scenario at SNR_{dB}^* of 7 dB and 1 dB. As seen from
 629 Fig. 12, the energy consumption of the IrCC-URC-STTC
 630 scheme and of the benchmark scheme decrease upon increasing

²The number of MA-RNs also includes the source and the destination. Again, the multi-antenna aided nodes are denoted as MA-RNs and single-antenna nodes are denoted as SA-RNs.

³In the IrCC-URC-STTC scenario the network consists of QPSK-assisted IrCC-URC-STTC aided MA-RNs and 8PSK-assisted IrCC-URC aided SA-RNs.

631 the number of MA-RNs n_{MA} . As mentioned in Section II-A,
 632 a low FER and a relatively high transmission range i.e. cov-
 633 erage area may be ensured by using the IrCC-URC-STTC
 634 scheme advocated. Furthermore, as justified in Section II-B,
 635 the specific routes having the lowest number of hops tend to be
 636 activated in the MA-RNs aided network considered. Therefore,
 637 having a high PHY-layer FER results in an increased number
 638 of retransmissions and hence may trigger route re-discovery,
 639 which results in more control packets being transmitted. Hence,
 640 more energy per payload bit is required for successfully de-
 641 livering the source data to the destination, as demonstrated
 642 in Fig. 12.

643 III. ROUTING DESIGN WITH PHY & 644 DL & NET COOPERATION

645 In recent years, numerous energy-efficient techniques have
 646 been proposed [26], [64], [65], [69], [83]–[106]. However,
 647 simply minimizing the energy consumption results in deficient
 648 designs. It is more beneficial to strike a tradeoff between the
 649 energy consumed and other metrics, such as the attainable
 650 throughput. For example, Multiple-Input and Multiple-Output
 651 (MIMO) schemes and near-capacity Space-Time Codes (STCs)
 652 were employed in [84] for optimizing the RN selection for
 653 the sake of maximizing the end-to-end throughput at a given
 654 total available power. While single-hop transmissions are more
 655 suitable for bandwidth-limited scenarios, multi-hop transmis-
 656 sions combined with spatial frequency-reuse tend to perform
 657 better in power-limited situations [69]. Spatial frequency-reuse
 658 employed in multi-hop scenarios may be beneficially com-
 659 bined with Interference Mitigation (IM) [69], [84] and transmit
 660 beamforming [84] for the sake of finding an attractive balance
 661 between energy minimization and throughput maximization in
 662 both single-hop and multi-hop schemes [69], [85], [86]. As a
 663 further advance, a beneficial tradeoff between the total energy
 664 consumption and throughput was found in [85] by considering
 665 both the transmission strategy of each node as well as the
 666 location of the RNs and the data rate of each node.

667 Moreover, the authors of [26], [57], [86], [89], [92], [95]–
 668 [98], [101]–[104], [107] invoked cross-layer design. For ex-
 669 ample, the impact of the link error rate on the route selection
 670 between a path associated with a large number of short-distance
 671 hops and another with a smaller number of long-distance hops
 672 was studied in [86]. In this paper, the link ‘cost’ was defined as
 673 a function of both the energy required for a single transmission
 674 attempt and the link error rate. This Objective Function (OF)
 675 captures the cumulative energy expended in reliable data trans-
 676 fer for both reliable and unreliable link layers. In [107], several
 677 routing algorithms were proposed, which opted for the route
 678 with minimum energy consumption in a mixed hop-by-hop and
 679 end-to-end retransmission mode. In the end-to-end retransmis-
 680 sion mode, a single unreliable link may require retransmissions
 681 from the source, and hence may require more energy for suc-
 682 cessfully delivering packets. Consequently, routing protocols
 683 play an important role in saving energy. The authors of [57]
 684 took into account both the energy consumed by data packets as
 685 well as by control packets and MAC retransmissions, because
 686 ignoring the energy consumption of exchanging control packets

might underestimate the actual energy consumption and thus 687
 688 may lead to inefficient designs. However, the energy OFs em-
 689 ployed in [57], [86], [107] exploited the assumption of having
 690 access to a potentially infinite number of MAC retransmissions,
 691 which is unrealistic. The employment of the OF proposed in
 692 [57], [86], [107] is feasible only when the affordable number of
 693 MAC retransmissions is infinite, which is formulated as

$$E_{total} = \sum_1^H \frac{E_i}{1 - FER_i}, \quad (5)$$

where $\frac{1}{1 - FER_i}$ is the expected number of transmission at- 694
 695 tempts required for successfully delivering a packet across
 696 link i . As seen from (5), the total energy of all hops is simply
 697 summed, which suggests that the success of the individual links
 698 in a route is deemed to be independent of each other, since the
 699 assumption that an infinite number of MAC retransmissions
 700 is affordable is given. Additionally, although the authors of
 701 [89] considered a limited number of MAC retransmissions, no
 702 specific OF was formulated.

Furthermore, TR relies on a route discovery process invoked 703
 704 for gleaning sufficient routing information for the source to
 705 make meritorious routing decisions, regardless, whether the
 706 routing protocol is proactive or reactive [108]. However, due to
 707 the rapid fluctuation of the channel conditions, the routing in-
 708 formation estimated on the basis of the average Channel Quality
 709 Information (CQI) may become stale, resulting in suboptimum
 710 routing. Therefore, OR [90]–[92], [96], [101], [103], [109]–
 711 [114] has been proposed for avoiding this problem. In OR no
 712 pre-selected route is employed, instead a so-called forwarder
 713 RN set is used for forwarding the packets along a benefi-
 714 cial route. The near-instantaneously varying characteristics of
 715 wireless channels is beneficially exploited considered by OR.
 716 Table V shows that OR is widely used in various networks, such
 717 as *ad hoc* networks [103], [115], wireless sensor networks [91],
 718 cognitive networks [116], vehicular networks [117], [118] and
 719 DTNs [119]–[121].

More specifically, Liu *et al.* [110] illustrated the basic idea 720
 721 behind OR and categorized the potential design criteria, includ-
 722 ing the Estimated Transmission count (ETX), the geographic
 723 distance aided and the energy consumption based philosophies.
 724 Biswas and Morris [101] proposed an Extremely Opportunistic
 725 Routing (ExOR) scheme, which employed the ETX metric at
 726 the destination for deciding the priority order of selecting a
 727 RN from the potential forwarder set. The proposed routing
 728 regime integrated the routing protocol and the MAC protocol
 729 for the sake of increasing the attainable throughput of multi-
 730 hop wireless networks. Their solution [101] also exploited
 731 the less reliable long-distance links, which would have been
 732 ignored by traditional routing protocols. Moreover, Dubois-
 733 Ferrière *et al.* [111] conceived the Least-Cost Anypath Routing
 734 (LCAR) regime, which finds the optimal choice of candidate
 735 RNs relying on the expected ETX cost of forwarding a packet
 736 to the destination. This LCAR algorithm considers the coordi-
 737 nation of the link layer protocols. Laufer *et al.* [114] proposed
 738 a ‘polynomial-time multirate anypath’ routing algorithm and
 739 provided the proof of its optimality. The proposed routing
 740 algorithm employed the Expected Anypath Transmission Time

TABLE V
OPPORTUNISTIC ROUTING PROTOCOLS IN VARIOUS NETWORKS

Year	Authors	Contribution
2006	Pelusi <i>et al.</i> [117]	Surveyed the most promising OR solutions and the taxonomy of the main routing and forwarding approaches in challenging environments.
2008	Conan <i>et al.</i> [121]	Proposed a single copy and multi-hop OR scheme for sparse Delay Tolerant Networks (DTNs).
2009	Khalife <i>et al.</i> [118]	Explored opportunistic forwarding without preestablished routing in multihop cognitive radio networks.
	Spyropoulos <i>et al.</i> [122]	Proposed a class of routing schemes that can identify the nodes of “highest utility” in intermittently connected wireless networks.
2010	Lee <i>et al.</i> [119]	Presented a topology-assisted Geo-OR designed for vehicular networks that combined topology-assisted geographic routing with opportunistic forwarding for mitigating the effects of unreliable wireless channels.
	Li <i>et al.</i> [123]	Investigated energy-efficient opportunistic forwarding and designed different forwarding policies for DTNs.
2011	Mao <i>et al.</i> [91]	Presented an energy-efficient OR strategy conceived for wireless sensor networks, which created a prioritized forwarder list to minimize the total energy consumption of all nodes.
2012	Wang <i>et al.</i> [103]	Proposed a cooperative OR scheme for mobile ad hoc networks for tackling the problem of opportunistic data transfer.
2013	Wu <i>et al.</i> [120]	Proposed a hybrid routing scheme for data dissemination in vehicular ad hoc networks (VANETs), using a carry-and-forward scheme for mitigating the forwarding disconnection problem of sparse VANETs.
2014	Yoon <i>et al.</i> [124]	Investigated the feasibility of OR in power line communications access networks and proposed a customized OR, which used static geographical information.

741 (EATT) as the routing metric, which is a generalization of the
 742 unidirectional ETX metric that takes into account that nodes
 743 transmit at multiple bit rates. The authors of [90], [109], [113]
 744 employed a geographic distance based metric for choosing the
 745 potential forwarder RN set. More specifically, Zorzi and Rao
 746 [109] proposed an OR scheme based on random forwarding,
 747 where the specific node, which is closest to the destination
 748 is chosen as the RN for the next hop. Additionally, they [90]
 749 analyzed the achievable energy as well as latency performance
 750 and provided a detailed description of a MAC scheme based
 751 on both opportunistic concepts and on collision avoidance.
 752 Zeng *et al.* [113] proposed a multirate OR by incorporating
 753 rate adaptation into their candidate-selection algorithm, which
 754 was shown to achieve a higher throughput and lower delay
 755 than the corresponding traditional single-rate routing and its
 756 opportunistic single-rate routing counterpart. The authors of
 757 [91], [92], [96] employed the energy consumption metric for
 758 choosing the potential forwarder RN set. More concretely,
 759 Mao *et al.* [91] presented an energy-efficient OR strategy
 760 relying on sophisticated PA, which prioritizes the forwarder
 761 RNs by directly minimizing the total energy consumption of
 762 all nodes. Dehghan *et al.* [92] developed a minimum-energy
 763 cooperative routing based on many-to-many cooperation and
 764 determines the optimal route with the aid of the Bellman-Ford
 765 algorithm [123]. Wei *et al.* [96] proposed an energy-conserving
 766 Assistant Opportunistic Routing (AsOR) protocol, which clas-
 767 sified a sequence of nodes into three different node sets, namely,
 768 the frame node, the assistant node and the unselected node.
 769 The frame nodes were indispensable for decode-and-forward
 770 operation, while the assistant nodes provided protection against
 771 unsuccessful opportunistic transmissions. Although the authors
 772 of [91], [92], [96] employed the energy consumption as their
 773 routing metric, they have not provided any theoretical bounds
 774 in their performance analysis. Moreover, these authors as-
 775 sumed that the number of affordable MAC retransmissions
 776 was infinite.

777 An appropriate PA scheme combined with an opportunistic
 778 scheme was introduced in [74]. The opportunistic scheme does

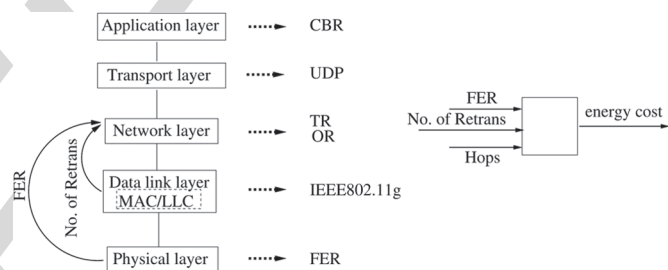


Fig. 13. System model of the energy-efficient routing with PHY & DL & NET cooperation in *ad hoc* networks.

not employ a pre-selected route, while it will fully utilize
 779 the time-variant characteristic of the hostile wireless channel,
 780 where any RN has the chance to forward a packet as long as
 781 the packet arrives at this RN successfully. A pair of energy-
 782 consumption-based OFs are constructed for TR and OR by
 783 exploiting the knowledge of both the corresponding FER within
 784 the PHY layer, as well as that of the number of MAC retrans-
 785 missions and of the number of RNs in the NET layer, as seen
 786 in the system model of Fig. 13. The above-mentioned TR and
 787 OR algorithms employ the corresponding energy-consumption-
 788 based OFs as their routing metrics, respectively. Apart from
 789 the energy consumption, the end-to-end throughput is evaluated
 790 as well. It was demonstrated that the algorithms **proposed in**
 791 [74] are capable of operating close to the theoretical bound
 792 found by the exhaustive search of all routes. In Fig. 13, the
 793 characteristics of the PHY layer are represented with the aid
 794 of the FER, while the DL layer employs the IEEE802.11g
 795 standard. In the NET layer, the above-mentioned TR and
 796 are employed, which make their decisions on the basis of the
 797 above energy-consumption-related OFs. The UDP is employed
 798 in the transport layer and the data streaming relies on a CBR
 799 service in the application layer. As in Section II, the channel
 800 imposes both free-space path-loss and uncorrelated Rayleigh
 801 fading, plus the ubiquitous AWGN.

Based on the system model of Fig. 13, the impact of the
 803 lowest three layers of the OSI model on the total energy 804

805 dissipated of the entire system is considered, which will be
 806 analyzed, whilst relying on an energy-consumption-based OF.
 807 In [73], [74], only the transmit energy consumed by the
 808 data packets during their transmission is considered, which are
 809 generated by the application layer. The energy consumed by
 810 other packets, such as routing and MAC control packets is not
 811 considered. In other words, the idealized simplifying assump-
 812 tion is that the energy consumed during the process of route
 813 discovery is negligible. The elimination of this simplification
 814 was set aside for the future work. **As detailed in** [73], [74],
 815 **the OF is** invoked for making routing-related decisions, which
 816 directly influence the energy consumed by future data packets.
 817 All nodes are assumed to be stationary. Only a single source-
 818 destination pair is supported in the network and only a single
 819 node has the chance of transmitting in a time slot, once the route
 820 was determined. All the data packets are also assumed to have
 821 the same length and all nodes have the same transmission rate.

822 A. Traditional Routing With Fixed Transmit Power

823 Naturally, having an infinite number of MAC retransmis-
 824 sions will impose a potentially infinite end-to-end delay at the
 825 destination, which is not realistic. In realistic environments,
 826 the wireless link may become broken owing to packet errors
 827 if the maximum number of MAC retransmissions has been
 828 exhausted. A broken link may trigger a route-repair or even
 829 route re-discovery for the sake of maintaining the current
 830 source-destination communications session. The route-repair
 831 is often required at the upper-node's broken link, while the
 832 route re-discovery should be initiated by the source. All these
 833 actions may consume more energy and naturally they reduce
 834 the attainable throughput. Additionally, the success of a specific
 835 hop emanating from a node relies on the success of all previous
 836 hops. If any of the previous links is broken, then no packet
 837 will be forwarded towards the destination. Naturally, any link
 838 is more likely to break if the number of MAC retransmissions
 839 is limited to N_r . The energy consumption considered is divided
 840 into two parts: the energy consumed by the data packets which
 841 succeed in reaching the destination and the energy consumed
 842 by the data packets which are dropped before reaching the
 843 destination. The time slot duration of a single transmission
 844 attempt across a given link is defined as T . Given the same data
 845 packet length and the same transmission rate at each node, T is
 846 a constant value. Here, the energy-conscious OF of a two-hop
 847 route is detailed as an example. p_s and p_f are used to denote
 848 the probability of a packet being successfully delivered to the
 849 destination successfully and being dropped before reaching the
 850 destination, respectively. Furthermore, the notation $p_s(\tau)$ repre-
 851 sents the probability that the packet is successfully delivered
 852 all the way from the source to the destination after a time
 853 duration of τ . First, the energy consumption analysis of a 2-hop
 854 route is considered in Fig. 14. The symbol \surd indicates that
 855 the link's transmission is successful after $1 \leq \frac{\tau}{T} \leq N_r$ MAC
 856 retransmission attempts. Hence the time duration of the link's
 857 transmission is $T \leq \tau \leq N_r T$. Fig. 14 shows that a packet's
 858 successful transmission over the link $S - R_1$ requires a time
 859 duration of τ_1 , while the successful transmission of a packet
 860 over the link $R_1 - D$ requires a time duration of τ_2 . Hence the

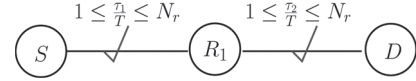


Fig. 14. A packet is successfully delivered from S to D in a 2-hop route.

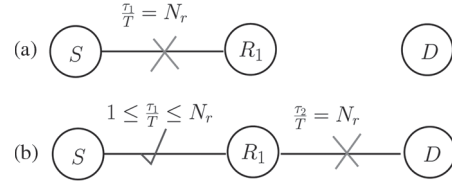


Fig. 15. A packet is dropped before reaching D in a 2-hop route.

total time duration of a packet's passage between S and D is 861
 862 $(\tau_1 + \tau_2)$, where $2T \leq \tau_1 + \tau_2 \leq 2N_r T$.

Therefore, 863

$$p_s(2T) = p_1 p_2, \quad (6)$$

$$p_s(3T) = (1 - p_1) p_1 p_2 + p_1 (1 - p_2) p_2, \quad (7)$$

$$p_s(4T) = (1 - p_1)^2 p_1 p_2 + (1 - p_1) p_1 (1 - p_2) p_2 + p_1 (1 - p_2)^2 p_2, \quad (8)$$

$$\vdots \quad \quad \quad \vdots$$

$$p_s(2N_r T) = (1 - p_1)^{N_r - 1} p_1 (1 - p_2)^{N_r - 1} p_2. \quad (9)$$

While p_s is given by 864

$$p_s = p_s(2T) + p_s(3T) + p_s(4T) + \dots + p_s(2N_r T), \quad (10)$$

$$= \sum_{i=1}^{N_r} \sum_{j=1}^{N_r} (1 - p_1)^{i-1} p_1 (1 - p_2)^{j-1} p_2. \quad (11)$$

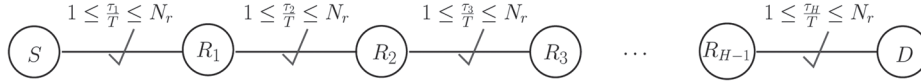
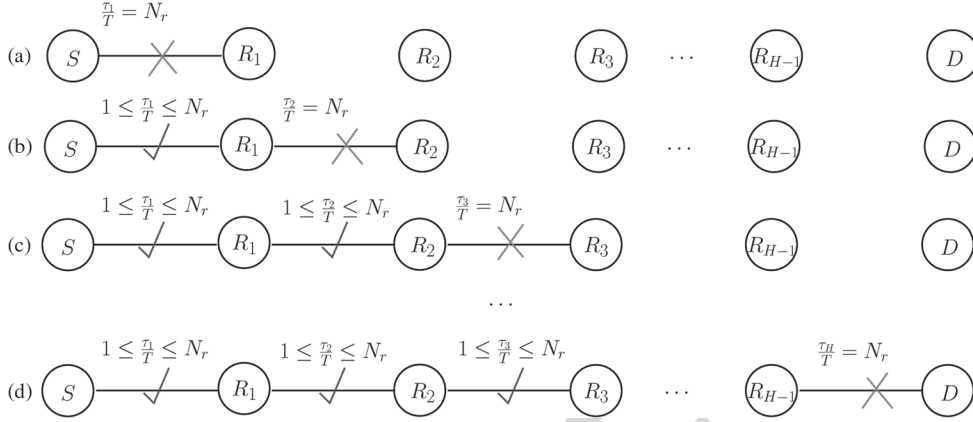
Since during a single time slot T the nodes consume an energy 865
 866 of E , the estimated total energy E_s consumed by a successfully
 867 delivered packet in a two-hop route is

$$E_s = [2p_s(2T) + 3p_s(3T) + 4p_s(4T) + \dots + 2N_r p_s(2N_r T)] E. \quad (12)$$

In a similar way, the time D_s required for a packet, which is 868
 869 successfully delivered from S to D is given by

$$D_s = [2p_s(2T) + 3p_s(3T) + 4p_s(4T) + \dots + 2N_r p_s(2N_r T)] T. \quad (13)$$

Additionally, the packets, which exhausted the maximum 870
 871 number N_r of MAC retransmissions and were finally dropped
 872 before reaching D due to poor channel conditions also consume
 873 energy. This energy should also be taken into account in the
 874 total energy consumption. The energy dissipation analysis of a
 875 packet dropped before reaching the destination in a 2-hop route
 876 is portrayed in Fig. 15. The symbol \times indicates that the link's
 877 transmission fails after $\frac{\tau}{T} = N_r$ MAC retransmission attempts.
 878 As seen in Fig. 15, a transmission failure may occur either in
 879 the $S - R_1$ link or in the $R_1 - D$ link of a 2-hop route. Hence,
 880 even when the data transmission in the $S - R_1$ link is successful
 881 within the time duration of $T \leq \tau_1 \leq N_r T$, the transmission
 882 might fail in the $R_1 - D$ link.


 Fig. 16. A packet is successfully delivered from S to D in a H -hop route.

 Fig. 17. A packet is dropped before reaching D in a H -hop route.

883 The probability of failure p_f of the two-hop route for a single
884 packet is described as follows:

$$p_f(1) = (1 - p_1)^{N_r}, \quad (14)$$

$$p_f(2) = [(1 - p_f(1))] (1 - p_2)^{N_r}, \quad (15)$$

$$p_f = p_f(1) + p_f(2), \quad (16)$$

885 where $p_f(h)$ represents the probability of the packet becoming
886 dropped during the h -th hop. Therefore, the energy E_f con-
887 sumed by a dropped packet is quantified as follows:

$$E_f = \left[N_r p_f(1) + \sum_1^{N_r} (1 - p_1)^{i-1} p_1 (1 - p_2)^{N_r} (i_1 + N_r) \right] E. \quad (17)$$

888 Similarly, the average time D_f required by a packet to propagate
889 from S up to the broken link is formulated as

$$D_f = \left[N_r p_f(1) + \sum_1^{N_r} (1 - p_1)^{i-1} p_1 (1 - p_2)^{N_r} (i_1 + N_r) \right] T. \quad (18)$$

890 The energy dissipation analysis of a packet's successful
891 delivery to the destination and that of a packet dropped before
892 reaching the destination in a H -hop route is characterized in
893 Fig. 16 and Fig. 17, respectively. Fig. 16 portrays the scenario,
894 where each link's transmission is successful after $1 \leq \frac{\tau}{T} \leq N_r$
895 MAC retransmission attempts. By contrast, Fig. 17 shows that
896 a transmission failure could take place within any of the links,
897 where all the previous links' transmissions were successful. The
898 time duration elapsed before reaching the failed link is $\tau = N_r T$,
899 while that elapsing during all the previous link's transmission is
900 $T \leq \tau \leq N_r T$.

901 Therefore, the total normalized transmit energy consumption
902 becomes:

$$\bar{E}_{total} = \frac{E_{total}}{p_s} = \frac{E_s + E_f}{p_s}. \quad (19)$$

Similarly, the end-to-end throughput R_{e2e} is given as

903

$$R_{e2e} = \frac{P_s}{D_s + D_f}. \quad (20)$$

A low-complexity routing algorithm is proposed in [73].
The process of route discovery is shown in Fig. 18, where
 S represents the source, D represents the destination, and the
other nodes are denoted by symbols A, B, C, E, F and G . $E_{S \rightarrow n, t}$
denotes the estimated NEC for the route spanning from S to
node n at time instant t , while $E_{S \rightarrow n}$ is used for storing the
minimum NEC for every node in every time-slot of duration
 T . The routing process may be divided into the following
four steps:

- **Step 1** Node S broadcasts the RREQ packet;
- **Step 2** Every node carries out the operations detailed in Fig. 19 upon receiving the RREQ packet;
- **Step 3** Node S receives the RREP packet and then updates the routing table;
- **Step 4** Then node S sends its data packet along the specific route having the lowest estimated \bar{E}_{total} .

A flow chart is provided in Fig. 19 for specifically highlight-
ing the operations, when each node receives an RREQ packet.
If S receives the RREQ packet, S will simply discard this RREQ
packet. By contrast, if another node $n (n \neq S)$ receives the
RREQ packet, it calculates the NEC $E_{S \rightarrow n, t}$ and then compares
 $E_{S \rightarrow n, t}$ to $E_{S \rightarrow n}$. If $E_{S \rightarrow n, t} > E_{S \rightarrow n}$, then node n will discard the
RREQ packet. Otherwise, if node n is D , then D will respond
with a newly created RREP packet. However, if node n is not
 D , node n will broadcast the RREQ packet again.

Now the process of routing discovery is explained in details
for further clarification. During time slot 1, node S broadcasts
the RREQ packet, nodes A, B and C receive the RREQ packet.
According to the actions seen in Fig. 19, nodes A, B and C first
calculate $E_{S \rightarrow A, 1}$, $E_{S \rightarrow B, 1}$ and $E_{S \rightarrow C, 1}$, respectively. Then they
compare these newly calculated values with the aid of $E_{S \rightarrow A}$,

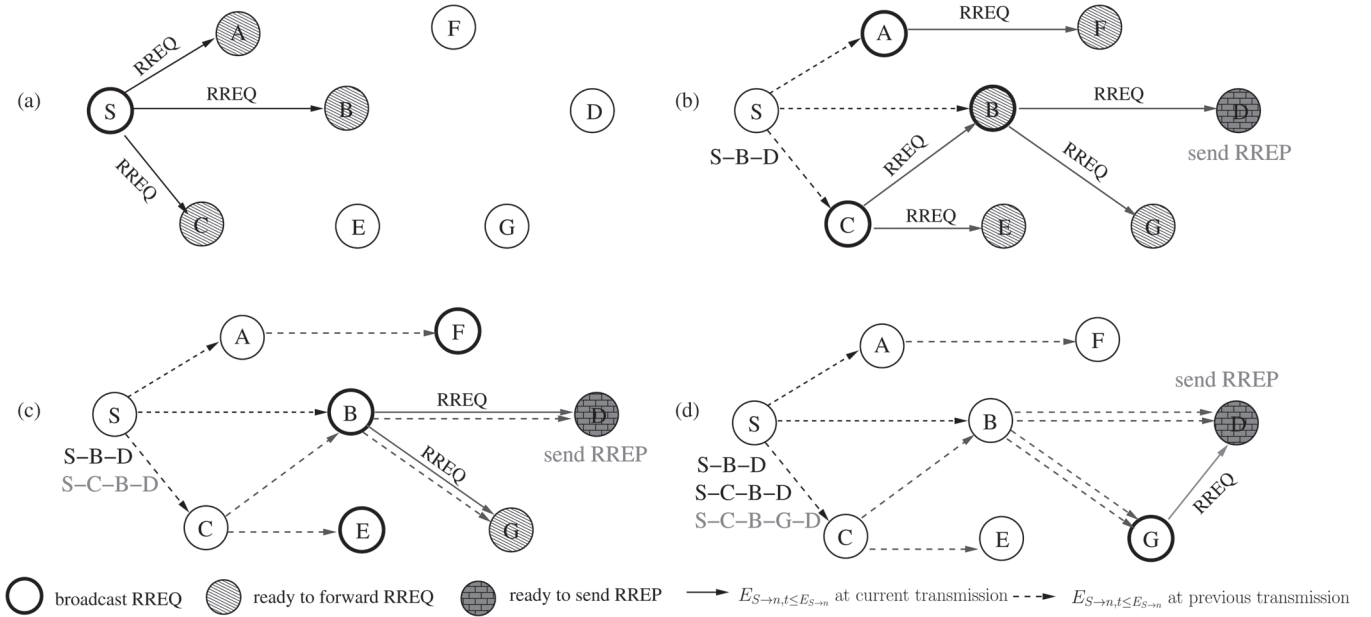


Fig. 18. The process of route discovery in the low-complexity routing algorithm. (a) Actions during time slot 1. (b) Actions during time slot 2 and node S updates its routing table with the route $S-B-D$. (c) Actions during time slot 3 and node S updates its routing table with the route $S-C-B-D$ since the estimated NEC of route $S-C-B-D$ is lower than that of route $S-B-D$. (d) Actions during time slot 4 and node S updates its routing table with the route $S-C-B-G-D$, since the estimated NEC of route $S-C-B-G-D$ is lower than that of route $S-C-B-D$.

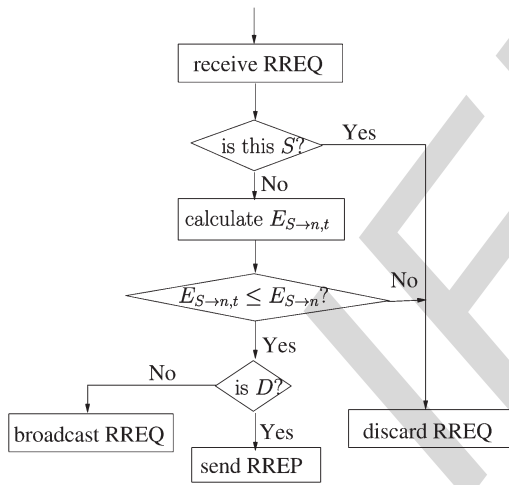


Fig. 19. Operations when each node receives an RREQ packet.

935 $E_{S \rightarrow B}$ and $E_{S \rightarrow A}$, respectively. If $E_{S \rightarrow A, 1} \leq E_{S \rightarrow A}$, then A will
 936 update $E_{S \rightarrow A}$ and will forward the RREQ packet during the
 937 next time slot, otherwise it will discard it. The same actions
 938 are carried out at node B and node C as well.

939 Then during time slot 2, node A , B and C forward the RREQ
 940 packet. According to the actions seen in Fig. 19, nodes B , E , F
 941 and G will forward the RREQ packet in the next time slot, since
 942 $E_{S \rightarrow B, 2} \leq E_{S \rightarrow B}$, $E_{S \rightarrow E, 2} \leq E_{S \rightarrow E}$, $E_{S \rightarrow F, 2} \leq E_{S \rightarrow F}$ and $E_{S \rightarrow G, 2} \leq$
 943 $E_{S \rightarrow G}$. Node D is ready to send back a newly created RREP
 944 packet in the next time slot, since node D is the destination and
 945 $E_{S \rightarrow D, 2} \leq E_{S \rightarrow D}$. Afterwards, S will receive the RREP packet
 946 and updates its routing table with the route $S-B-D$ obtained.
 947 S will send the data packet along the route $S-B-D$.

948 During time slot 3, nodes B , E , F and G forward the RREQ
 949 packet. According to the actions portrayed in Fig. 19, node G
 950 will forward the RREQ packet during the next time slot, since

$E_{S \rightarrow G, 3} \leq E_{S \rightarrow G}$. Node D will then send back a newly created
 951 RREP packet during the next time slot, since node D is the
 952 destination and $E_{S \rightarrow D, 3} \leq E_{S \rightarrow D}$. Afterwards, S will receive the
 953 second RREP packet and updates its routing table again with
 954 the route $S-C-B-D$ obtained, since the estimated NEC of
 955 route $S-C-B-D$ is lower than that of route $S-B-D$. Finally,
 956 node S will send the next data packet along the updated route
 957 $S-C-B-D$. 958

959 During time slot 4, node G forwards the RREQ packet,
 960 then nodes B , E and D receive it. According to the actions
 961 of Fig. 19, then D is ready to send back a newly created
 962 RREP packet during the next time slot, since node D is the
 963 destination and $E_{S \rightarrow D, 4} \leq E_{S \rightarrow D}$. Afterwards, S will receive the
 964 third RREP packet and updates its routing table again with the
 965 route $S-C-B-G-D$ obtained, since the estimated NEC of
 966 route $S-C-B-G-D$ is lower than that of route $S-C-B-D$.
 967 Finally, node S will send the next data packet along the updated
 968 route $S-C-B-G-D$. 968

969 The analytically estimated NEC associated both with an
 970 infinite number as well as a finite number of N_r MAC re-
 971 transmissions was calculated from (5) and (19), respectively.
 972 A simple linear network topology was studied, where all N
 973 nodes are equi-spaced along a line. The frame length of the
 974 data packets, which are generated from the application layer,
 975 is $L_{app} = 1024$ Bytes. The 802.11g standard is employed in the
 976 DL layer. The transmit power is set to $P_{t_i} = 0.016$ mW and the
 977 IrCC-URC-QPSK defined in Section II is employed in the PHY
 978 layer. The channel model is the AWGN channel subjected to
 979 inverse second-power free-space path loss. The other system
 980 parameters employed for the simulations of Figs. 20 and 21 are
 981 listed in Table IV. 981

982 The NEC and the end-to-end throughput evaluated both from
 983 (19) and (20) as well as by simulations are portrayed in Figs. 20
 984 and 21. 984

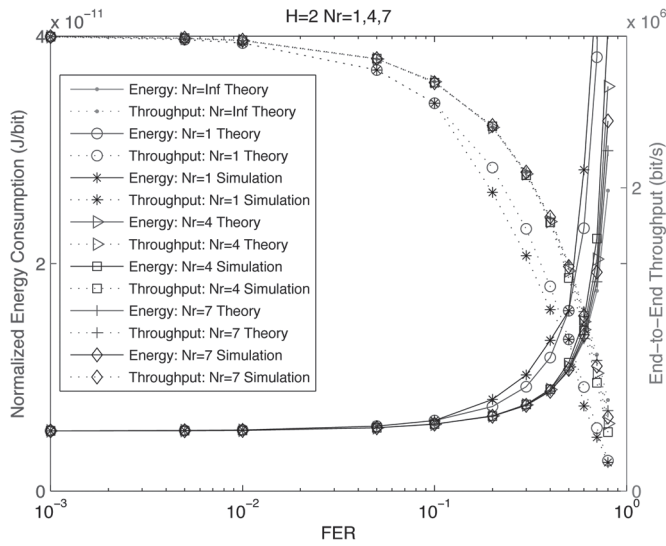


Fig. 20. The NEC and the end-to-end throughput versus FER ($10^{-3} \leq FER \leq 1$) and the maximum number of MAC retransmissions N_r ($N_r = 1, 4, 7$) with the number of hops $H = 2$ for comparing the theoretically analyzed values and simulation based values.

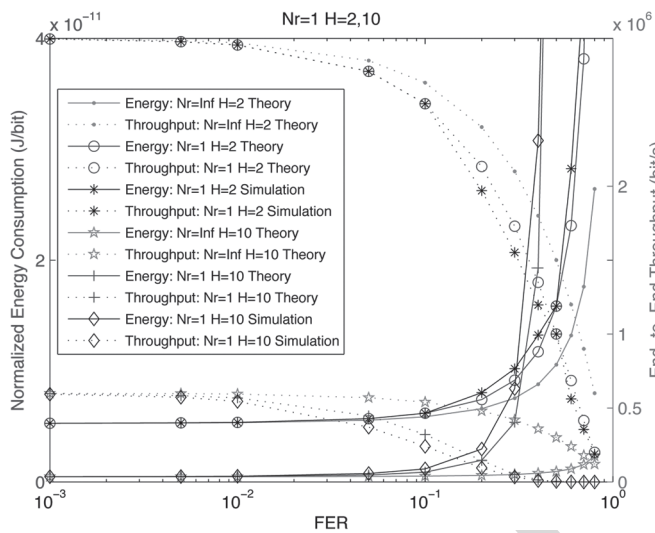


Fig. 21. The NEC and the end-to-end throughput versus FER ($10^{-3} \leq FER \leq 1$) and the number of hops H ($H = 2, 10$) with the maximum number of MAC retransmissions $N_r = 1$ for comparing the theoretically analyzed values and simulation based values.

985 Fig. 20 displays three groups of performance curves recorded
 986 at $N_r = 1, 4$ and 7 , respectively, for both the NEC and for the
 987 end-to-end throughput, where N_r is the maximum number of
 988 MAC retransmissions. The performance figures recorded for
 989 the infinite number of MAC retransmissions scenario, namely
 990 for $N_r = \infty$ are identical for the theory evaluated from (5)
 991 and for the simulations. All the analytical and the simulation
 992 based values recorded for the NEC increase, when the FER
 993 increases. By contrast, the curves representing the end-to-end
 994 throughput decrease, when the FER increases. The reason for
 995 this observation is that a high FER in a link indicates a high
 996 breakage probability not only for the specific link and but
 997 also for the entire route, when retransmissions are required.
 998 However, if N_r is sufficiently high, then the success probability
 999 of a packet across a link or even the entire route becomes higher.

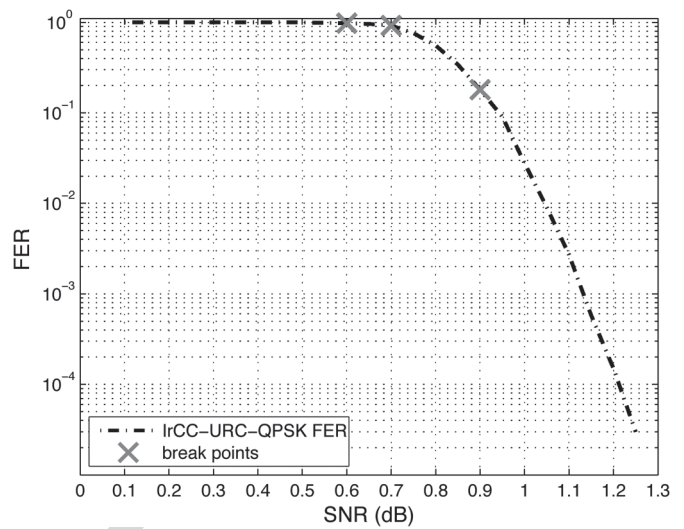


Fig. 22. FER versus SNR for the IrCC-URC-QPSK scheme of Section II-A for the average code rate of $R_c = 0.5$ in an AWGN channel.

This trend is presented in Fig. 20, where the curve recorded for 1000
 $N_r = 7$ is seen to be close to that of $N_r = \infty$. The discrepancy 1001
 between the theoretical value and the simulation-based value 1002
 becomes higher when N_r is reduced and simultaneously the 1003
 FER is increased. Fig. 20 also shows that the theoretical energy 1004
 consumption of (19) based on the energy-conscious OF is closer 1005
 to the simulation based values than those based on the OF rely- 1006
 ing on an infinite number of MAC retransmissions. Naturally, 1007
 the advantage of the OF is more substantial for $N_r = 1$. 1008

Fig. 21 also displays two groups of performance curves, 1009
 one group for the NEC and the other group for the end-to- 1010
 end throughput, which are associated with $H = 2$ and 1011
 respectively. When H is increased, the normalized energy 1012
 consumption is reduced and the end-to-end throughput is de- 1013
 creased, because the distance between a pair of adjacent nodes 1014
 is reduced and therefore the transmit power required at each 1015
 node for successfully delivering a packet is reduced. Similarly, 1016
as discussed in [73], the theoretical values estimated based 1017
 on the proposed OF are closer to the simulated values than 1018
 to those estimated on the basis of an infinite number of MAC 1019
 retransmissions, especially when both H and the FER are high. 1020

Hence, **as elaborated on in [73], the conclusion is reached** 1021
from Figs. 20 and 21 that the proposed energy-conscious OF 1022
 is more accurate than the one assuming an infinite number of 1023
 MAC retransmissions at high FERs, or for a high number of 1024
 hops at a low maximum number of MAC retransmissions. 1025

B. Traditional Routing With Adjustable Transmit Power 1026

The FER curve was generated for the AWGN channel model 1027
 with the aid of simulation [74]. According to the approach 1028
 of [102], this will allow us to determine the average FER 1029
 for arbitrary fading channels upon weighting the AWGN-FER 1030
 by the Probability Distribution Function (PDF) of the fading 1031
 channel and averaging it over the legitimate dynamic range. 1032
 More specifically, the channel model considered is the uncor- 1033
 related, non-dispersive Rayleigh fading channel. The average 1034
 FER expression $FER_{Rayleigh}$ is determined for the Rayleigh 1035
 fading channel considered by integrating the specific FER_{AWGN} 1036

1037 value of the AWGN channel experienced at a given SNR after
1038 weighting it by the probability of that specific SNR, which is
1039 given by:

$$FER_{Rayleigh} = \int_0^{\infty} e^{-\gamma} FER_{AWGN}(\gamma) d\gamma, \quad (21)$$

1040 where γ is the channel SNR, $e^{-\gamma}$ represents the Rayleigh
1041 channel while the $FER_{AWGN}(\gamma)$ versus the SNR curve is ap-
1042 proximated by the following four-segment FER vs. SNR model
1043 representing the AWGN channel:

$$FER_{AWGN}(\gamma) \approx \begin{cases} 1, & \text{if } 0 \leq \gamma < \eta_1, \\ 10a_1 \log(\gamma) + a_2, & \text{if } \eta_1 \leq \gamma < \eta_2, \\ 10a_3 \log(\gamma) + a_4, & \text{if } \eta_2 \leq \gamma < \eta_3, \\ a_5 e^{-10a_6 \log(\gamma)}, & \text{if } \gamma \geq \eta_3, \end{cases} \quad (22)$$

1044 with η_1 , η_2 and η_3 being the break-points of the four-segment
1045 FER versus SNR approximation $FER_{AWGN}(\gamma)$. Eqs. (21) and
1046 (22) are suitable for approximating different FER curves by ap-
1047 propriately setting the corresponding parameter values invoked.
1048 Eq. (21) may be readily extended to arbitrary channel models.
1049 Given $FER_{Rayleigh}$, the successful reception probability of a
1050 link can be calculated as $[1 - (FER_{Rayleigh})^{N_r}]$ if the maximum
1051 number of MAC retransmissions (including the first MAC
1052 retransmission attempt) is N_r . Specifically, for the IrCC-URC-
1053 QPSK scheme of Section II-A[72] employed, $a_1 = -0.5889$,
1054 $a_2 = 1.3341$, $a_3 = -3.705$, $a_4 = 3.5169$, $a_5 = 4.4669 \times 10^6$
1055 and $a_6 = 18.9118$. Additionally, the values of the break-points
1056 η_1 , η_2 and η_3 are determined for the SNR points of 0.6 dB,
1057 0.7 dB, and 0.9 dB, which are based on the curves seen
1058 in Fig. 22. Fig. 22 shows the FER performance versus the
1059 SNR, when the IrCC-URC-QPSK scheme of Section II-A is
1060 employed, relying on the average code rate of $R_c = 0.5$ in an
1061 AWGN channel. As seen from Fig. 22, the corresponding hori-
1062 zontal points of the symbol 'x' are 0.6 dB, 0.7 dB and 0.9 dB.
1063 Therefore, by employing a practical coding scheme, such as
1064 the IrCC-URC-QPSK scheme of Section II with the aid of (19),
1065 it arrives at

$$\bar{E}_{total} = \frac{P_{t1}}{p_1} T, \quad (23)$$

1066 which shows that \bar{E}_{total} is independent of the number of retrans-
1067 missions in a single-hop route. In this context, the NEC is the
1068 same as that of a transmitter operating without a transmission
1069 limit, i.e. when $N_r = \text{inf}$. As indicated in [74], optimizing
1070 the transmit power of the source was formulated as a convex
1071 optimization problem.

1072 Once the closed-form expression of (23) for the NEC \bar{E}_{total}
1073 of a single hop, the optimized transmit power P_{t1} may be
1074 calculated by setting the derivative of (23) with respect to P_{t1}
1075 to zero, which yields

$$\frac{1}{p_1} + \frac{P_{t1}}{p_1^2} \frac{d(1-p_1)}{dP_{t1}} = 0$$

$$\frac{p_1}{-P_{t1}} = \frac{d(1-p_1)}{dP_{t1}}, \quad (24)$$

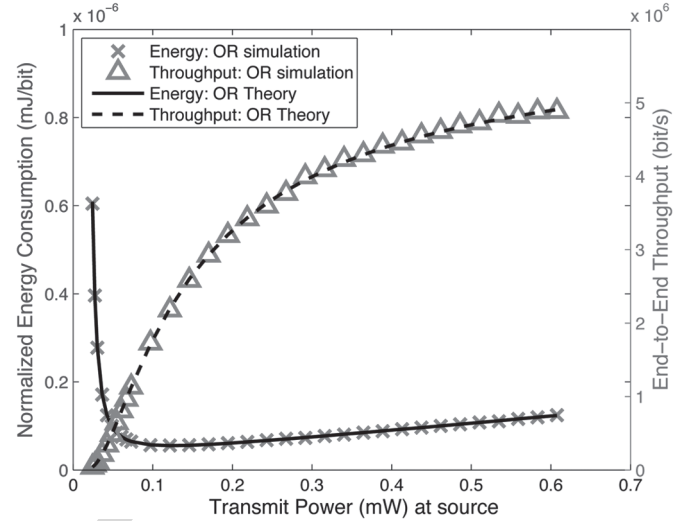


Fig. 23. The NEC \bar{E}_{total} and the end-to-end throughput R_{e2e} versus the transmit power P_{tS} .

1076 where $1 - p_1 = FER_1$. Finally, the analytical expression of the
1077 optimized transmit power P_{t1} can be found. The existence of the
1078 optimized transmit power at the source of a single-hop route
1079 is shown in Fig. 23. Moreover, the end-to-end throughput R_{e2e}
1080 of the TR relying on an adjustable transmit power also obeys
1081 the same expression of (20). Therefore, the NEC \bar{E}_{total} and the
1082 end-to-end throughput R_{e2e} are compared both in terms of sim-
1083 ulation and theoretical results in Fig. 23, where the maximum
1084 number of MAC retransmissions is $N_r = 7$. The frame length
1085 of the data packets, which are generated from the application
1086 layer, is 1024 Bytes. The 802.11g standard is employed in the
1087 DL layer. The distance between S and D is 1000 m. The other
1088 simulation configurations are listed in Table IV.

1089 Fig. 23 shows that the NEC initially decreases and then
1090 increases slowly beyond the transmit power of 0.12 mW, where
1091 0.12 mW is the optimal transmit power obtained by using
1092 (24). The end-to-end throughput increases upon increasing the
1093 transmit power at S . Observe that the simulation results closely
1094 match the theoretical curve.

1095 The idealized multi-hop linear network researched in
1096 Section III-A may be extended to a more realistic random net-
1097 work relying on Dijkstra's routing algorithm [124] and invoking
1098 the NEC \bar{E}_{total} for route selection. **Hence, a heuristic routing**
1099 **algorithm, namely the TR having an adjustable transmit**
1100 **power is invoked in [74] (referred to as Algorithm 1 in [74]),**
1101 **which may be adapted to the random network scenario**
1102 **considered for guaranteeing a high energy efficiency. For**
1103 **ease of interpretation, in this paper, the TR having an**
1104 **adjustable transmit power is exemplified with the aid of**
1105 **its step-by-step execution using the NEC metric \bar{E}_{total} , as**
1106 **shown in Fig. 24. It is assumed that \mathcal{V} is the vertex set, v is**
1107 **a node in the set \mathcal{V} and \bar{E}_{Sv} denotes the NEC. Moreover, \mathcal{S}**
1108 **represents the set of selected nodes, while $P_t^{opt}(u, v)$ denotes**
1109 **the optimal transmit power of node u assigned for transmission**
1110 **to node v .**

1111 As an example, the positions of S , D , R_1 and R_2 are as-
1112 sumed to be (100, 100), (900, 100), (500, 500), and (300,
1113 400), respectively. The IrCC-URC-QPSK is employed in the

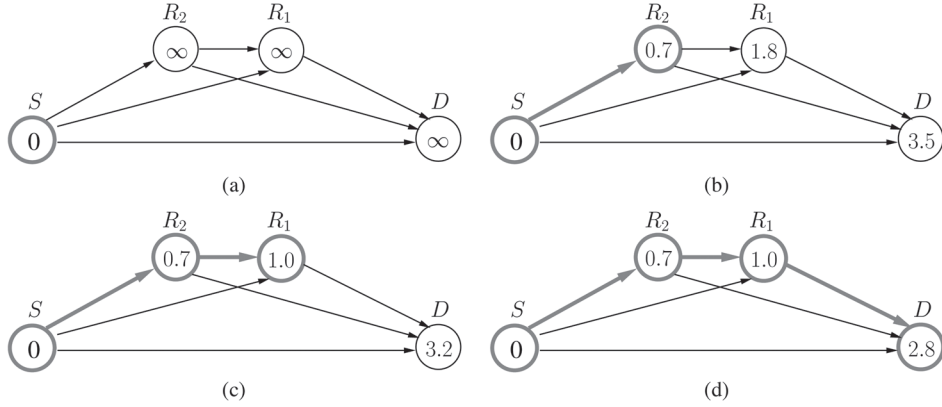


Fig. 24. Execution of the TR associated with an adjustable transmit power in a specific instance, where the positions of S , D , R_1 and R_2 are assumed to be (100, 100), (900, 100), (500, 500), and (300, 400), respectively. The value within a node v is its energy cost $\bar{E}_{total} (\times 10^{-8}$ mJ/bit) for transmission from S to node v . After each iteration one node is incorporated into the set S . The nodes in boldface denote the nodes in S after each iteration and the arrows in boldface represent the shortest route from S to the nodes in boldface after each iteration. Due to the adjustable transmit power of node u , the probability $p_f(u, v)$ of a packet, which is dropped at any link $u-v$ after $N_r = 7$ retransmissions, has nearly the same value of $p_f(u, v) = 0.041$, hence this value next to the arrows is not plotted for simplicity. (a) The situation just after the initialization, where $S = \{S\}$. (b) The first iteration of the algorithm, where $S = \{S\}$ before the iteration, while after the iteration R_2 is incorporated into the set S with the optimum power of $P_t^{opt}(S, R_2) = 0.16$ mW, yielding $S = \{S, R_2\}$. (c) The second iteration of the algorithm, where $S = \{S, R_2\}$ before the iteration, while after the iteration R_1 is incorporated into the set S with the optimum power of $P_t^{opt}(R_2, R_1) = 0.06$ mW, yielding $S = \{S, R_2, R_1\}$. (d) The final iteration of the algorithm, where $S = \{S, R_2, R_1\}$ before the iteration, while after the iteration D is incorporated into the set S with the optimum power of $P_t^{opt}(R_1, D) = 0.39$ mW, yielding $S = \{S, R_2, R_1, D\}$. The algorithm terminates.

1114 PHY layer. The channel imposes both free-space path-loss and
 1115 uncorrelated Rayleigh fading, plus the ubiquitous AWGN. The
 1116 other relevant parameters are listed in Table IV. Each node is
 1117 assumed to be aware of the other nodes' position, hence also
 1118 of their distance. In a compact form, $\mathcal{V} = \{S, R_1, R_2, D\}$ and
 1119 $S = \{S\}$, as shown in Fig. 24(a). In Fig. 24(b), S calculates its
 1120 transmit power optimized for minimizing the NEC from (24),
 1121 which is $\bar{E}_{SR_1} = 1.8 \times 10^{-8}$ mJ/bit, $\bar{E}_{SR_2} = 0.7 \times 10^{-8}$ mJ/bit,
 1122 $\bar{E}_{SD} = 3.5 \times 10^{-8}$ mJ/bit for transmission from S to R_1 , R_2 and
 1123 D , respectively. Since $\bar{E}_{SR_2} = 0.7 \times 10^{-8}$ mJ/bit is the lowest
 1124 in the set of the three energies, S is updated to $\{S, R_2\}$. Then
 1125 in Fig. 24(c), R_2 calculates its transmit power optimized for
 1126 minimizing the NEC from (24) for the transmission, which
 1127 is spanning from S to node R_1 and D via R_2 , respectively.
 1128 Since the updated NEC $\bar{E}_{SR_1} = 1.0 \times 10^{-8}$ mJ/bit is lower than
 1129 $\bar{E}_{SD} = 3.2 \times 10^{-8}$ mJ/bit, S is updated to $\{S, R_2, R_1\}$. Finally, in
 1130 Fig. 24(d), R_1 adjusts its own transmit power to the optimal one,
 1131 which minimizes the NEC $\bar{E}_{SD} = 2.8 \times 10^{-8}$ mJ/bit from S to
 1132 D via R_2 and R_1 . At this stage, D is incorporated into S . Since
 1133 $S = \{S, R_2, R_1, D\}$, the TR with adjustable transmit power may
 1134 be deemed to have converged and the route $S-R_2-R_1-D$ is
 1135 deemed to be the optimal route for transmission from S to D .

1136 The computational complexity has three main contributing
 1137 factors: a) the calculation of a single NEC in a specific case;
 1138 b) the number of NEC calculations; c) and finally, finding the
 1139 minimum NEC in each round. They denote the complexity of
 1140 E_s , E_f and p_s , where $p_s = \prod_1^H B(p_i)$, by $C(E_s)$, $C(E_f)$ and
 1141 $C(p_s)$. The complexity of evaluating D_s and D_f is the same
 1142 as that of E_s and E_f , apart from a multiplicative constant.
 1143 The number of NEC calculations is given by the number of
 1144 node pairs, which is $\mathcal{V}(\mathcal{V}-1)/2$. The minimum NEC can be
 1145 found based on the Fibonacci heap approach of [125], which
 1146 has a complexity on the order of $O(\log \mathcal{V})$. Therefore, the
 1147 complexity imposed by the TR with adjustable transmit power
 1148 is $O[\mathcal{V}^2[C(E_s) + C(E_f) + C(p_s)] + \mathcal{V} \log \mathcal{V}]$.

The performance of TR relying on an adjustable transmit
 power will be characterized in Section III-C in comparison to
 that of the OR of Section III-C.

C. Opportunistic Routing With Adjustable Transmit Power

The TR transmits the packet along the specific pre-selected
 route having the lowest estimated NEC. This pre-selected route
 is determined after the estimation and comparison of the NEC
 of each potential candidate route. The information invoked
 for routing decisions is gleaned during the process of route
 discovery, but this information may become stale owing to
 node-mobility. Instead, OR considers the potential chances of
 success for each candidate RN, bearing in mind their time-
 variant channel conditions. Regardless of which particular RN
 receives the packet from the source successfully, if this RN has
 the highest priority in the forwarder RN list, it will forward the
 packet to the next RN. Naturally, the challenge in the design
 of the OR procedure is the beneficial selection of the forwarder
 RN set, the specific priority order of the potential forwarders
 and the avoidance of duplicate transmissions [110]. All the
 nodes in a node's neighbor list are assumed to belong to this
 node's forwarder R-list. The metric used for determining the
 priority order is the normalized energy required by this par-
 ticular RN for reaching D . Acknowledgement (ACK) packets
 are employed for avoiding the duplicate transmissions. The
 particular RN in the forwarder R-set, which has the highest
 priority owing to requiring the lowest energy will send the ACK
 first. The other RNs, which overhear the ACK will withdraw
 from the competition [126], [127].

A two-hop network is shown in Fig. 25, which has a sin-
 gle source S , a single destination D and M RNs $R_1, R_2, \dots,$
 R_{M-1}, R_M . S and D are capable of communicating with all
 the RNs, as well as with each other. By contrast, the M RNs
 are unable to communicate with each other. The idealized

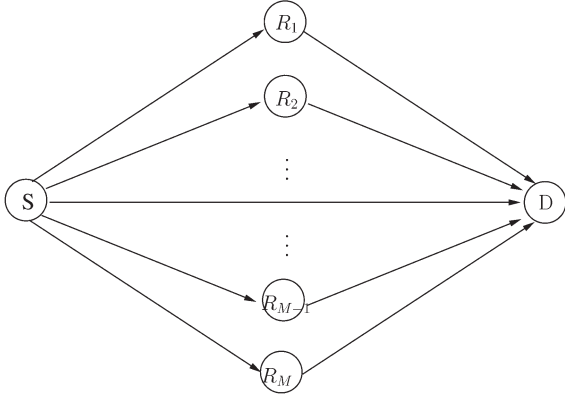


Fig. 25. A two-hop network assisted by a number of RNs.

1182 simplifying assumption is stipulated furthermore that each node
 1183 knows the position of all other nodes. For each RN $R_m, m =$
 1184 $1 \dots M$, the total average energy consumption $E_{R_m D}$ required
 1185 for transmission from R_m to D is given by $E_{R_m D} = E_{R_m D}^s + E_{R_m D}^f$
 1186 where $E_{R_m D}^s$ represents the energy dissipated by a packet, which
 1187 is successfully delivered from R_m to D while $E_{R_m D}^f$ represents
 1188 the energy dissipated by a packet, which is dropped before
 1189 reaching D from R_m after N_r MAC retransmissions. Let E_S
 1190 denote the energy dissipated while sending a packet from
 1191 the source S to any of the RNs R_m , which is $E_S = P_S T$. It
 1192 is assumed that $E_{R_1 D} < E_{R_2 D} < \dots < E_{R_M D}$. Furthermore, for
 1193 convenience, the destination node D is represented as R_0 and
 1194 $\prod_{m=0}^M (1 - p_{SR_m}) = \zeta$, where p_{SR_m} denotes the probability of a
 1195 packet, which is successfully delivered from S to R_m .
 1196 If S successfully sends a packet to the m -th RN, $m =$
 1197 $0, 1, \dots, M$, with the aid of n_r transmissions, the probability of
 1198 this event is

$$p_0(n_r) = \zeta^{n_r-1} p_{SR_0}, \text{ if } m = 0 \quad (25)$$

$$p_m(n_r) = \zeta^{n_r-1} \prod_{i=0}^{m-1} (1 - p_{SR_i}) p_{SR_m}, \text{ if } 1 \leq m \leq M. \quad (26)$$

1199 Correspondingly, the energy dissipated becomes

$$E_0(n_r) = n_r E_S, \text{ if } m = 0 \quad (27)$$

$$E_m(n_r) = n_r E_S + E_{R_m D}, \text{ if } 1 \leq m \leq M. \quad (28)$$

1200 Let $D_{R_m D}$ denote the average delay of a packet travers-
 1201 ing from $R_m, m = 1, \dots, M$, to D , including the delay $D_{R_m D}^s$
 1202 encountered by a packet that is successfully delivered to D
 1203 and the delay $D_{R_m D}^f$ experienced when a packet is dropped
 1204 before reaching D . Then $D_{R_m D} = D_{R_m D}^s + D_{R_m D}^f$, where $D_{R_m D}^s$
 1205 represents D_s and $D_{R_m D}^f$ corresponds to D_f , provided that the
 1206 number of hops is 1. Consequently,

$$D_0(n_r) = n_r D_S, \text{ if } m = 0 \quad (29)$$

$$\begin{aligned} D_m(n_r) &= n_r D_S + D_{R_m D} \\ &= n_r D_S + \left(D_{R_m D}^s + D_{R_m D}^f \right), \text{ if } 1 \leq m \leq M, \end{aligned} \quad (30)$$

1207 where D_S is T , which denotes the duration of a Time Slot (TS).

Consequently, when taking into account all the possible 1208
 events, the total energy consumption is 1209

$$\begin{aligned} E_{total} &= \sum_{n_r=1}^{N_r} p_0(n_r) E_0(n_r) \\ &\quad + \sum_{n_r=1}^{N_r} \sum_{m=1}^M p_m(n_r) E_m(n_r) + \zeta^{N_r} (N_r E_S), \end{aligned} \quad (31)$$

while the total delay becomes: 1210

$$\begin{aligned} D_{total} &= \sum_{n_r=1}^{N_r} p_0(n_r) D_0(n_r) \\ &\quad + \sum_{n_r=1}^{N_r} \sum_{m=1}^M p_m(n_r) D_m(n_r) + \zeta^{N_r} (N_r D_S), \end{aligned} \quad (32)$$

Meanwhile, the packet transmitted from S may be dropped 1211
 in the $S - D$, $S - R_m$ or $R_m - D$ link, where $m = 1, \dots, M$ and 1212
 again, the destination can be replaced by R_0 . Then the end-to- 1213
 end outage probability p_f may be formulated as 1214

$$p_f = p_{f,S-R_0} + p_{f,S-R_m} + p_{f,R_m-D}, \quad m = 1, \dots, M. \quad (33)$$

Furthermore, the NEC \bar{E}_{total} may be formulated as 1215

$$\bar{E}_{total} = \frac{E_{total}}{1 - p_f}, \quad (34)$$

while the end-to-end throughput R_{e2e} is given by 1216

$$R_{e2e} = \frac{1 - p_f}{D_{total}}. \quad (35)$$

Although the network topology in Fig. 25 has only two hops, 1217
 this algorithm may be extended to a large network, where 1218
 the OR principle is employed for each hop. Meanwhile, the 1219
 optimal transmit power of each node is found for the sake 1220
 of minimizing the NEC required for the successful passage 1221
 of a packet from that node to the destination. Therefore, **the** 1222
heuristic routing algorithm, namely the OR associated with 1223
an adjustable transmit power is conceived in [74] (referred 1224
to as Algorithm 2 in [74]), for calculating the minimum NEC 1225
by carrying out optimum distance-dependent power alloca- 1226
tion at each node, hop-by-hop. For ease of interpretation, in 1227
this paper, the OR having an adjustable transmit power is 1228
exemplified with the aid of its step-by-step execution using 1229
the NEC metric \bar{E}_{total} , as shown in Fig. 26. Here, for any 1230
 node v in a given vertex set \mathcal{V} , \bar{E}_{vD} denotes the NEC \bar{E}_{total} 1231
 necessitated for transmission from node v to the destination 1232
 D , where the potential set of receiver nodes is denoted by 1233
 \mathcal{R} . Furthermore, $P_i^{opt}(v)$ is the optimal transmit power, which 1234
 minimizes the NEC required for transmission from node v to 1235
 the destination D . 1236

Again, **as a specific example**, both the topology and the 1237
 relevant parameters **used in** Fig. 26 are similar to those used 1238
in Fig. 24. It was also assumed that each node is aware of 1239
 the other nodes' position, hence also of their distance. In a 1240
 compact form, $\mathcal{V} = \{S, R_1, R_2, D\}$ and $\mathcal{R} = \{D\}$, as shown in 1241

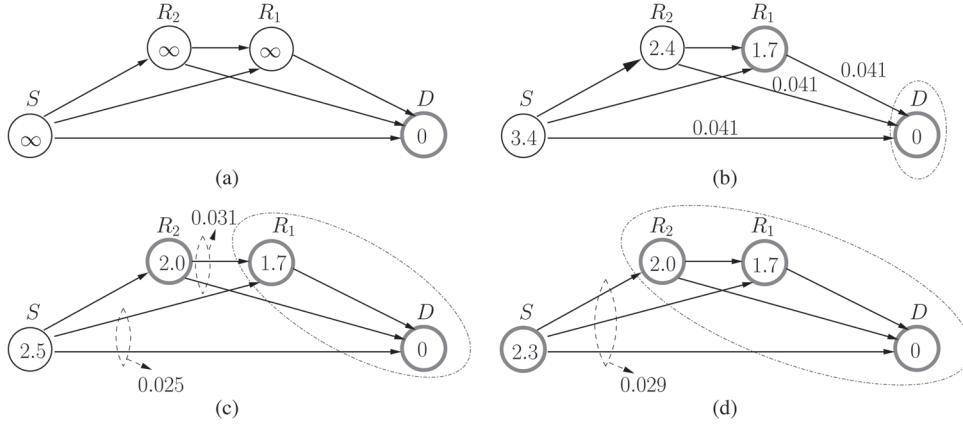


Fig. 26. Execution of the OR associated with an adjustable transmit power in a specific instance, where the positions of S , D , R_1 and R_2 are assumed to be (100, 100), (900, 100), (500, 500) and (300, 400), respectively. The value within a node u is its cost \bar{E}_{total} ($\times 10^{-8}$ mJ/bit) incurred by its transmission from node u to D and the dash-dot ellipse represents the receiver set \mathcal{R} before each iteration. After each iteration one node is incorporated into the set \mathcal{R} . The nodes in boldface denote the nodes in \mathcal{R} after each iteration. The values next to the arrows or the dashed ellipses represent the probability $p_f(u, \mathcal{R})$ of a packet being transmitted from S in conjunction with the event that none of the nodes in the receiver set \mathcal{R} receives it after $N_r = 7$ retransmissions. (a) The situation just after the initialization, where $\mathcal{R} = \{D\}$. (b) The first iteration of the algorithm, where $\mathcal{R} = \{D\}$ before the iteration, while after the iteration R_1 is incorporated into the set \mathcal{R} with the optimum power of $P_t^{opt}(R_1) = 0.39$ mW, yielding $\mathcal{R} = \{R_1, D\}$. (c) The second iteration of the algorithm, where $\mathcal{R} = \{R_1, D\}$ before the iteration while after the iteration R_2 is incorporated into the set \mathcal{R} with the optimum power of $P_t^{opt}(R_2) = 0.36$ mW, yielding $\mathcal{R} = \{R_2, R_1, D\}$. (d) The final iteration of algorithm, where $\mathcal{R} = \{R_2, R_1, D\}$ before the iteration, while after the iteration S is incorporated into the set \mathcal{R} with the optimum power of $P_t^{opt}(S) = 0.41$ mW, yielding $\mathcal{R} = \{S, R_2, R_1, D\}$. The algorithm terminates.

1242 Fig. 26(a). In Fig. 26(b), S , R_1 and R_2 calculate their transmit
 1243 power optimized for minimizing the NEC from (34), yielding
 1244 $\bar{E}_{SD} = 3.4 \times 10^{-8}$ mJ/bit, $\bar{E}_{R_1D} = 1.7 \times 10^{-8}$ mJ/bit, $\bar{E}_{R_2D} =$
 1245 2.4×10^{-8} mJ/bit for transmission to D . Since $\bar{E}_{R_1D} = 1.7 \times$
 1246 10^{-8} mJ/bit is the lowest in the set of the three energies, \mathcal{R} is
 1247 updated to $\{R_1, D\}$. Then in Fig. 26(c), S and R_2 adjust their
 1248 own transmit power and update their NEC for transmission
 1249 to node D by considering $\{R_1, D\}$ as their forwarder relay
 1250 set. Since $\bar{E}_{R_2D} = 2.0 \times 10^{-8}$ mJ/bit is lower than $\bar{E}_{SD} =$
 1251 2.5×10^{-8} mJ/bit, \mathcal{R} is updated to $\{R_2, R_1, D\}$. Finally, in
 1252 Fig. 26(d), S adjusts its own transmit power to the optimal one,
 1253 which minimizes $\bar{E}_{SD} = 2.3 \times 10^{-8}$ mJ/bit, where $\{R_2, R_1, D\}$
 1254 is the resultant forwarder relay set. At this stage, the OR with
 1255 adjustable transmit power may be deemed to have converged,
 1256 since S is incorporated into \mathcal{R} and $\mathcal{R} = \{S, R_2, R_1, D\}$. In this
 1257 algorithm, every node has to find its own forwarder R-set
 1258 by itself upon exploiting the knowledge of the other nodes'
 1259 positions. If more than one node in a node's forwarder R-
 1260 list receives the packet from that node successfully, then that
 1261 particular one, which requires the lowest NEC for transmission
 1262 to the destination has the highest priority for forwarding this
 1263 packet. The nodes of the forwarder R-set communicate with
 1264 each other similarly to the technique of [126] and again, the
 1265 NEC required for successful transmission to D is invoked for
 1266 deciding the priority order of the forwarders.

1267 The complexity of finding the transmit power and the for-
 1268 warder set also depends on three contributing factors, just like
 1269 for the TR scenario. They denote the complexity of E_{total} in
 1270 (34) and of p_f in (33) by $C(E_{total})$ and $C(p_f)$, respectively.
 1271 The OR with adjustable transmit power has to invoke \mathcal{V} times
 1272 for the sake of adding a further node into \mathcal{R} in each round. The
 1273 optimal transmit power of any node in $(\mathcal{V} - \mathcal{R})$ is calculated
 1274 in a specific round and the complexity of this calculation is
 1275 given by $C(E_{total}) + C(p_f)$. Again, the complexity of finding
 1276 the optimal transmit power can be calculated by Fibonacci

heap [125] which has a complexity on the order of $O(\log \mathcal{V})$.
 Therefore, the complexity of the OR with adjustable transmit
 power is $O[\mathcal{V}^2[C(E_{total}) + C(p_f)] + \mathcal{V} \log \mathcal{V}]$.

Now the performance of the networks associated with a total
 of $N = 4$ and 15 nodes are analyzed. The positions of S and
 D are (100, 100) and (900, 100), respectively, while the other
 nodes are uniformly located within a circle centered at (400,
 100) with a radius of 400 m. The NEC \bar{E}_{total} and the end-
 to-end throughput R_{e2e} are shown in Fig. 27 and Fig. 28 as
 a function of the maximum number of MAC retransmissions
 N_r . The theoretical NEC bound of both TR and OR was also
 investigated when $N = 4$, which was found by the exhaustive
 search of all the routes spanning from S to D , while for $N = 15$
 no theoretical bounds were given, since the exhaustive search
 has an excessive computation complexity.

Fig. 27 shows that the performance of the energy-
 consumption OF based algorithm is close to the theoretical
 bound when $N = 4$, especially in the case of a high N_r . Both
 Figs. 27 and 28 show that the energy-efficient OR outperforms
 both the Adjustable Energy-Efficient Opportunistic Routing
 (A-EEOR) algorithm defined in [91] and the energy-efficient
 TR. Here, the A-EEOR algorithm selects and prioritizes the
 forwarding set during the initialization stage according to the
 total energy cost of forwarding a packet to the destination node,
 which is estimated under the assumption of allowing a poten-
 tially infinite number of MAC retransmissions N_r . However,
 N_r is finite in practical scenarios. Hence, more specifically,
 compared to the A-EEOR algorithm the OR algorithm has
 a lower normalized energy consumption for $N_r < 4$, as seen
 in Fig. 27, while exhibiting a higher end-to-end throughput
 for $N_r < 6$, as shown in Fig. 28. Moreover, both the OR and
 TR simulation results closely match the theoretical curves.
 When $N_r = 1$ or 2 for the network topology of $N = 4$, both
 the exhaustive search, labelled by "TR bound" and the TR
 algorithm proposed in [74], labelled by "TR theory", selected

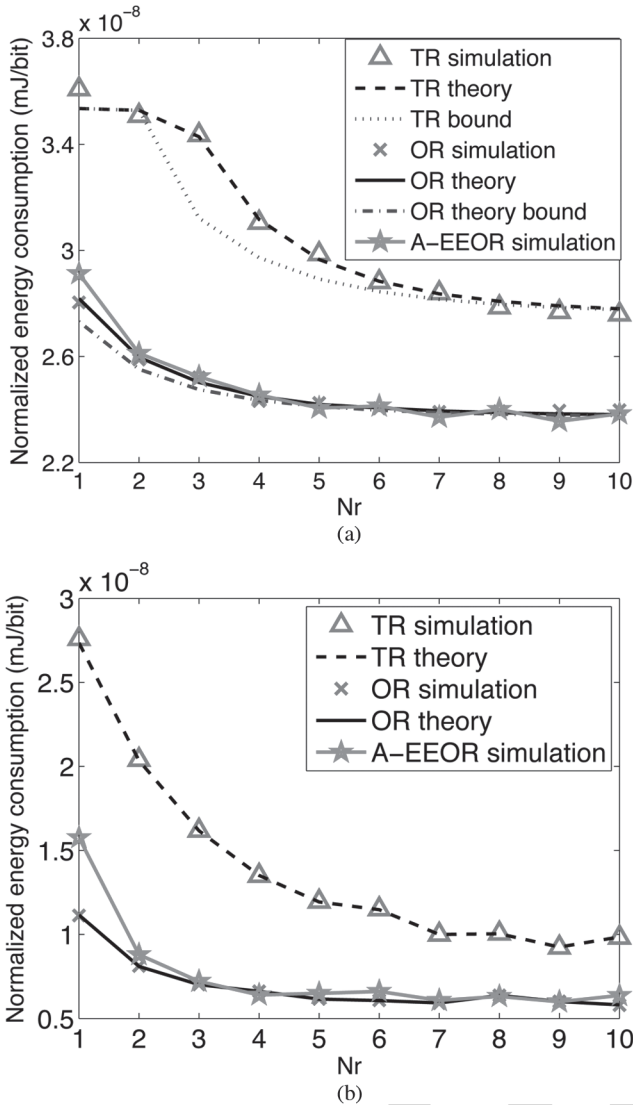


Fig. 27. The NEC \bar{E}_{total} versus the maximum number of MAC retransmissions N_r , when $N = 4$ and 15. (a) Network topology $N = 4$. (b) Network topology $N = 15$.

1312 the route ‘S-D’. Hence the NEC is the same for both. When
 1313 $2 < N_r < 8$, the exhaustive search and **the TR algorithm**
 1314 **proposed in [74]** choose different routes, since the exhaustive
 1315 search represents the globally optimal algorithm, while the TR
 1316 algorithm is a locally optimal algorithm. More specifically, the
 1317 TR algorithm is optimal for every single hop. Moreover, the
 1318 simulation results corresponding to the ‘TR simulation’ label
 1319 closely match the theoretical value represented by the label
 1320 ‘TR theory’. Therefore, the ‘TR simulation/theory’ and the ‘TR
 1321 bound’ scenarios exhibit a performance discrepancy, when $2 <$
 1322 $N_r < 8$, as seen in Fig. 27. Note that the NEC \bar{E}_{total} decreases
 1323 upon increasing N_r . However, the end-to-end throughput R_{e2e} of
 1324 the A-EEOR and OR regimes first increases and then saturates.
 1325 Additionally, the end-to-end throughput of TR is in fact higher
 1326 than that of OR for $N_r = 1$ and 2 when $N = 4$, but it is lower
 1327 for $N_r \geq 3$, as seen in Fig. 28. This is because in case of a low
 1328 number of MAC retransmissions, the direct near-line-of-sight
 1329 route spanning from S to D in the TR has a more dominant
 1330 priority than the other routes.

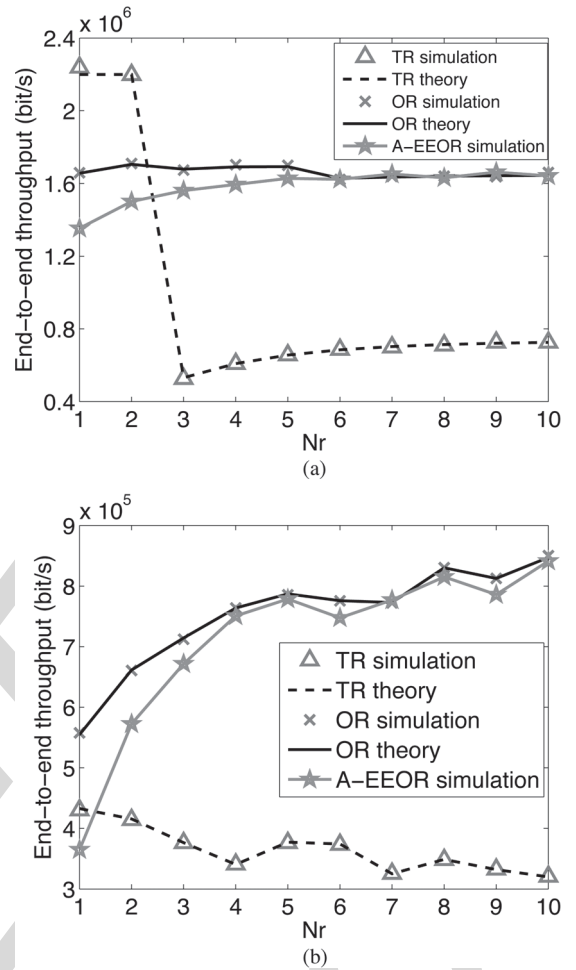


Fig. 28. The end-to-end throughput R_{e2e} versus the maximum number of MAC retransmissions N_r , when $N = 4$ and 15. (a) Network topology $N = 4$. (b) Network topology $N = 15$.

IV. CONCLUSIONS AND DESIGN GUIDELINES

1331

A. Conclusions

1332

In this paper diverse routing schemes were studied, investi- 1333
 gating the benefits of multi-antenna aided RNs, the FER, the 1334
 number of MAC retransmissions and the number of hops on 1335
 the performance energy consumption. 1336

- In Section I, we described the main functions of the OSI 1337
 model layer by layer, then we highlighted the common 1338
 methods of cross-layer design. The historical develop- 1339
 ment of cross-layer aided routing protocol designs was 1340
 portrayed in Table II. Then, we categorized the family 1341
 of *ad hoc* routing protocols, which were improved in the 1342
 following chapters. 1343
- In Section II, we focused our attention on the reduction 1344
 of the energy consumption by exploiting the benefits of 1345
 the coordination between the PHY layer and the NET 1346
 layer. Specifically, the advantages of near-capacity coding 1347
 schemes were quantified in terms of their energy saving. A 1348
 near-capacity three-stage concatenated IrCC-URC-STTC 1349
 relay-transceiver equipped with two transmit antennas was 1350
 proposed in [72] for the *ad hoc* network considered, 1351
 since it achieved a low FER at a low transmit power. 1352

1353 The high effective transmission range of the IrCC-URC-
1354 STTC aided MA-RNs facilitated cross-layer design for
1355 activating beneficial routes having the lowest number of
1356 longer hops.

1357 • Section III was specifically dedicated to minimizing the
1358 energy consumed by the data packets during the process
1359 of data transmission, where the NEC was quantified by
1360 considering both the PHY layer as well as the DL layer
1361 and the NET layer. Additionally, a cross-layer operation
1362 aided energy-efficient OR algorithm for *ad hoc* networks
1363 and an energy-consumption-based OF combined with PA
1364 was analyzed, which was proposed in [74] both for finding
1365 a theoretical bound and for conveying the packets through
1366 the network.

1367 B. Design Guidelines

1368 In general, three basic steps may be identified, when design-
1369 ing routing algorithms in *ad hoc* networks, which are:

- 1370 1) Determining the design targets, such as the network's
1371 throughput and/or energy consumption;
- 1372 2) Determining the key factors, which influence the design
1373 targets most crucially. These key factors may be related
1374 to different layers, including the channel categories, the
1375 protocol parameters and so on;
- 1376 3) Determining the routing metrics used for making routing
1377 decisions, such as the number of hops and/or the normal-
1378 ized end-to-end energy consumption.

1379 Let us now detail these three design steps as follows:

- 1380 • Throughput and energy consumption constitute a pair of
1381 important specifications in analyzing a network's perfor-
1382 mance, which critically depend on the parameters of the
1383 different OSI layers. Hence, combining the functions of
1384 multiple layers with the aid of cross-layer operation is ben-
1385 efiticial in terms of improving the attainable performance, as
1386 demonstrated in this tutorial with the assistance of several
1387 cross-layer aided routing algorithms designed for *ad hoc*
1388 networks.
- 1389 • The number of hops is one of the most popular routing
1390 metrics in routing design, as we demonstrated in the con-
1391 text of the classic routing algorithm, namely the DYMO
1392 protocol.
- 1393 • One of the most important factors we have to consider
1394 in the PHY layer is constituted by the specific charac-
1395 teristics of the time-variant wireless channel, which in-
1396 flict bit/symbol errors and even packet loss events at the
1397 receiver node. Hence, strong and robust channel coding
1398 schemes have to be employed for mitigating the channel-
1399 induced degradations. The BER and FER are the two rep-
1400 resentative parameters, which are capable of characteriz-
1401 ing the influence of both the time-variant wireless channel
1402 and of the FEC coding schemes, hence representing the
1403 overall performance of the PHY layer.
- 1404 • For the sake of reducing the system's total transmit energy
1405 consumption, a near-capacity coding scheme, such as the
1406 IrCC-URC-STTC scheme of Section II-A is the most
1407 appropriate choice, since it requires a reduced transmit

power at a given BER/FER value, which may also be
viewed as reducing the BER/FER at a given transmit
power. This is the reason, why the IrCC-URC-STTC aided
MA transceivers operate close to the achievable capacity
and this is, why they are capable of reducing the num-
ber of hops spanning from the source to the destination.
Requiring less hops implies that less nodes are involved,
hence reducing the energy dissipation. An energy-efficient
routing algorithm relying on the employment of IrCC-
URC-STTC aided MA transceivers [72] was analyzed in
Section II-B and Section II-C, showing that the system's
total transmit energy consumption was reduced.

1419
1420 • Furthermore, having considered the factors influencing the
1421 design of both the PHY layer and of the NET layer, we
1422 have to proceed by characterizing the influence of the DL
1423 layer in the cross-layer aided routing design. Our goal
1424 is that of achieving a throughput improvement and for
1425 energy reduction. One of the representative factors in the
1426 DL layer is constituted by the number of maximum MAC
1427 retransmissions. The larger the number of maximum MAC
1428 retransmissions, the more energy will be consumed and
1429 the higher the delay becomes. As a benefit, the success-
1430 ful packet reception probability is improved. Hence, we
1431 have to find the most appropriate number of maximum
1432 MAC retransmissions for the sake of striking an attractive
1433 compromise.

1434 • Additionally, we emphasize that the energy assigned to
1435 the data packets plays a dominant role in determining the
1436 system's total energy dissipation, which hence has to be
1437 optimized. For the sake of achieving an improved network
1438 throughput and a reduced energy consumption, the joint
1439 influence of the FER in the PHY layer, of the maximum
1440 number of retransmissions in the DL layer and of the
1441 number of hops in the NET layer has to be carefully con-
1442 sidered. Additionally, opting for the NEC as the routing
1443 metric instead of the number of hops is more beneficial in
1444 terms of reducing energy consumption. Hence, an accurate
1445 energy-consumption-based OF is required for combining
1446 all the three factors corresponding to the lower three
1447 layers of the seven-layer OSI architecture, as indicated
1448 in Section III-A of the tutorial. The routing algorithm
1449 proposed strikes an attractive tradeoff between the normal-
1450 ized energy consumption and the end-to-end throughput
1451 in the context of real-world scenarios, as exemplified in
1452 Section III-A.

1453 • A hop-length-dependent PA is beneficial in terms of re-
1454 ducing the energy consumption. If the transmit power of
1455 each node is assumed to be the same, a certain amount of
1456 extra energy will be dissipated, since the distance between
1457 each pair of nodes is different, which would necessitate a
1458 different amount of transmit energy. An energy-efficient
1459 TR algorithm was designed with the aid of the hop-length-
1460 dependent power allocation of Section III-B, which also
1461 jointly considered the FER in the PHY layer, the maximum
1462 number of retransmissions in the DL layer and the number
1463 of hops in the NET layer. A reliable routing metric is
1464 constituted by the NEC quantified in terms of the energy-
1465 based OF exemplified in Section III-B.

1466 • Additionally, the violently time-varying fading channel
 1467 will impose extra energy dissipation as well, because it
 1468 may render a pre-selected route inadequate for reliable
 1469 data transmission. This led to the concept of OR, which
 1470 is capable of reducing the energy consumption. Hence an
 1471 energy-efficient OR regime was designed with the aid of
 1472 hop-length-dependent PA in Section III-C, which also re-
 1473 lied on cross-layer operation across the lower three layers
 1474 of the TCP/IP model. Again, a reliable routing metric is
 1475 constituted by the NEC quantified in terms of the energy-
 1476 based OF exemplified in Section III-C.

1477 **All operational systems rely on a vital form of cross-**
 1478 **layer operation, which makes wireless systems different**
 1479 **from wireline based systems. Explicitly, both handovers and**
 1480 **power-control rely on cross-layer cooperation in all wireless**
 1481 **systems. This is why they are usually shown diagrammati-**
 1482 **cally as a block bridging the lowest three layers. Going back**
 1483 **as far as the old second-generation GSM system, the total**
 1484 **control-channel bitrate was as low as 961 bits/sec, which**
 1485 **limited the efficiency of the power-control and handover**
 1486 **operations, especially at high velocity and for small traffic**
 1487 **cells, when handovers are frequent. For the 3G systems the**
 1488 **control-channel rates were increased by an order of mag-**
 1489 **nitude to about 10 kbits/s, which facilitated more prompt**
 1490 **handovers and power-control actions, when for example**
 1491 **the mobile turned at a street-corner. The 4G LTE system**
 1492 **also followed this trend, since an increased control-channel**
 1493 **rate supports more sophisticated cross-layer cooperation.**
 1494 Although the main focus of this tutorial is on the energy dis-
 1495 sipated by data packets during the process of data transmission,
 1496 we note that cross-layer cooperation imposes an extra network
 1497 overhead, since the control **information also plays** an impor-
 1498 tant role in determining the system's total energy consumption,
 1499 especially in mobile scenarios where the control **information**
 1500 **assists** in maintaining seamless communications [128]. **The**
 1501 **extra control information is generated, when the informa-**
 1502 **tion exchange takes place amongst layers or different nodes,**
 1503 **including the control bits and the extra control packets.**
 1504 Additionally, a plethora of control packets are required for both
 1505 route discovery and for route maintenance. For example, node-
 1506 mobility might cause the following problems:

- 1507 • In TR, both the pre-selected route and the pre-stored
 1508 backup routes become invalid, which will activate route
 1509 re-discovery and hence may deplete the residual energy of
 1510 each node;
- 1511 • In OR, both the pre-computed optimal transmit power and
 1512 the forwarder set might become invalid, which requires the
 1513 re-computation of these two parameters. Hence, the effects
 1514 of the route life-time have to be considered for estimating
 1515 the energy consumption in a mobile scenario [128]–[131].

1516 Hence, the energy-consumption-based OFs formulated in the
 1517 stationary scenario may require further adjustments, if the en-
 1518 ergy dissipated by the control packets is also considered. It may
 1519 be promising to employ bio-inspired algorithms, such as the
 1520 ant colony algorithm [132], for accommodating a dynamically
 1521 changing topology, which requires future research.

REFERENCES

- 1522
- [1] H. Labiod, Ed., *Wireless Ad Hoc and Sensor Networks*. Hoboken, NJ, USA: Wiley, 2008. 1523
 - [2] R. Ramanathan and J. Redi, "A brief overview of Ad Hoc networks: Challenges and directions," *IEEE Commun. Mag.*, vol. 40, no. 5, pp. 20–22, May 2002. 1524
 - [3] H. Zimmermann, "OSI reference model—the ISO model of architecture for open systems interconnection," *IEEE Trans. Commun.*, vol. 28, no. 4, pp. 425–432, Apr. 1980. 1525
 - [4] *Reference Model of Open Systems Interconnection*, ISO/TC97/SC16 Std. Doc. N227, 1979. 1526
 - [5] A. Goldsmith, *Wireless Communications*. New York, NY, USA: Cambridge Univ. Press, 2005. 1527
 - [6] W. Stallings, *Wireless Communications & Networks*, 2nd ed. Englewood Cliffs, NJ, USA: Prentice-Hall, 2005. 1528
 - [7] *Information Technology-Telecommunications and Information Exchange Between Systems-Local and Metropolitan Area Networks-Specific Requirements*, IEEE Std. 802.11, 2007. 1529
 - [8] "Internet protocol," IETF Draft, 1981. 1530
 - [9] S. Deering and R. Hinden, "Internet protocol, version 6 (IPv6) specification," IETF Draft, 1998. 1531
 - [10] "Transmission control protocol," IETF Draft, 1981. 1532
 - [11] "User datagram protocol," IETF Draft, 1980. 1533
 - [12] *Definitions of Terms Related to Quality of Service*, ITU-T E.800, 2008. 1534
 - [13] V. Srivastava and M. Motani, "Cross-layer design: A survey and the road ahead," *IEEE Commun. Mag.*, vol. 43, no. 12, pp. 112–119, Dec. 2005. 1535
 - [14] M. Conti, G. Maselli, G. Turi, and S. Giordano, "Cross-layering in mobile Ad Hoc network design," *Computer*, vol. 37, no. 2, pp. 48–51, Feb. 2004. 1536
 - [15] R. Jurdak, *Wireless Ad Hoc and Sensor Networks: A Cross-layer Design Perspective*. New York, NY, USA: Springer-Verlag, 2010. 1537
 - [16] F. Fu and M. V. D. Schaar, "A new systematic framework for autonomous cross-layer optimization," *IEEE Trans. Veh. Technol.*, vol. 58, no. 4, pp. 1887–1903, May 2009. 1538
 - [17] R. Winter, J. H. Schiller, N. Nikaein, and C. Bonnet, "Crosstalk: Cross-layer decision support based on global knowledge," *IEEE Commun. Mag.*, vol. 44, no. 1, pp. 93–99, Jan. 2006. 1539
 - [18] E. Setton, T. Yoo, X. Zhu, A. Goldsmith, and B. Girod, "Crosslayer design of Ad Hoc networks for real-time video streaming," *IEEE Wireless Commun.*, vol. 12, no. 4, pp. 59–65, Aug. 2005. 1540
 - [19] Q. Liu, X. Wang, and G. B. Giannakis, "A cross-layer scheduling algorithm with QoS support in wireless networks," *IEEE Trans. Veh. Technol.*, vol. 55, no. 3, pp. 839–847, May 2006. 1541
 - [20] W. L. Huang and K. B. Letaief, "Cross-layer scheduling and power control combined with adaptive modulation for wireless Ad Hoc networks," *IEEE Trans. Commun.*, vol. 55, no. 4, pp. 728–739, Apr. 2007. 1542
 - [21] Q. Zhang and Y.-Q. Zhang, "Cross-layer design for QoS support in multihop wireless networks," *Proc. IEEE*, vol. 96, no. 1, pp. 64–76, Jan. 2008. 1543
 - [22] B. J. Oh and C. W. Chen, "A cross-layer approach to multichannel MAC protocol design for video streaming over wireless Ad Hoc networks," *IEEE Trans. Multimedia*, vol. 11, no. 6, pp. 1052–1061, Oct. 2009. 1544
 - [23] S. Chu and X. Wang, "Opportunistic and cooperative spatial multiplexing in MIMO Ad Hoc networks," *IEEE/ACM Trans. Netw.*, vol. 18, no. 5, pp. 1610–1623, Oct. 2010. 1545
 - [24] A. Ghosh and W. Hamouda, "Cross-layer antenna selection and channel allocation for MIMO cognitive radios," *IEEE Trans. Wireless Commun.*, vol. 10, no. 11, pp. 3666–3674, Nov. 2011. 1546
 - [25] M. Mardani, S.-J. Kim, and G. B. Giannakis, "Cross-layer design of wireless multihop random access networks," *IEEE Trans. Signal Process.*, vol. 60, no. 5, pp. 2562–2574, May 2012. 1547
 - [26] M. Uddin, C. Rosenberg, W. Zhuang, P. Mitran, and A. Girard, "Joint routing and medium access control in fixed random access wireless multihop networks," *IEEE/ACM Trans. Netw.*, vol. 22, no. 1, pp. 80–93, Feb. 2014. 1548
 - [27] F. Tang, L. Barolli, and J. Li, "A joint design for distributed stable routing and channel assignment over multihop and multiframe mobile Ad Hoc cognitive networks," *IEEE Trans. Ind. Informat.*, vol. 10, no. 2, pp. 1606–1615, May 2014. 1549
 - [28] V. Kawadia and P. R. Kumar, "A cautionary perspective on cross-layer design," *IEEE Wireless Commun.*, vol. 12, no. 1, pp. 3–11, Feb. 2005. 1550
 - [29] E. M. Royer and C.-K. Toh, "A review of current routing protocols for Ad Hoc mobile wireless networks," *IEEE Pers. Commun.*, vol. 6, no. 2, pp. 46–55, Apr. 1999. 1551
 - [30] C. E. Perkins and P. Bhagwat, "Highly dynamic destination-sequenced distance vector (DSDV) for mobile computers," in *Proc. ACM SIGCOMM*, Aug. 31–Sep. 2, 1994, pp. 234–244. 1552

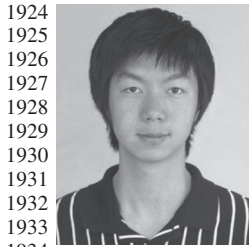
- 1599 [31] T. Clausen and P. Jacquet, "Optimized Link State Routing Protocol
1600 (OLSR) (RFC 3626) 2003, IETF Draft.
- 1601 [32] *The Dynamic Source Routing Protocol (DSR) for Mobile Ad Hoc Net-*
1602 *works for IPv4*. [Online]. Available: <http://tools.ietf.org/html/rfc4728>
- 1603 [33] *Ad hoc On-Demand Distance Vector (AODV) Routing*. [Online]. Avail-
1604 able: <http://tools.ietf.org/html/rfc3561>
- 1605 [34] *Dynamic MANET On-Demand (DYMO) Routing Routing*. [Online].
1606 Available: <http://tools.ietf.org/html/draft-ietf-manet-dymo-19>
- 1607 [35] *The Zone Routing Protocol (ZRP) for Ad Hoc Networks*. [Online]. Avail-
1608 able: <http://tools.ietf.org/html/draft-ietf-manet-zone-zrp-04>
- 1609 [36] A. Goldsmith and S. B. Wicker, "Design challenges for energycon-
1610 strained Ad Hoc wireless networks," *IEEE Wireless Commun.*, vol. 9,
1611 no. 4, pp. 8–27, Aug. 2002.
- 1612 [37] M. R. Souryal, B. R. Vojcic, and R. L. Pickholtz, "Information efficiency
1613 of multihop packet radio networks with channel-adaptive routing," *IEEE*
1614 *J. Sel. Areas Commun.*, vol. 23, no. 1, pp. 40–50, Jan. 2005.
- 1615 [38] S.-H. Lee, E. Choi, and D.-H. Cho, "Timer-based broadcasting for
1616 power-aware routing in power-controlled wireless Ad Hoc networks,"
1617 *IEEE Commun. Lett.*, vol. 9, no. 3, pp. 222–224, Mar. 2005.
- 1618 [39] M. Johansson and L. Xiao, "Cross-layer optimization of wireless
1619 networks using nonlinear column generation," *IEEE Trans. Wireless*
1620 *Commun.*, vol. 5, no. 2, pp. 435–445, Feb. 2006.
- 1621 [40] S. Mao *et al.*, "On routing for multiple description video over wireless
1622 Ad Hoc networks," *IEEE Trans. Multimedia*, vol. 8, no. 5, pp. 1063–
1623 1074, Oct. 2006.
- 1624 [41] A. Abdroubou and W. H. Zhuang, "A position-based QoS routing scheme
1625 for UWB mobile Ad Hoc networks," *IEEE J. Sel. Areas Commun.*,
1626 vol. 24, no. 4, pp. 850–856, Apr. 2006.
- 1627 [42] J. Zhang, Q. Zhang, B. Li, X. Luo, and W. Zhu, "Energy-efficient routing
1628 in mobile Ad Hoc networks: Mobility-assisted case," *IEEE Trans. Veh.*
1629 *Technol.*, vol. 55, no. 1, pp. 369–379, Jan. 2006.
- 1630 [43] S. Kompella, S. Mao, Y. T. Hou, and H. D. Sherali, "Cross-layer opti-
1631 mized multipath routing for video communications in wireless net-
1632 works," *IEEE J. Sel. Areas Commun.*, vol. 25, no. 4, pp. 831–840,
1633 May 2007.
- 1634 [44] M. Chiang, S. H. Low, A. R. Calderbank, and J. C. Doyle, "Layering as
1635 optimization decomposition: A mathematical theory of network archi-
1636 tectures," *Proc. IEEE*, vol. 95, no. 1, pp. 255–312, Jan. 2007.
- 1637 [45] K. T. Phan, H. Jiang, C. Tellambura, S. A. Vorobyov, and R. Fan,
1638 "Joint medium access control, routing and energy distribution in multi-
1639 hop wireless networks," *IEEE Trans. Wireless Commun.*, vol. 7, no. 12,
1640 pp. 5244–5249, Dec. 2008.
- 1641 [46] J. Liu, Y. T. Hou, Y. Shi, and H. D. Sherali, "Cross-layer optimization
1642 for MIMO-based wireless Ad Hoc networks: Routing, power allocation,
1643 bandwidth allocation," *IEEE J. Sel. Areas Commun.*, vol. 26, no. 6,
1644 pp. 913–926, Aug. 2008.
- 1645 [47] A. Abdroubou and W. H. Zhuang, "Statistical QoS routing for IEEE
1646 802.11 multihop Ad Hoc networks," *IEEE Trans. Wireless Commun.*,
1647 vol. 8, no. 3, pp. 1542–1552, Mar. 2009.
- 1648 [48] P. Li, Q. Shen, Y. Fang, and H. Zhang, "Power controlled network proto-
1649 cols for multi-rate Ad Hoc networks," *IEEE Trans. Wireless Commun.*,
1650 vol. 8, no. 4, pp. 2142–2149, Apr. 2009.
- 1651 [49] L. Ding, T. Melodia, S. N. Batalama, J. D. Matyjas, and M. J. Medley,
1652 "Cross-layer routing and dynamic spectrum allocation in cognitive radio
1653 Ad Hoc networks," *IEEE Trans. Veh. Technol.*, vol. 59, no. 4, pp. 1969–
1654 1979, May 2010.
- 1655 [50] Y. Lu, J. Guan, Z. Wei, and Q. Wu, "Joint channel assignment and cross-
1656 layer routing protocol for multi-radio multi-channel Ad Hoc networks,"
1657 *J. Syst. Eng. Electron.*, vol. 21, no. 6, pp. 1095–1102, Dec. 2010.
- 1658 [51] Z. Ding and K. K. Leung, "Cross-layer routing using cooperative trans-
1659 mission in vehicular Ad-Hoc networks," *IEEE Journal on Selected Areas*
1660 *in Communications*, vol. 29, no. 3, pp. 571–581, Mar. 2011.
- 1661 [52] B. Tavli and W. B. Heinzelman, "Energy-efficient real-time multicast
1662 routing in mobile Ad Hoc networks," *IEEE Trans. Comput.*, vol. 60,
1663 no. 5, pp. 707–722, May 2011.
- 1664 [53] S.-J. Syue, C.-L. Wang, T. Aguilar, V. Gauthier, and H. Afifi, "Coop-
1665 erative geographic routing with radio coverage extension for SER con-
1666 strained wireless relay networks," *IEEE J. Sel. Areas Commun.*, vol. 30,
1667 no. 2, pp. 271–279, Feb. 2012.
- 1668 [54] M. Pan, H. Yue, C. Zhang, and Y. Fang, "Path selection under budget
1669 constraints in multihop cognitive radio networks," *IEEE Trans. Mobile*
1670 *Comput.*, vol. 12, no. 6, pp. 1133–1145, Jun. 2013.
- 1671 [55] J. G. Li, D. Cordes, and J. Y. Zhang, "Power-aware routing protocols
1672 in Ad Hoc wireless networks," *IEEE Wireless Commun.*, vol. 12, no. 6,
1673 pp. 69–81, Dec. 2005.
- 1674 [56] S. D. Muruganathan, D. C. F. Ma, R. I. Bhasin, and A. Fapojuwo, "A cen-
1675 tralized energy-efficient routing protocol for wireless sensor networks,"
1676 *IEEE Commun. Mag.*, vol. 43, no. 3, pp. S8–S13, Mar. 2005.
- [57] J. Zhu, C. Qiao, and X. Wang, "On accurate energy consumption models
1677 for wireless Ad Hoc networks," *IEEE Trans. Wireless Commun.*, vol. 5,
1678 no. 11, pp. 3077–3086, Nov. 2006. 1679 AQ2
- [58] S. J. Baek and G. Veciana, "Spatial energy balancing through proactive
1680 multipath routing in wireless multihop networks," *IEEE/ACM Trans.*
1681 *Netw.*, vol. 15, no. 1, pp. 93–104, Feb. 2007. 1682
- [59] S. Eidenbenz, G. Resta, and P. Santi, "The COMMIT protocol for
1683 truthful and cost-efficient routing in Ad Hoc networks with self-
1684 ish nodes," *IEEE Trans. Mobile Comput.*, vol. 7, no. 1, pp. 19–33,
1685 Jan. 2008. 1686
- [60] W. Liang, R. Brent, Y. Xu, and Q. Wang, "Minimum-energy all-
1687 toall multicasting in wireless Ad Hoc networks," *IEEE Trans. Wireless*
1688 *Commun.*, vol. 8, no. 11, pp. 5490–5499, Nov. 2009. 1689
- [61] M. Li, L. Ding, Y. Shao, Z. Zhang, and B. Li, "On reducing broadcast
1690 transmission cost and redundancy in Ad Hoc wireless networks using di-
1691 rectional antennas," *IEEE Trans. Veh. Technol.*, vol. 59, no. 3, pp. 1433–
1692 1442, Mar. 2010. 1693
- [62] C. Ma and Y. Yang, "A battery-aware scheme for routing in wireless
1694 Ad Hoc networks," *IEEE Trans. Veh. Technol.*, vol. 60, no. 8, pp. 3919–
1695 3932, Oct. 2011. 1696
- [63] A. M. Akhtar, M. R. Nakhai, and A. H. Aghvami, "Power aware cooper-
1697 ative routing in wireless mesh networks," *IEEE Commun. Lett.*, vol. 16,
1698 no. 5, pp. 670–673, May 2012. 1699
- [64] T. Lu and J. Zhu, "Genetic algorithm for energy-efficient QoS multicast
1700 routing," *IEEE Commun. Lett.*, vol. 17, no. 1, pp. 31–34, Jan. 2013. 1701
- [65] J. Vazifehdan, R. Prasad, and I. Niemegeers, "Energy-efficient reliable
1702 routing considering residual energy in wireless Ad Hoc networks," *IEEE*
1703 *Trans. Mobile Comput.*, vol. 13, no. 2, pp. 434–447, Feb. 2014. 1704
- [66] G. Ferrari, S. A. Malvassori, and O. K. Tonguz, "On physical layeror-
1705 ientiated routing with power control in Ad Hoc wireless networks," *IET*
1706 *Commun.*, vol. 2, no. 2, pp. 306–319, Feb. 2008. 1707
- [67] J. C. Fricke, M. M. Butt, and P. A. Hoehner, "Quality-oriented adaptive
1708 forwarding for wireless relaying," *IEEE Commun. Lett.*, vol. 12, no. 3,
1709 pp. 200–202, Mar. 2008. 1710
- [68] M. Haenggi and D. Puccinelli, "Routing in Ad Hoc networks: A case
1711 for long hops," *IEEE Commun. Mag.*, vol. 43, no. 10, pp. 93–101,
1712 Oct. 2005. 1713
- [69] M. Sikora, J. N. Laneman, M. Haenggi, D. J. Costello, and T. E. Fuja,
1714 "Bandwidth-and power-efficient routing in linear wireless networks,"
1715 *IEEE Trans. Inf. Theory*, vol. 52, no. 6, pp. 2624–2633, Jun. 2006. 1716
- [70] C. Bae and W. E. Stark, "End-to-end energy and bandwidth tradeoff in
1717 multihop wireless networks," *IEEE Trans. Inf. Theory*, vol. 55, no. 9,
1718 pp. 4051–4066, Sep. 2009. 1719
- [71] J. Niu, L. Cheng, Y. Gu, L. Shu, and S. K. Das, "R3E: Reliable reactive
1720 routing enhancement for wireless sensor networks," *IEEE Trans. Ind.*
1721 *Informat.*, vol. 10, no. 1, pp. 784–794, Feb. 2014. 1722
- [72] J. Zuo, H. V. Nguyen, S. X. Ng, and L. Hanzo, "Energy-efficient relay
1723 aided Ad Hoc networks using iteratively detected irregular convolu-
1724 tional coded, unity-rate coded and space-time trellis coded transceivers,"
1725 in *Proc. IEEE WCNC*, Quintana-Roo, Mexico, Mar. 28–31, 2011,
1726 pp. 1179–1184. 1727
- [73] J. Zuo, C. Dong, S. X. Ng, L.-L. Yang, and L. Hanzo, "Energy-efficient
1728 routing in Ad Hoc networks relying on channel state information and
1729 limited mac retransmissions," in *Proc. IEEE VTC-Fall*, San Francisco,
1730 CA, USA, Sep. 5–8, 2011, pp. 1–5. 1731
- [74] J. Zuo *et al.*, "Cross-layer aided energy-efficient opportunistic routing in
1732 Ad Hoc networks," *IEEE Trans. Commun.*, vol. 62, no. 2, pp. 522–535,
1733 Feb. 2014. 1734
- [75] D. Feng *et al.*, "A survey of energy-efficient wireless communications,"
1735 *IEEE Commun. Surveys Tuts.*, vol. 15, no. 1, pp. 167–178, 2013. 1736
- [76] M. C. Vuran and I. F. Akyildiz, "Error control in wireless sensor net-
1737 works: A cross layer analysis," *IEEE/ACM Trans. Netw.*, vol. 17, no. 4,
1738 pp. 1186–1199, Aug. 2009. 1739
- [77] H. V. Nguyen, S. X. Ng, and L. Hanzo, "Distributed three-stage concate-
1740 nated irregular convolutional, unity-rate and space-time trellis coding for
1741 single-antenna aided cooperative communications," in *Proc. IEEE 72nd*
1742 *VTC-Fall*, Ottawa, ON, Canada, Sep. 6–9, 2010, pp. 1–5. 1743
- [78] S. T. Brink, "Convergence behavior of iteratively decoded parallel con-
1744 catenated codes," *IEEE Trans. Commun.*, vol. 49, no. 10, pp. 1727–1737,
1745 Oct. 2001. 1746
- [79] L. Hanzo, O. Alamri, M. El-Hajjar, and N. Wu, *Near-Capacity Multi-*
1747 *Functional MIMO Systems*. New York, NY, USA: Wiley, 2009. 1748
- [80] *User Datagram Protocol*. [Online]. Available: [http://tools.ietf.org/html/](http://tools.ietf.org/html/rfc768)
1749 [rfc768](http://tools.ietf.org/html/rfc768) 1750
- [81] L. Hanzo, S.-X. Ng, T. Keller, and W. Webb, *Quadrature Amplitude*
1751 *Modulation: From Basics to Adaptive Trellis-Coded, Turbo-Equalised*
1752 *and Space-Time Coded OFDM, CDMA, and MC-CDMA Systems*,
1753 2nd ed. Hoboken, NJ, USA: Wiley-IEEE Press, 2004. 1754

- [82] J. Zuo, S. X. Ng, and L. Hanzo, "Fuzzy logic aided dynamic source routing in cross-layer operation assisted Ad Hoc networks," in *Proc. IEEE 72nd VTC-Fall*, Ottawa, ON, Canada, Sep. 6–9, 2010, pp. 1–5.
- [83] A. Ibrahim, H. Zhu, and K. J. R. Liu, "Distributed energy-efficient cooperative routing in wireless networks," *IEEE Trans. Wireless Commun.*, vol. 7, no. 10, pp. 3930–3941, Oct. 2008.
- [84] E. Baccarelli, M. Biagi, C. Pelizzoni, and N. Cordeschi, "Maximum-rate node selection for power-limited multi-antenna relay backbones," *IEEE Trans. Mobile Comput.*, vol. 8, no. 6, pp. 807–820, Jun. 2009.
- [85] C. Bae and W. E. Stark, "End-to-end energy-bandwidth tradeoff in multihop wireless networks," *IEEE Trans. Inf. Theory*, vol. 55, no. 9, pp. 4051–4066, Sep. 2009.
- [86] S. Banerjee and A. Misra, "Minimum energy paths for reliable communication in multi-hop wireless networks," in *Proc. 3rd ACM Int. Symp. MobiHoc*, Lausanne, Switzerland, Jun. 9–11, 2002, pp. 146–156.
- [87] S. Cui, R. Madan, A. Goldsmith, and S. Lall, "Cross-layer energy and delay optimization in small-scale sensor networks," *IEEE Trans. Wireless Commun.*, vol. 6, no. 10, pp. 3688–3699, Oct. 2007.
- [88] H. Alwan and A. Agarwal, "Multi-objective QoS routing for wireless sensor networks," in *Proc. ICNC*, Jan. 28–31, 2013, pp. 1074–1079.
- [89] X.-Y. Li *et al.*, "Reliable and energy-efficient routing for static wireless Ad Hoc networks with unreliable links," *IEEE Trans. Parallel Distrib. Syst.*, vol. 20, no. 10, pp. 1408–1421, Oct. 2009.
- [90] M. Zorzi and R. R. Rao, "Geographic random forwarding (GeRaF) for Ad Hoc and sensor networks: Energy and latency performance," *IEEE Trans. Mobile Comput.*, vol. 2, no. 4, pp. 349–365, Oct.–Dec. 2003.
- [91] X. Mao, S. Tang, X. Xu, X.-Y. Li, and H. Ma, "Energy-efficient opportunistic routing in wireless sensor networks," *IEEE Trans. Parallel Distrib. Syst.*, vol. 22, no. 11, pp. 1934–1942, Nov. 2011.
- [92] M. Dehghan, M. Ghaderi, and D. Goeckel, "Minimum-energy cooperative routing in wireless networks with channel variations," *IEEE Trans. Wireless Commun.*, vol. 10, no. 11, pp. 3813–3823, Nov. 2011.
- [93] J. Zhu and X. Wang, "Model and protocol for energy-efficient routing over mobile Ad Hoc networks," *IEEE Trans. Mobile Comput.*, vol. 10, no. 11, pp. 1546–1557, Nov. 2011.
- [94] T. Luo, M. Motani, and V. Srinivasan, "Energy-efficient strategies for cooperative multichannel MAC protocols," *IEEE Trans. Mobile Comput.*, vol. 11, no. 4, pp. 553–566, Apr. 2012.
- [95] S. Kwon and N. B. Shroff, "Energy-efficient SINR-based routing for multihop wireless networks," *IEEE Trans. Mobile Comput.*, vol. 8, no. 5, pp. 668–681, May 2009.
- [96] C. Wei, C. Zhi, P. Fan, and K. B. Letaief, "AsOR: An energy efficient multi-hop opportunistic routing protocol for wireless sensor networks over Rayleigh fading channels," *IEEE Trans. Wireless Commun.*, vol. 8, no. 5, pp. 2452–2463, May 2009.
- [97] M. C. Vuran and I. F. Akyildiz, "XLP: A cross-layer protocol for efficient communication in wireless sensor networks," *IEEE Trans. Mobile Comput.*, vol. 9, no. 11, pp. 1578–1591, Nov. 2010.
- [98] H. Kwon, T. H. Kim, S. Choi, and B. G. Lee, "A cross-layer strategy for energy-efficient reliable delivery in wireless sensor networks," *IEEE Trans. Wireless Commun.*, vol. 5, no. 12, pp. 3689–3699, Dec. 2006.
- [99] A. N. Pantazis, S. A. Nikolidakis, and D. D. Vergados, "Energy efficient routing protocols in wireless sensor networks: A survey," *IEEE Commun. Surveys Tuts.*, vol. 15, no. 2, pp. 551–591, 2013.
- [100] M. A. Rahman, S. Anwar, M. I. Pramanik, and M. F. Rahman, "A survey on energy efficient routing techniques in wireless sensor network," in *Proc. 15th ICACT*, Jan. 27–30, 2013, pp. 200–205.
- [101] S. Biswas and R. Morris, "Opportunistic routing in multi-hop wireless networks," *ACM SIGCOMM Comput. Commun. Rev.*, vol. 34, no. 1, pp. 69–74, Jan. 2004.
- [102] Q. W. Liu, S. L. Zhou, and G. B. Giannakis, "Cross-layer combining of adaptive modulation and coding with truncated ARQ over wireless links," *IEEE Trans. Wireless Commun.*, vol. 3, no. 5, pp. 1746–1755, Sep. 2004.
- [103] Z. Wang, Y. Chen, and C. Li, "CORMAN: A novel cooperative opportunistic routing scheme in mobile Ad Hoc networks," *IEEE J. Sel. Areas Commun.*, vol. 30, no. 2, pp. 289–296, Feb. 2012.
- [104] A. M. Akhtar, M. R. Nakhai, and A. H. Aghvami, "On the use of cooperative physical layer network coding for energy efficient routing," *IEEE Trans. Commun.*, vol. 61, no. 4, pp. 1498–1509, Apr. 2013.
- [105] R. C. Shah and J. M. Rabaey, "Energy aware routing for low energy Ad Hoc sensor networks," in *Proc. IEEE Wireless Commun. Netw. Conf.*, Mar. 2002, vol. 1, pp. 350–355.
- [106] Y. Xu, J. Heidemann, and D. Estrin, "Geography-informed energy conservation for Ad Hoc routing," in *Proc. 7th Annu. Int. Conf. MobiCom*, Rome, Italy, Jul. 2001, pp. 70–84.
- [107] Q. F. Dong and S. Banerjee, "Minimum energy reliable paths using unreliable wireless links," in *Proc. 6th ACM Int. Symp. MobiHoc*, Urbana-Champaign, IL, USA, May 25–28, 2005, pp. 449–459.
- [108] C.-E. Perkins, E.-M. Royer, S.-R. Das, and M.-K. Marina, "Performance comparison of two on-demand routing protocols for Ad Hoc networks," *IEEE Pers. Commun.*, vol. 8, no. 1, pp. 16–28, Feb. 2001.
- [109] M. Zorzi and R. R. Rao, "Geographic random forwarding (GeRaF) for Ad Hoc and sensor networks: Multihop performance," *IEEE Trans. Mobile Comput.*, vol. 2, no. 4, pp. 337–348, Oct.–Dec. 2003.
- [110] H. Liu, B. Zhang, H. Mouttah, X. Shen, and J. Ma, "Opportunistic routing for wireless Ad Hoc and sensor networks: Present and future 24 directions," *IEEE Commun. Mag.*, vol. 47, no. 12, pp. 103–109, Dec. 2009.
- [111] H. Dubois-Ferrière, M. Grossglauser, and M. Vetterli, "Valuable detours: Least-cost anypath routing," *IEEE/ACM Trans. Netw.*, vol. 19, no. 2, pp. 333–346, Apr. 2011.
- [112] A. A. Bhorkar, M. Naghshvar, T. Javidi, and B. D. Rao, "Adaptive opportunistic routing for wireless Ad Hoc networks," *IEEE/ACM Trans. Netw.*, vol. 20, no. 1, pp. 243–256, Feb. 2012.
- [113] K. Zeng, Z. Yang, and W. Lou, "Location-aided opportunistic forwarding in multirate and multihop wireless networks," *IEEE Trans. Veh. Technol.*, vol. 58, no. 6, pp. 3032–3040, Jul. 2009.
- [114] R. Laufer, H. Dubois-Ferrière, and L. Kleinrock, "Polynomial-time algorithms for multirate anypath routing in wireless multihop networks," *IEEE/ACM Trans. Netw.*, vol. 20, no. 3, pp. 742–755, Jun. 2012.
- [115] L. Pelusi, A. Passarella, and M. Conti, "Opportunistic networking: Data forwarding in disconnected mobile Ad Hoc networks," *IEEE Commun. Mag.*, vol. 44, no. 11, pp. 134–141, Nov. 2006.
- [116] H. Khalife, N. Malouch, and S. Fdida, "Multihop cognitive radio networks: To route or not to route," *IEEE Netw.*, vol. 23, no. 4, pp. 20–25, Jul. 2009.
- [117] K. C. Lee, U. Lee, and M. Gerla, "Geo-opportunistic routing for vehicular networks [topics in automotive networking]," *IEEE Commun. Mag.*, vol. 48, no. 5, pp. 164–170, May 2010.
- [118] D. Wu, Y. Zhang, L. Bao, and A. C. Regan, "Location-based crowdsourcing for vehicular communication in hybrid networks," *IEEE Trans. Intell. Transp. Syst.*, vol. 14, no. 2, pp. 837–846, Jun. 2013.
- [119] V. Conan, J. Leguay, and T. Friedman, "Fixed point opportunistic routing in delay tolerant networks," *IEEE J. Sel. Areas Commun.*, vol. 26, no. 5, pp. 773–782, Jun. 2008.
- [120] T. Spyropoulos, T. Turtletti, and K. Obraczka, "Routing in delay-tolerant networks comprising heterogeneous node populations," *IEEE Trans. Mobile Comput.*, vol. 8, no. 8, pp. 1132–1147, Aug. 2009.
- [121] Y. Li *et al.*, "Energy-efficient optimal opportunistic forwarding for delay-tolerant networks," *IEEE Trans. Veh. Technol.*, vol. 59, no. 9, pp. 4500–4512, Nov. 2010.
- [122] S.-G. Yoon, S. Jang, Y.-H. Kim, and S. Bahk, "Opportunistic routing for smart grid with power line communication access networks," *IEEE Trans. Smart Grid*, vol. 5, no. 1, pp. 303–311, Jan. 2014.
- [123] T. H. Cormen, C. E. Leiserson, R. L. Rivest, and C. Stein, *Introduction to Algorithms*, 3rd ed. Upper Saddle River, NJ, USA: MIT Press, 2009.
- [124] E. W. Dijkstra, "A note on two problems in connexion with graphs," *Numerische Mathematik*, vol. 1, no. 1, pp. 269–271, 1959.
- [125] M. L. Fredman and R. E. Tarjan, "Fibonacci heaps and their uses in improved network optimization algorithms," *J. Assoc. Comput. Mach.*, vol. 34, no. 3, pp. 596–615, Jul. 1987.
- [126] C. Dong, L.-L. Yang, and L. Hanzo, "Multi-hop diversity aided multihop communications: A cumulative distribution function aware approach," *IEEE Trans. Commun.*, vol. 61, no. 11, pp. 4486–4499, Nov. 2013.
- [127] C. Dong, L.-L. Yang, and L. Hanzo, "Performance analysis of multihop-diversity-aided multihop links," *IEEE Trans. Veh. Technol.*, vol. 61, no. 6, pp. 2504–2516, Jul. 2012.
- [128] W. C. Tan, S. K. Bose, and T.-H. Cheng, "Power and mobility aware routing in wireless Ad Hoc networks," *IET Commun.*, vol. 6, no. 11, pp. 1425–1437, Jul. 2012.
- [129] F. D. Rango, F. Guerriero, and P. Fazio, "Link-stability and energy aware routing protocol in distributed wireless networks," *IEEE Trans. Parallel Distrib. Syst.*, vol. 23, no. 4, pp. 713–726, Apr. 2012.
- [130] A. A. Jeng and R.-H. Jan, "Adaptive topology control for mobile Ad Hoc networks," *IEEE Trans. Parallel Distrib. Syst.*, vol. 22, no. 12, pp. 1953–1960, Dec. 2011.
- [131] G. Ferrari and O. K. Tonguz, "Impact of mobility on the BER performance of Ad Hoc wireless networks," *IEEE Trans. Veh. Technol.*, vol. 56, no. 1, pp. 271–286, Jan. 2007.
- [132] S. L. Correia, J. Celestino, and O. Cherkaoui, "Mobility-aware ant colony optimization routing for vehicular Ad Hoc networks," in *Proc. IEEE WCNC*, Quintana-Roo, Mexico, Mar. 28–31, 2011, pp. 1125–1130.



1911
1912
1913
1914
1915
1916
1917
1918
1919
1920
1921
1922 current research interests include protocols and algorithms design, cross-layer
1923 optimization and opportunistic communications.

Jing Zuo received the B.Eng. degree in communications engineering and the M.Sc. degree in communications and information system from Jilin University, Changchun, China, in 2006 and 2008, respectively, and the Ph.D. degree in wireless communications from University of Southampton, U.K., in 2013. She is the recipient of scholarship under the UK-China Scholarships for Excellence programme from 2008 to 2011. From 2009 to 2013, she was involved in the OPTIMIX and CONCERTO European projects. She is currently with Huawei, Shenzhen, China and her



1924
1925
1926
1927
1928
1929
1930
1931
1932
1933
1934
1935 Best Paper Award at IEEE VTC 2014-Fall. His research interests include
1936 applied math, relay system, channel modelling and cross-layer optimization.

Chen Dong received the B.S. degree in electronic information sciences and technology from University of Science and Technology of China (USTC), Hefei, China, in 2004, and the M.Eng. degree in pattern recognition and automatic equipment from the University of Chinese Academy of Sciences, Beijing, China in 2007. He received the Ph.D. degree from the University of Southampton, UK. In 2014. Now he is a post-doc in the same University. He was the recipient of scholarship under the UK-China Scholarships for Excellence programme and he has been awarded



1948
1949
1950
1951
1952
1953
1954
1955
1956
1957

Soon Xin Ng (S'99–M'03–SM'08) received the B.Eng. degree (first class) in electronic engineering and the Ph.D. degree in telecommunications from the University of Southampton, Southampton, U.K., in 1999 and 2002, respectively. From 2003 to 2006, he was a postdoctoral research fellow working on collaborative European research projects known as SCOUT, NEWCOM and PHOENIX. Since August 2006, he has been a member of academic staff in the School of Electronics and Computer Science, University of Southampton. He is involved in the

OPTIMIX and CONCERTO European projects as well as the IU-ATC and UC4G projects. He is currently an associate professor in telecommunications at the University of Southampton. His research interests include adaptive coded modulation, coded modulation, channel coding, space-time coding, joint source and channel coding, iterative detection, OFDM, MIMO, cooperative communications, distributed coding, quantum error correction codes and joint wireless-and-optical-fiber communications. He has published over 180 papers and co-authored two John Wiley/IEEE Press books in this field. He is a Chartered Engineer and a Fellow of the Higher Education Academy in the U.K.



of Southampton, United Kingdom, where he is the professor of wireless communications in the School of Electronics and Computer Science. His research has covered a wide range of topics in wireless communications, networking and signal processing. He has published over 300 research papers in journals and conference proceedings, authored/co-authored three books and also published several book chapters. The details about his publications can be found at <http://www-mobile.ecs.soton.ac.uk/lly/>. He is a Fellow of the IET, served as an associate editor to the *IEEE TRANSACTIONS ON VEHICULAR TECHNOLOGY* and *JOURNAL OF COMMUNICATIONS AND NETWORKS* (JCN), and is currently an associate editor to the *IEEE Access* and the *Security and Communication Networks (SCN) Journal*.

Lie-Liang Yang (M'98–SM'02) received the 1958 B.Eng. degree in communications engineering from 1959 Shanghai TieDao University, Shanghai, China, 1960 in 1988, and the M.Eng. and Ph.D. degrees in 1961 communications and electronics from Northern 1962 (Beijing) Jiaotong University, Beijing, China in 1963 1991 and 1997, respectively. From June 1997 to 1964 December 1997 he was a visiting scientist of the 1965 Institute of Radio Engineering and Electronics, 1966 Academy of Sciences of the Czech Republic. Since 1967 December 1997, he has been with the University 1968



co-authored 20 John Wiley/IEEE Press books on mobile radio communications totalling in excess of 10 000 pages, published 1460 research entries at IEEE Xplore, acted both as TPC and General Chair of IEEE conferences, presented keynote lectures and has been awarded a number of distinctions. Currently he is directing a 60-strong academic research team, working on a range of research projects in the field of wireless multimedia communications by industry, the Engineering and Physical Sciences Research Council (EPSRC) UK, the European Research Council's Advanced Fellow Grant and the Royal Society's Wolfson Research Merit Award. He is an enthusiastic supporter of industrial and academic liaison and he offers a range of industrial courses. He is also a Governor of the IEEE VTS. During 2008–2012 he was the Editor-in-Chief of the *IEEE Press* and a Chaired Professor also at Tsinghua University, Beijing. His research is funded by the European Research Council's Senior Research Fellow Grant. For further information on research in progress and associated publications please refer to <http://www-mobile.ecs.soton.ac.uk>.

Lajos Hanzo received the degree in electronics in 1980 1976 and the doctorate degree in 1983. In 2009 he 1981 was awarded the honorary doctorate "Doctor Honoris Causa" by the Technical University of Budapest. 1983 During his 37-year career in telecommunications he 1984 has held various research and academic posts in 1985 Hungary, Germany and the UK. Since 1986 he has 1986 been with the School of Electronics and Computer 1987 Science, University of Southampton, UK, where he 1988 holds the chair in telecommunications. He has suc- 1989 cessfully supervised more than 80 Ph.D. students, 1990

AUTHOR QUERIES

AUTHOR PLEASE ANSWER ALL QUERIES

AQ1 = Note that reference [26] and [105] are the same. Therefore, reference [105] was deleted from the list.
Citations were renumbered accordingly. Please check.

AQ2 = Note that reference [57] and [109] are the same. Therefore, reference [109] was deleted from the list.
Citations were renumbered accordingly. Please check.

END OF ALL QUERIES

IEEE
Proof